Effects of temperature and pCO_2 on the degradation of organic matter in the ocean

Judith Piontek

Dissertation zur Erlangung des akademischen Grades eines Doktors der Naturwissenschaften (Dr. rer. nat.)

Fachbereich 2 (Biologie/Chemie)
Universität Bremen

Alfred-Wegener-Institut für Polar- und Meeresforschung
in der Helmholtz-Gemeinschaft

Bremen, Januar 2009

1. Gutachter: Dr. Anja Engel

2. Gutachter: Prof. Dr. Karin Lochte

Promotionskolloquium: 9. Februar 2009

"I presume that the numerous lower pelagic animals persist on the infusoria, which are known to abound in the open ocean: but on what, in the clear blue water, do these infusoria subsist?"

CHARLES DARWIN (1845)

Table of contents

Summary

This thesis deals with effects of temperature and the partial pressure of carbon dioxide (pCO_2) on the degradation of organic matter in the ocean. Ocean temperature and pCO_2 are subject to natural spatiotemporal variability, but changes in the world's climate currently evoke strong anthropogenic impacts on these two parameters in seawater. The sea surface temperature will rise by up to 5°C in global average until the end of this century. Concurrently, the equilibration with rising atmospheric pCO_2 will increase seawater pCO_2 from the present-day level of 380 µatm up to 900 µatm, and thus decrease the ocean pH by up to 0.6 units.

An increase of temperature and pCO_2 as expected for the near future led to a substantial acceleration of organic matter degradation in experimental studies. Higher degradation rates were primarily induced by temperature and pH effects on bacterial extracellular enzymes that increased rates of polymer hydrolysis.

Effects of rising *in-situ* temperature on the bacterial degradation of diatom aggregates formed from a natural plankton community of the Kiel Fjord (Baltic Sea) accelerated both the dissolution of diatom silica frustules and the remineralization of particulate organic carbon (POC). Elevated temperature increased activities of bacterial extracellular enzymes in aggregates and their surrounding seawater, and promoted bacterial metabolism and growth. Degradation of diatom aggregates at higher rate will potentially decrease the export of organic carbon in the warmed future ocean. The accelerated degradation of aggregates in the experimental treatment of elevated temperature was counteracted by temperature effects that supported organic matter aggregation and thus may enhance export. Whether elevated temperature will decrease or increase the export of aggregated organic matter in marine

ecosystems will depend on additional abiotic and biotic factors like depth and stratification of the water body and conditions for phytoplankton growth.

The production of organic carbon by phytoplankton and the subsequent degradation by bacterioplankton were investigated during field studies in the northern Bay of Biscay (Atlantic Ocean). Carbon in transparent exopolymer particles (TEP) accounted in average for 12% of POC during the decline of a coccolithophorid bloom. Heterotrophic bacterial activity was examined with focus on the degradation of polysaccharides that are the main component of TEP and contain also a considerable fraction of organic carbon in phytoplankton biomass. The polysaccharide hydrolysis by bacterial extracellular glucosidases and the subsequent utilization of glucose monomers co-determined the biomass production of bacterioplankton in the Bay of Biscay. Bacterial degradation activity altered the chemical composition of polysaccharides produced from the coccolithophore *Emiliania huxleyi* and relatively enriched surface-active carbohydrate species. Polysaccharide-rich TEP were degraded as efficiently as POC derived from phytoplankton biomass. A series of incubation experiments demonstrated that lowered seawater pH increased the activity of bacterial extracellular glucosidases, and thus substantially accelerated the breakdown of polysaccharides. Linear regression revealed that glucosidase rates were directly related to the increase of the hydrogen ion concentration in seawater. The experimental decrease of seawater pH simulating ocean acidification also increased the loss of POC during incubation. Experimental results suggest that effects of ocean acidification on bacterial organic matter degradation will provide a positive feedback to increasing atmospheric CO_2.

This thesis clearly shows that effects of rising temperature and decreasing pH on the activity of heterotrophic bacterioplankton have the potential to substantially affect the marine carbon cycle. In order to evaluate potential feedback mechanisms of marine

biogeochemical cycles in response to climate change, it is essential to investigate effects of projected changes in ocean temperature and pCO_2 on bacterial heterotrophic processes and on autotrophic processes with similar effort.

Zusammenfassung

Die vorliegende Arbeit befasst sich mit Auswirkungen von Temperatur und Kohlendioxid-Partialdruck (pCO_2) auf den Abbau von organischem Material im Ozean. Temperatur und pCO_2, die im Ozean auch natürlichen räumlichen und zeitlichen Schwankungen unterliegen, werden zunehmend von den Folgen des anthropogenen globalen Klimawandels beeinflusst. Die Oberflächentemperatur des Ozeans wird in diesem Jahrhundert weltweit um bis zu 5°C ansteigen. Im selben Zeitraum wird die Equilibrierung mit steigendem atmosphärischem pCO_2 zu einem Anstieg des pCO_2 in Seewasser von derzeit 380 µatm auf bis zu 900 µatm führen und so den pH-Wert des Ozeans um bis zu 0.6 Einheiten senken.

Ein Anstieg von Temperatur und pCO_2, wie sie für die nahe Zukunft zu erwarten sind, haben in experimentellen Studien zu einem deutlich beschleunigten Abbau von organischem Material geführt. Ursache für höhere Abbauraten waren in erster Linie Effekte von Temperatur und pH auf bakterielle extrazelluläre Enzyme, die zu erhöhten Raten der Hydrolyse von Polymeren geführt haben.

Auswirkungen steigender *in-situ* Temperatur auf den bakteriellen Abbau von Diatomeen-Aggregaten, die aus einer natürlichen Plankton-Gemeinschaft der Kieler Bucht (Ostsee) gebildet wurden, haben sowohl die Lösung der Diatomeen-Silikatschalen als auch die Remineralisierung des partikulären organischen Kohlenstoffs (POC) beschleunigt. Die erhöhte Temperatur förderte die Aktivität der bakteriellen extrazellulären Enzyme in Aggregaten und ihrem Umgebungswasser, sowie Metabolismus und Wachstum der Bakterien. Erhöhte Abbauraten von Diatomeen-Aggregaten haben das Potential den Export von organischem Kohlenstoff bei Erwärmung der Ozeane zu verringern. Erhöhten Abbauraten bei experimentell erhöhter Temperatur standen Temperatur-Effekte gegenüber, die die Aggregation des organischen Materials begünstigten und so wiederum den Export

steigern könnten. Ob ein Anstieg der Temperatur den Export von aggregiertem organischem Material in marinen Ökosystemen letztlich verringert oder steigert, wird deshalb von weiteren abiotischen und biotischen Faktoren wie zum Beispiel Tiefe und Stratifizierung des Wasserkörpers und Wachstumsbedingungen für das Phytoplankton abhängen.

In Feldstudien wurden die Produktion von organischem Kohlenstoff durch Phytoplankton und der Abbau durch das Bakterioplankton in der nördlichen Biskaya (Atlantik) untersucht. Während einer absterbenden Coccolithophoriden-Blüte betrug der Kohlenstoff-Anteil von transparenten exopolymeren Partikeln (TEP) am POC durchschnittlich 12%. Die bakterielle Aktivität wurde speziell im Hinblick auf den Abbau von Polysacchariden untersucht, die der Hauptbestandteil von TEP sind und ebenfalls einen erheblichen Anteil des organischen Kohlenstoffes in Phytoplankton-Biomasse beinhalten. Die Hydrolyse von Polysacchariden durch bakterielle extrazelluläre Glucosidasen und die nachfolgende Verwertung von Glucose-Monomeren beeinflussten die Biomasse-Produktion der Bakterioplankton-Gemeinschaft in der Biskaya. Bakterielle Abbauaktivität veränderte die chemische Zusammensetzung von Polysacchariden produziert durch den Coccolithophoriden *Emiliania huxleyi* und führte zu einer relativen Anreicherung von oberflächenaktiven Zuckern. Polysaccharidreiche TEP sind mit gleicher Effizienz abgebaut worden wie POC, das sich von der Phytoplankton Biomasse ableitet. Eine Reihe von Inkubationsexperimenten zeigte, dass ein gesenkter pH-Wert die Aktivität der bakteriellen extrazellulären Glucosidasen erhöhte und so den Abbau von Polysacchariden deutlich beschleunigte. Eine lineare Regression belegte einen direkten Zusammenhang zwischen den Raten der extrazellulären Glucosidasen und dem Anstieg der Protonen-Konzentration im Seewasser. Die experimentelle Absenkung des pH-Wertes in Seewasser, die die Versauerung der Ozeane simulierte, erhöhte auch die Verluste des POC während der

Inkubation. Die experimentellen Ergebnisse weisen darauf hin, dass Auswirkungen der Ozeanversauerung auf den bakteriellen Abbau von organischem Material eine positive Rückkopplung zur ansteigenden atmosphärischen CO_2 Konzentration auslösen können.

Diese Arbeit zeigt deutlich, dass Effekte von steigender Temperatur und sinkendem pH-Wert auf die Aktivität des heterotrophen Bakterioplanktons das Potential haben, den marinen Kohlenstofkreislauf erheblich zu beeinflussen. Um mögliche Rückkopplungs-Mechanismen mariner biogeochemischer Kreisläufe in Bezug auf den weltweiten Klimawandel zu bewerten, ist es deshalb notwendig, Auswirkungen der prognostizierten Veränderungen von Temperatur und pCO_2 im Ozean auf autotrophe Prozesse und auf bakterielle heterotrophe Prozesse mit gleicher Sorgfalt zu untersuchen.

1. General introduction

Anthropogenic emissions have increased the concentration of a number of greenhouse gases in the atmosphere, and of carbon dioxide (CO_2) in particular, during the last 200 years (Houghton et al. 2001, Parry et al. 2007). Since radiative forcing by greenhouse gases plays an essential role in maintaining the Earth's temperature, increasing emissions have led to an observed warming of the atmosphere and the ocean (Houghton et al. 2001, Parry et al. 2007). Furthermore, the absorption of excess atmospheric CO_2 by the ocean has increased the acidity of seawater at global scale (Sabine et al. 2004, Raven et al. 2005). The assessment of potential consequences for marine biota and biogeochemical cycles in the ocean requires an integrated scientific approach. Effects of increasing temperature and decreasing pH on bacterial organic matter degradation are thereby of outstanding importance, but yet hardly considered. Heterotrophic bacteria are the main consumers of organic matter in the ocean, efficiently remineralizing biogenic carbon back to CO_2 (Azam 1998, Sherr & Sherr 2000). Less than 10% of organic carbon removed from the surface ocean via particle sinking is sequestered to the deep ocean (Martin et al. 1987). The loss of organic carbon within and below the euphotic zone is mainly mediated by the degradation activity of bacteria, colonizing sinking particles and their surroundings (Cho & Azam 1988, Karl et al. 1988, Smith et al. 1992). Metabolism and growth of marine bacteria are significantly affected by temperature and pH (Rivkin et al. 1996, Arnosti 1998, Pomeroy & Wiebe 2001). Potential effects of current changes in ocean temperature and pH on bacterial activity and consequences for the cycling of organic matter need to be investigated, since they are highly relevant for marine organic carbon fluxes and the ocean-atmosphere CO_2 exchange.

1.1 Temperature and pH in the ocean - natural variability and current trends induced by human activities

Temperature and pH show distinct spatial and temporal variations in the ocean. The largest variability of temperature occurs at the ocean's surface, driven by the seasonal solar radiation. The annual amplitude of sea surface temperature (SST) in the open ocean exceeds 4.5°C at latitudes of 30 to 40° and decreases towards the equator and the poles (Dietrich et al. 1975). Oceanic regions with high annual amplitudes of SST are stratified during summer. The warmer upper 20 to 200 metres of the water column are separated from the cold deep water by the thermocline, which restricts the vertical exchange of solutes.

The pH in seawater is determined by the proportioning of the different inorganic carbon species, namely dissolved CO_2, carbonate, and bicarbonate. At present day, natural seawater typically has a pH of 8.2 and bicarbonate accounts for approx. 90% of dissolved inorganic carbon (Zeebe & Wolf-Gladrow 2001). On global scale and on time scales longer than 1000 years, the carbonate chemistry of seawater is controlled by the riverine input of inorganic carbon, whose composition is determined by the weathering of rocks. However, on time scales of oceanic circulation (1000 years and less), the proportions of inorganic carbon species in the ocean are primarily determined by biological processes, in particular by calcification, photosynthesis, and the degradation of organic matter (Zeebe & Wolf-Gladrow 2001).

Beside natural spatial and temporal variability of temperature and pH in the ocean, current changes in the world's climate evoke changes of these two parameters with a speed not experienced by marine organisms during their recent evolutionary history (Raven et al. 2005). There is clear scientific consensus that the main explanation for current climate change is human activity (Parry et al. 2007). The mean global atmospheric CO_2 concentration has

increased from 280 ppm in the 18th century to 380 ppm in 2005 due to the combustion of fossil fuels at a progressively faster rate each decade (Houghton et al. 2001, Parry et al. 2007). Emissions of CO_2 in the recent past were at the upper edge of the envelope of IPCC emission scenarios (Raupach et al. 2007). Therefore, it seems likely that atmospheric CO_2 concentration will reach a level of 970 ppm by the year 2100 (Houghton et al. 2001). Changes of temperature and pH in marine environments induced by climate change are frequently termed ocean warming and ocean acidification (Fig. 1).

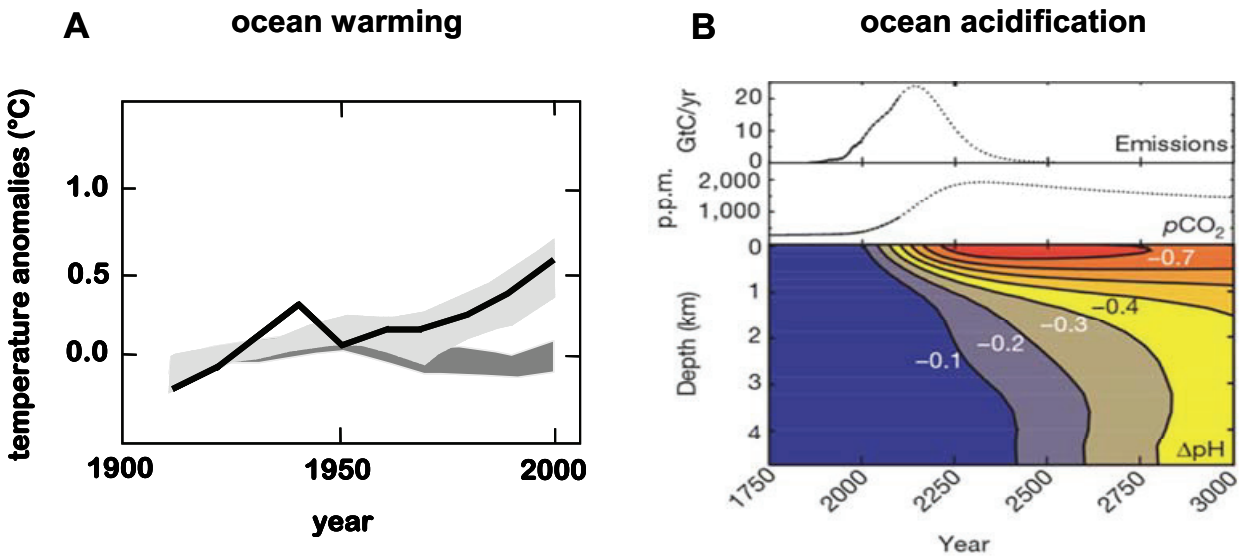

Figure 1. Effects of global change on the world ocean - ocean warming and ocean acidification.

(A) Ocean warming: Observations of sea surface temperature (SST) over the last 100 years. Anomalies were calculated relative to the mean SST of the period 1961 to 1990. Dark grey shaded bands show the 5-95% range for 19 simulations from 5 climate models using only the natural forcing due to solar activity and volcanoes. Bands shaded in light grey show the 5-95% range for 58 simulations from 14 climate models using both natural and anthropogenic forcing. Redrawn from IPCC (2007).
(B) Ocean acidification: Release of CO_2 and emissions predicted for the future related to changes in ocean pH. Reproduced from Caldeira & Wickett (2003).

The SST of the world ocean has already increased by 0.6°C in average during the last 100 years (Fig. 1 A) and will further rise by 3 to 5°C during the 21st century. The increase of SST in temperate climate zones will be pronounced during winter and spring, when it will

potentially amount to 5 to 10°C (Houghton et al. 2001, Parry et al. 2007). The equilibration of seawater with increasing atmospheric CO_2 concentration generates changes in carbonate chemistry already measurable today. The ocean pH has lowered by approx. 0.1 units from the surface to depth since pre-industrial times, representing a 30% increase in the concentration of hydrogen ions (Raven et al. 2005). The increase in atmospheric CO_2 concentration predicted for the near future will further decrease the ocean pH by up to 0.6 units in the surface layer and by approx. 0.3 units in depths below 1000 m within the next 150 years (Caldeira & Wickett 2003) (Fig. 1 B). A doubling of seawater CO_2 concentration as projected for the surface ocean by the middle of this century will be accompanied by a decrease in average carbonate concentration of 35%. Current changes in carbonate chemistry of seawater are essentially irreversible during our lifetimes.

1.2 The bacterial cycling of organic matter in the ocean

The scientific knowledge is by far insufficient to predict with precision the evolution and consequences of global change in marine environments. Potential effects of ocean warming and acidification on heterotrophic bacteria and their degradation activity are yet not adequately included in experimental studies and model predictions, despite the well-known fact that heterotrophic bacteria play a major role in degradation and remineralization of organic matter in the ocean (Cho & Azam 1988, Smith et al. 1992).

The microbial loop

The world's oceans are estimated to contain more than 10^{29} bacteria (Whitman 1998). Members of the microbial foodweb, including protozoan microzooplankton, are typically five to ten times the biomass of all multicellular marine organisms (Pomeroy 2007). The

consumption of dissolved organic matter (DOM) by marine bacteria and the subsequent production of bacterial biomass provide the basis for the microbial loop. DOM is reintroduced to higher trophic levels after grazing of bacteria by protozoans that in turn are grazed by larger zooplankton (Azam et al. 1983) The microbial loop is a major pathway of organic carbon in the ocean, channelling about 50% of primary production (Azam 1998).

The role of bacteria in the marine carbon cycle

The ocean is one of the major sinks for atmospheric CO_2 on Earth, but also a very dynamic global carbon reservoir. The functioning of the heterotrophic bacterial community largely controls carbon fluxes in the ocean and provides a feedback to the net flux of CO_2 from the atmosphere to the sea. Marine bacteria contribute by far the largest proportion to community respiration in the pelagic ocean, remineralizing about 75% of the contemporary annual net primary production of 45 Gt of carbon (Falkowski et al. 1998). Bacterial respiration thus largely determines the production of CO_2 in the ocean, suggesting a substantial bacterial control of the net CO_2 exchange across the air-sea interface. The second main function of heterotrophic bacteria in the marine carbon cycle is the solubilization of particulate organic carbon (POC). The transition of organic carbon from the particulate to the dissolved pool is mediated by the activity of bacterial extracellular enzymes (Smith et al. 1992). The bacterial solubilization of sinking particles co-determines the efficiency of the biological carbon pump, i.e. the export of organic carbon to the deep ocean via particle sinking (Volk & Hoffert 1985) that in turn drives the flux of atmospheric CO_2 to the ocean.

The bioreactivity of marine organic matter

A large fraction of organic matter in the open ocean is derived from phytoplankton biomass, debris and exudates (Fig. 2 A). In particular phytoplankton blooms have a profound effect on

the input of organic matter into marine systems (Falkowski et al. 1998). The bioreactivity of particulate and dissolved organic matter is determined by its biochemical composition and diagenetic state. Diagenetically young or fresh material is most bioreactive, and becomes continuously smaller in size and less bioreactive owing to chemical modifications during the decomposition process (Amon & Benner 1996) (Fig. 2 B). The distribution of organic matter along the size continuum is highly skewed to smaller size classes, since 60 to 80% of organic matter is smaller than 1 kDa (Benner 2002).

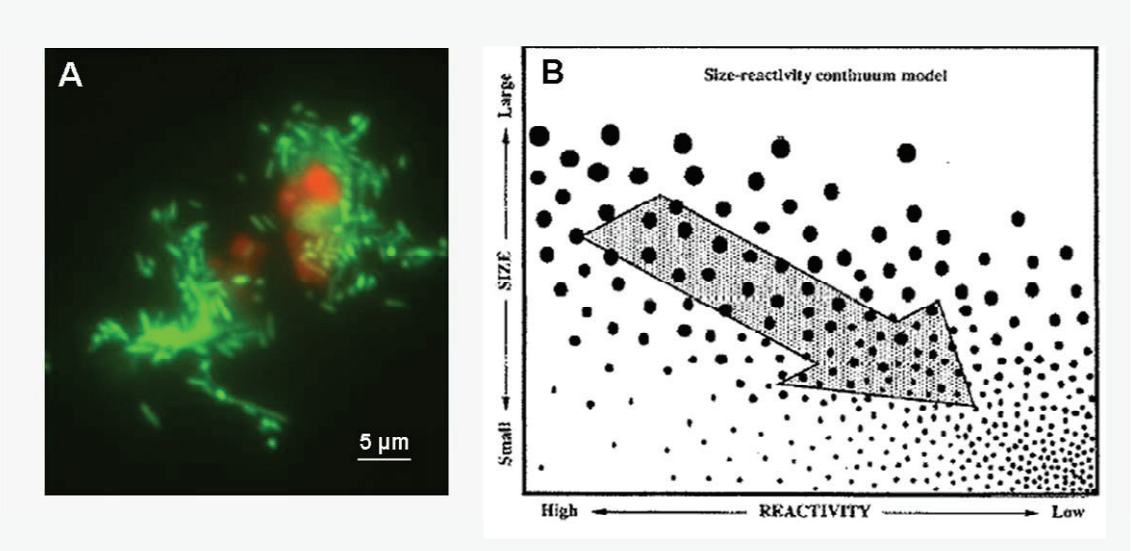

Figure 2. Changes in bioreactivity of organic matter during its degradation.

(A) Bacteria (stained with Sybr Green I) colonizing cells and debris of *Emiliania huxleyi* (red chlorophyll fluorescence). The picture was taken by epifluorescence microscopy at 1000fold magnification.
(B) Schematic diagram of the size-reactivity continuum model. The arrow denotes the major pathway of degradation from bioreactive organic matter like phytoplankton cells and components of high molecular weight to small refractory compounds. Reproduced from Amon & Benner (1996).

Following the size continuum of organic matter in seawater, degradation starts with the decomposition of particles. The flux of particulate organic matter (POM) sinking through the water column is reduced by approx. 90% before the deep ocean is reached. According to an exponential decay, more than 75% of the net loss occurs in the upper 500 m of the water column (Martin et al. 1987). The loss of POM in transit to the deep ocean is mainly driven by

the activity of bacterial extracellular enzymes that shifts organic matter from the particulate to the dissolved phase. Proceeding bacterial degradation activity reduces continuously the proportion of amino acids, carbohydrates, and lipids in particles that accounts for up to 80% of POC in the euphotic zone (Hedges et al. 2001). A consistent preferential loss of one particular component, however, could not be determined. Incubation experiments and field studies provide examples for the selective degradation of both carbohydrates and amino acids (Wakeham et al. 1997, Panagiotopoulos et al. 2002).

The bioreactivity of DOM derived from particle solubilization or other biological processes like phytoplankton exudation and cell lysis can be characterized by the classification of metabolic categories. The pools of labile, semilabile, and refractory DOM are defined by their turnover times, ranging from days in case of labile DOM over several months for the semilabile fraction to centuries and millennia for refractory DOM (Kirchman 1993, Carlson & Ducklow 1995). Concentrations of the different DOM pools in the open ocean reflect the different scales of turnover times. The concentration of labile DOM is usually in the nanomolar range, while semilabile DOM accumulates in surface waters, where it includes highly variable proportions of bulk DOM (Carlson 2002). The largest pool of DOM is refractory, accounting for up to 80% of dissolved organic carbon (DOC) (Carlson & Ducklow 1995). In contrast to labile and semilabile DOM, refractory DOM is uniformly distributed throughout the water column (Druffel et al. 1992). The metabolic categories of DOM differ considerably with regard to their chemical composition. Important components of labile DOM are dissolved free neutral sugars and amino acids. Semilabile DOM is dominated by carbohydrates (Benner et al. 1992, Pakulski & Benner 1994), while nitrogenous compounds such as amino acids represent a relatively minor proportion (McCarthy et al. 1996). Refractory DOM mostly consists of chemically not characterized compounds (Cowie & Hedges 1994, Skoog & Benner 1997) that are mostly of low molecular weight (Carlson

2002). Nevertheless, also DOM older than 500 years is partly metabolized by marine bacteria (Cherrier et al. 1999).

Organic macroaggregates - hotspots of bacterial activity in the ocean

Organic particles offer a niche for bacterial life in the ocean. Macroscopic organic aggregates ("marine snow") are the upper limit of the particle size scale. Their formation is induced by physical coagulation of smaller primary particles derived from phytoplankton cells and debris (McCave 1984, Jackson 1990) or by zooplankton grazing and subsequent production of faecal pellets (Turner 2002) (Fig. 3 A). Aggregates are considered as the main vehicle for the export of organic matter to the deep ocean (Fowler & Knauer 1986). While sinking through the water column, they are microbial hotspots characterized by high bacterial abundances relative to the surrounding seawater (Alldredge & Youngbluth 1985). The bacterial community associated with macroaggregates is fundamentally different from that of free-living bacteria co-occurring in the same water mass. Assemblages attached to particles are dominated by the *Cytophaga-Flavobacterium-Bacteroides* group and the order *Planctomycetales* (DeLong et al. 1993). Bacterial cells associated with aggregates often exhibit a capsular envelope, and attach to particle surfaces by fibrillar structures (Heissenberger et al. 1996) (Fig. 3 B).

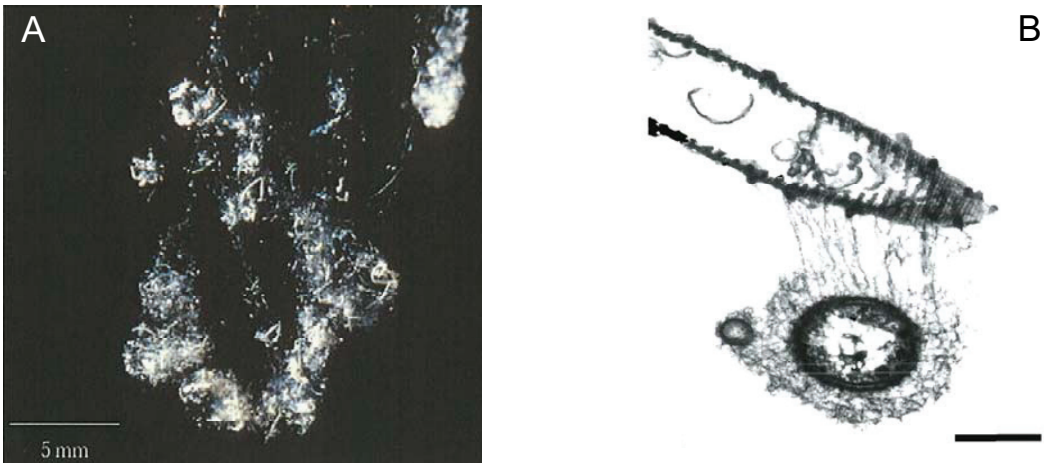

Figure 3. Organic macroaggregates and their colonization by marine bacteria.

(A) *In-situ* micrograph of a diatom aggregate. Picture by A. Alldredge, reproduced from Kiørboe (2001).
(B) Bacterial cells attached with fibrils to diatom debris. Pictures taken by means of transmission electron microscopy, scale bar = 250 nm. Reproduced from Heissenberger et al. (1996).

The cell-specific extracellular enzyme activity of particle-attached bacteria is several times higher compared to free-living bacteria (Karner & Herndl 1992, Grossart et al. 2007). A large proportion of hydrolysates derived from aggregate solubilization is not taken up by the attached bacterial community. Instead, leaking solutes diffuse to the ambient seawater, where they fuel growth of free-living bacteria or remain in dissolved form (Smith et al. 1992). The decoupling of aggregate solubilization by extracellular enzymes from bacterial utilization of the dissolved components is an important mechanism for large-scale transition of organic matter from sinking particles to the dissolved phase (Smith et al. 1992, Kiorboe & Jackson 2001).

1.3 The microbiology of organic matter degradation and its sensitivity to temperature and pH

Bacterial phylogenetic types in the upper ocean are highly diverse, but members of the alpha *Proteobacteria*, particularly the *Roseobacter* clade, SAR 11, and SAR 116, seem to dominate (DeLong et al. 1993, Giovannoni & Rappé 2000). Most strains of the marine bacterioplankton community are heterotrophic, thus obtaining almost all requirements for life from the oxidation of organic molecules (Fig. 4).

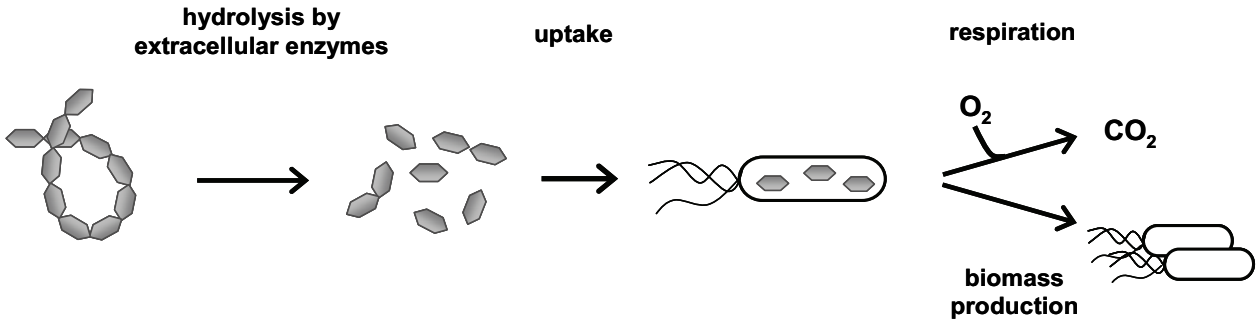

Figure 4. Simplified scheme of organic matter degradation by heterotrophic bacteria.

The hydrolysis of organic macromolecules by extracellular enzymes provides organic compounds of low molecular weight. The uptake and the subsequent metabolization of low-molecular-weight compounds fuel bacterial respiration and biomass production. See text for further explanation.

The vast majority of organic matter in the ocean, providing the basis for growth of heterotrophic bacteria, is of high molecular weight (> 1 kDa) and thus not available for direct bacterial uptake and utilization. Therefore, marine bacteria release extracellular enzymes to accomplish the initial step in organic matter degradation outside of the cell. The term "extracellular enzymes" includes ectoenzymes, which are cell-surface bound and enzymes that are freely dispersed in seawater. Bacterial extracellular enzymes act as endo- or exohydrolases, splitting the sensitive linkage either in the interior of the substrate or in terminal position. After enzymatic breakdown of polymers, specific membrane-bound permeases transport subunits of up to 600 Da across the bacterial cytoplasmic membrane

(Weiss et al. 1991). Within the bacterial cell, consumed carbon is distributed between catabolic and anabolic reactions that generate energy and biomass, respectively. The dominating catabolic pathway of bacteria in marine pelagic ecosystems is aerobic respiration, resulting in the formation of CO_2 (Sherr & Sherr 2000). Organic substrates are oxidized by the use of oxygen as terminal electron acceptor to release energy that is stored as adenosine-5'-triphosphate (ATP). The ratio of anabolic to catabolic processes is represented by the bacterial growth efficiency (BGE) that is defined by

$$BGE = BBP/(BBP + BR),$$

where BBP is the bacterial biomass production and BR the bacterial respiration. The BGE at open ocean sites ranges from 0.05 to 0.3, meaning that between 5 and 30% of organic carbon consumed by bacteria are converted into biomass, while 70 to 95% are remineralized to CO_2 (del Giorgio & Cole 1998).

Studies about temperature and pH effects on marine bacteria conducted in the past decades were primarily focused on physiological responses. The Q_{10} factor, which is defined as the factorial increase of the rate of a physiological process in response to a temperature increase of 10°C, assesses the overall response of biological activity to increasing temperature and compares the temperature sensitivity of different processes. Bacterial activities typically reveal a higher Q_{10} factor ($2 < Q_{10} < 3$) than phytoplankton growth and photosynthesis ($1 < Q_{10} < 2$), showing a higher sensitivity to temperature changes in their environment (Pomeroy & Wiebe 2001). A concept that allows the evaluation of pH effects on biological processes like the Q_{10} factor for temperature effects does currently not exist. The most relevant findings of studies dealing with effects of temperature and pH on the degradation activity of marine bacteria are summarized in the following.

The activity of protein- and polysaccharide-degrading bacterial extracellular enzymes in marine sediments and of arctic isolates increases at rising temperature, showing optima well above the ambient environmental temperatures (King 1986, Helmke & Weiland 1991, Christian & Karl 1995, Arnosti et al. 1998). The membrane-bound transporters of mesophilic and psychrotolerant marine bacteria respond with decreased substrate affinities to temperatures at the lower end of their specific temperature range (Wiebe et al. 1993, Nedwell & Rutter 1994). The BGE in the ocean was shown to be an inverse function of temperature (Rivkin & Legendre 2001). Hence, a smaller proportion of consumed carbon is converted into biomass at increasing temperature for the benefit of respiratory CO_2 production. This finding is based on observations of increased BR at lower latitudes compared to higher latitudes. However, changes in *in-situ* BR may partly result from factors other than temperature, since there are gradients of major environmental factors like inorganic and organic nutrients superimposed on the latitudinal temperature range (Carlson 2007). In contrast to results from field studies, BGE was found to increase at rising temperature in laboratory studies under substrate-replete conditions (Jimenez-Mercado et al. 2007). Temperature explains almost all the variation of BBP in short-term incubation experiments that exclude variability in all parameters except temperature. The *in-vitro* BBP clearly increases with rising temperature (Hoch & Kirchman 1993, Shiah & Ducklow 1994). However, no temperature dependence of BBP could be observed along natural temperature gradients through the Pacific, because BBP was predominantly controlled by variations in the supply of dissolved organic substrates (Kirchman et al. 2001).

There are less studies dealing with pH effects on the bacterial degradation activity in marine environments. The activity of polysaccharide-degrading extracellular enzymes in lakes but also in intertidal sediments shows a clear dependence on pH (King 1986, Chróst 1991, Münster 1991). Similar to the enzymatic temperature optima mentioned above, the pH optima

of *in-situ* extracellular enzyme activity do not match with the ambient pH. Furthermore, changing pH was shown to affect the functioning of permeases in cultures of isolated bacterial strains (e.g. Rauner et al. 2006), suggesting impacts of changing ocean pH on *in-situ* bacterial uptake rates in marine systems. However, there are no studies available investigating pH effects on the bacterial uptake of organic compounds in marine environments. Also studies about effects of pH on the *in-situ* respiration of marine bacterioplankton are currently missing. Changes in pH are known to affect the respiratory electron transfer due to alterations of the redox potential of electron carriers (Kolber 2007). Therefore, effects of ocean acidification on bacterial respiration seem likely.

1.4 Aims and outline of this thesis

Current changes in ocean temperature and pH require integrated studies focused on interactive and combined effects of temperature and pH changes in small intervals as predicted by future scenarios. There is urgency to develop a mechanistic understanding of how ongoing changes in ocean temperature and pH affect processes on small scales and how these effects are transferred to the community and ecosystem level. This thesis is focused on effects of temperature and pH on the bacterial degradation of organic matter. It intends to fill gaps in the knowledge about direct temperature and pH effects on the activity of marine bacteria that exist in particular with regard to pH. Emphasis is put on the linkage between microbial ecology and biogeochemistry, two disciplines that are often separated from each other in marine research. Impacts of increasing temperature and decreasing pH on the bacterial degradation activity in the ocean are discussed with respect to consequences for the cycling of marine organic matter.

Manuscript I is focused on temperature effects on marine diatom aggregates. In order to assess consequences of increasing temperature on the formation and degradation of macroaggregates both the associated bacterial activity and the biogeochemical characteristics of aggregates incubated at different temperatures were investigated. The winter/spring bloom in the Kiel Fjord (Western Baltic Sea) served as model system to test the effect of temperature increase projected by the Intergovernmental Panel of Climate Change (IPCC).

Manuscript II and **manuscript III** present results from two field studies in the Gulf of Biscay, and are focused on the relevance of polysaccharides for the marine carbon cycle. Manuscript II investigates the concentration and size-frequency distribution of transparent exopolymer particles (TEP) during the decline of a coccolithophorid bloom. Manuscript III deals with the role of polysaccharides derived from coccolithophores as carbon source for heterotrophic bacteria. Field data are combined with results from a laboratory experiment to assess the impact of decreasing ocean pH on the cycling of carbohydrates.

Manuscript IV reports effects of lowered ocean pH on the bacterial degradation of polysaccharides and POC induced by biochemical effects of changing pH on the activity of extracellular glucosidases. Consequences for biological and biogeochemical processes in the future ocean are discussed.

Main results of this thesis are summarized, and their contribution to current research is discussed in a concluding section. Effects of temperature and pH on the bacterial degradation of marine organic matter are evaluated with regard to future impacts of global change on marine environments.

1.5 References

ALLDREDGE AL, YOUNGBLUTH MJ (1985) The significance of macroscopic aggregates (marine snow) as sites for heterotrophic bacterial production in the mesopelagic zone of the subtropical atlantic. Deep-Sea Res Part A 32:1445-1456

AMON RMW, BENNER R (1996) Bacterial utilization of different size classes of dissolved organic matter. Limnol Oceanogr 41:41-51

ARNOSTI C (1998) Rapid potential rates of extracellular enzymatic hydrolysis in Arctic sediments. Limnol Oceanogr 43:315-324

ARNOSTI C, JØRGENSEN BB, SAGEMANN J, THAMDRUP B (1998) Temperature dependence of microbial degradation of organic matter in marine sediments: polysaccharide hydrolysis, oxygen consumption, and sulfate reduction. Mar Ecol Prog Ser 165:59-70

AZAM F (1998) Microbial control of oceanic carbon flux: The plot thickens. Science 280:694-696

AZAM F, FENCHEL T, FIELD JG, GRAY JS, MEYER-REIL LA, THINGSTAD F (1983) The ecological role of water-column microbes in the sea. Mar Ecol Prog Ser 10:257–263

BENNER R (2002) Chemical Composition and Reactivity. In: Hansell DA, Carlson CA (eds) Biogeochemistry of Marine Dissolved Organic Matter. (Elsevier Science, Orlando)

BENNER R, PAKULSKI JD, MCCARTHY M, HEDGES JL, HATCHER PG (1992) Bulk chemical characterization of dissolved organic matter in the ocean. Science 255:1561-1564

CALDEIRA K, WICKETT ME (2003) Anthropogenic carbon and ocean pH. Nature 425:365-365

CARLSON CA (2002) Production and Removal Processes. In: Hansell DA, Carlson CA (eds) Biogeochemistry of Marine Dissolved Organic Matter. (Elsevier Science, Orlando)

CARLSON CA, DUCKLOW HW (1995) Dissolved organic-carbon in the upper ocean of the central equatorial pacific-ocean, 1992 - daily and finescale vertical variations. Deep-Sea Res Part II 42:639-656

CARLSON CA, DEL GIORGIO PA, HERNDL GJ (2007) Microbes and the dissipation of energy and respiration: from cells to ecosystems. Oceanogr 20(2):89-100

CHERRIER J, BAUER JE, DRUFFEL ERM, COFFIN RB, CHANTON JP (1999) Radiocarbon in marine bacteria: Evidence for the age of assimilated carbon. Limnol Oceanogr 44:730-736.

CHO BC, AZAM F (1988) Major role of bacteria in biogeochemical fluxes in the oceans interior. Nature 332:441-443

CHRISTIAN JR, KARL DM (1995) Bacterial ectoenzymes in marine waters: activity ratios and temperature responses in three oceanographic provinces. Limnol Oceanogr 40:1042-1049

CHRÓST RJ (1991) Environmental control of the synthesis and activity of aquatic microbial ectoenzymes. In: Chróst RJ (ed) Microbial enzymes in aquatic environments (Springer Verlag, Heidelberg)

COWIE GL, HEDGES JI (1994) Biochemical indicators of diagenetic alteration in natural organic matter mixtures. Nature 369:304-307

DEL GIORGIO PA, COLE JJ (1998) Bacterial growth efficiency in natural aquatic systems. Annu Rev Ecol Syst 29:503-541

DELONG EF, FRANKS DG, ALLDREDGE AL (1993) Phylogenetic diversity of aggregate-attached vs. free-living marine bacterial assemblages. Limnol Oceanogr 38:924-934

DIETRICH G, KALLE K, KRAUSS W, SIEDLER G (1975) Allgemeine Meereskunde (Gebrüder Bornträger, Berlin)

DRUFFEL ERM, WILLIAMS PM, BAUER JE, ERTEL JR (1992) Cycling of dissolved and particulate organic matter in the ocean. J Geophys Res 97:15639-15659

FALKOWSKI PG, BARBER RT, SMETACEK V (1998) Biogeochemical controls and feedbacks on ocean primary production. Science 281:200-206

FOWLER SW, KNAUER GA (1986) Role of large particles in the transport of elements and organic compounds through the oceanic water column. Prog. Oceanogr. 16:147–194

GIOVANNONI S, RAPPÉ M (2000) Evolution, Diversity, and Molecular Ecology of Marine Prokaryotes. In: Kirchman DL (ed) Microbial Ecology of the Ocean. (Wiley-Liss, Inc., p 47-85

GROSSART HP, TANG KW, KIORBOE T, PLOUG H (2007) Comparison of cell-specific activity between free-living and attached bacteria using isolates and natural assemblages. FEMS Microbiol Lett 266:194-200

HEDGES JI, BALDOCK JA, GELINAS Y, LEE C, PETERSON M, WAKEHAM SG (2001) Evidence for non-selective preservation of organic matter in sinking marine particles. Nature 409:801-804

HEISSENBERGER A, LEPPARD GG, HERNDL GJ (1996) Ultrastructure of marine snow .2. Microbiological considerations. Mar Ecol Prog Ser 135:299-308

HELMKE E, WEYLAND H (1991) Effect of temperature on extracellular enzymes occurring in permanently cold marine environments. Kiel Meeresforsch Sonderh 8:198-204

HOCH M, KIRCHMAN D (1993) Seasonal and interannual variability in bacterial production and biomass in a temperate estuary. Mar Ecol Prog Ser 98:283-295

HOUGHTON JT, DING Y, GRIGGS DJ, NOGUER M, VAN DER LINDEN PJ, DAI X, MASKELL K, JOHNSON CA (2001) Climate Change 2001: The Scientific Basis: Contribution of Working Group I to the Third Assessment Report of the Intergovernmental Panel of Climate Change, (Cambridge University Press)

JACKSON GA (1990) A model of the formation of marine algal flocs by physical coagulation processes. Deep-Sea Res 37:1197–1211

JIMENEZ-MERCADO A, CAJAL-MEDRANO R, MASKE H (2007) Marine heterotrophic bacteria in continuous culture, the bacterial carbon growth efficiency, and mineralization at excess substrate and different temperatures. Microb Ecol 54:56-64

KARL DM, KNAUER GA, MARTIN JH (1988) Downward flux of particulate organic-matter in the ocean - a particle decompostion paradox. Nature 332:438-441

KARNER M, HERNDL GJ (1992) Extracellular enzymatic-activity and secondary production in free-living and marine-snow-associated bacteria. Mar Biol 113:341-347

KING GM (1986) Characterization of β-glucosidase activity in intertidal marine sediments. Appl Envrionm Microbiol 51(2):373-380

KIORBOE T, JACKSON GA (2001) Marine snow, organic solute plumes, and optimal chemosensory behavior of bacteria. Limnol Oceanogr 46:1309-1318

KIRCHMAN DL (1993) Biomass and Production of Heterotrophic Bacterioplankton in the Oceanic Sub-Arctic Pacific. Deep-Sea Res Part I 40:967-988

KIRCHMAN DL, MEON B, DUCKLOW HW, CARLSON CA, HANSELL DA, STEWARD GF (2001) Glucose fluxes and concentrations of dissolved combined neutral sugars (polysaccharides) in the Ross Sea and Polar Front Zone, Antarctica. Deep-Sea Res Part II 48:4179-4197

KOLBER Z (2007) Energy Cycle in the ocean: powering the microbial world. Oceanogr 20 (2):79-88

MARTIN JH, KNAUER GA, KARL DM, BROENKOW WW (1987) VERTEX - Carbon cycling in the northeast pacific. Deep-Sea Res Part A 34:267-285

MCCAVE IN (1984) Size spectra and aggregation of suspended particles in the deep ocean. Deep-Sea Res 31:329–352

MÜNSTER U (1991) Extracellular enzyme activity in eutrophic and polyhumic lakes. In: Chróst RJ (ed) Microbial enzymes in aquatic environments (Springer Verlag, Heidelberg)

NEDWELL DB, RUTTER M (1994) Influence of temperature on growth-rate and competition between 2 psychrotolerant antarctic bacteria - low-temperature diminishes affinity for substrate uptake. Appl Environ Microbiol 60:1984-1992

PAKULSKI JD, BENNER R (1994) Abundance and distribution of carbohydrates in the ocean. LIMNOL OCEANOGR 39:930-940

PANAGIOTOPOULOS C, SEMPERE R, OBERNOSTERER I, STRIBY L, GOUTX M, VAN WAMBEKE F, GAUTIER S, LAFONT R (2002) Bacterial degradation of large particles in the southern Indian Ocean using in vitro incubation experiments. Org Geochem 33:985-1000

PARRY M, CANZIANI O, PALUTIKOF J, VAN DER LINDEN PJ, HANSON C (2007) Climate Change 2007: Impact, Adaption and Vulnerability: Contribution of Working Group II to the Fourth Assessment Report of the Intergovernmental Panel of Climate Change, (Cambridge University Press)

POMEROY LR, WIEBE WJ (2001) Temperature and substrates as interactive limiting factors for marine heterotrophic bacteria. Aquat Microb Ecol 23:187-204

POMEROY LR, LE B. WILLIAMS PJ, AZAM F, HOBBIE JE (2007) The microbial loop. Oceanogr 20 (2):28-33

RAUPACH MR, MARLAND G, CIAIS P, LE QUÉRÉ C, CANADELL JG, KLEPPNER G, FIELD CB (2007) Global and regional drivers accelerating CO_2 emissions. PNAS 104 (24):10288-10293

RAVEN J, CALDEIRA K, ELDERFIELD H, HOEGH-GULDBERG O, LISS PS, RIEBESELL U, SHEPHERD J, TURLEY C, WATSON A (2005) Ocean acidification due to increasing atmospheric carbon dioxide. The Royal Society 12:68

RIVKIN RB, ANDERSON MR, LAJZEROWICZ C (1996) Microbial processes in cold oceans .1. Relationship between temperature and bacterial growth rate. Aquat Microb Ecol 10:243-254

RIVKIN RB, LEGENDRE L (2001) Biogenic carbon cycling in the upper ocean: Effects of microbial respiration. Science 291:2398-2400

SABINE CL, FEELY RA, GRUBER N, KEY RM, LEE K, BULLISTER JL, WANNINKHOF R, WONG CS, WALLACE DWR, TILBROOK B, MILLERO FJ, PENG TH, KOZYR A, ONO T, RIOS AF (2004) The oceanic sink for anthropogenic CO2. Science 305:367-371

SHERR E, SHERR B (2000) Marine Microbes: An Overview. In: Kirchman DL (ed) Microbial Ecology of the Ocean. (Wiley-Liss, Inc., p 13-47

SHIAH FK, DUCKLOW H (1994) Temperature regulation of heterotrophic bacterioplankton abundance, production, and specific growth-rate in Chesapeake Bay. Limnol and Oceanogr 39:1416-1425

SKOOG A, BENNER R (1997) Aldoses in various size fractions of marine organic matter: Implications for carbon cycling. Limnol Oceanogr 42:1803-1813

TURNER JT (2002) Zooplankton fecal pellets, marine snow and sinking phytoplankton blooms. Aquat Microb Ecol 27:57-102

SMITH DC, SIMON M, ALLDREDGE AL, AZAM F (1992) Intense hydrolytic enzyme-activity on marine aggregates and implications for rapid particle dissolution. Nature 359:139-142

VOLK T, HOFFERT MI (1985) The Carbon Cycle and Atmospheric CO2. Natural Variations Archean to Present (Am Geophys Union, Washington DC)

WAKEHAM SG, LEE C, HEDGES JI, HERNES PJ, PETERSON ML (1997) Molecular indicators of diagenetic status in marine organic matter. Geochim Cosmochim Acta 61:5363-5369

WEISS MS, ABELE U, WECKESSER J, WELTE W, SCHLITZ E, SCHULZ GE (1991) Molecular architecture and electrostatic properties of a bacterial porin. Science 254:1627-1630

WHITMAN WB, COLEMAN DC, WIEBE WJ (1998) Prokaryotes. The unseen majority. PNAS 95:6578-6583

WIEBE WJ, SHELDON JR. WM, POMEROY LR (1993) Evidence for enhanced substrate requirement by marine mesophilic bacterial isolates at minimal growth temperatures. Microb Ecol 25:151-159

ZEEBE RE, WOLF-GLADROW D (2001) CO_2 in seawater: Equilibrium, Kinetics, Isotopes. Elsevier Oceanography Series

2. Manuscripts

2.1 List of manuscripts

This thesis includes the following manuscripts, partly submitted or already accepted for publication.

I. Judith Piontek, Nicole Händel, Gerald Langer, Julia Wohlers, Ulf Riebesell, Anja Engel

(accepted for publication in Aquatic Microbial Ecology)

Effects of rising temperature on the formation and microbial degradation of marine diatom aggregates.

Contribution of the authors: J. Piontek wrote the manuscript in cooperation with A. Engel, supported by all co-authors. The experiment was conducted by J. Piontek together with N. Händel and G. Langer.

II. Jérôme Harlay, Caroline de Bodt, Anja Engel, Sandra Jansen, Quentin d'Hoop, Judith Piontek, Nicolas van Oostende, Steve Groom, Koen Sabbe, Lei Chou

(submitted to Deep Sea Research Part I)

Abundance and size distribution of transparent exopolymer particles (TEP) in a coccolithophorid bloom in the northern Bay of Biscay (June 2006)

Contribution of the authors: The manuscript was written by J. Harlay in discussion with all co-authors. Sampling was conducted by J. Harlay, C. de Bodt, J. Piontek, Q. d'Hoop, N. van Oostende, and L. Chou.

III. Judith Piontek, Nicole Händel, Corinna Borchard, Mirko Lunau, Anja Engel

(to be submitted)

The bacterial utilization of polysaccharides derived from *Emiliania huxleyi* and the impact of ocean acidification.

Contribution of the authors: J. Piontek wrote the manuscript in cooperation with A. Engel. Experiments were conducted by J. Piontek together with N. Händel and C. Borchard. N. Händel and M. Lunau contributed to sample analyses.

IV. Judith Piontek, Mirko Lunau, Nicole Händel, Corinna Borchard, Mascha Wurst, Anja Engel

(to be submitted)

Acidification increases microbial carbohydrate degradation in the ocean.

Contribution of the authors: J. Piontek wrote the manuscript in close cooperation with A. Engel, supported by M. Lunau. Experiments were conducted by J. Piontek together with N. Händel, M. Lunau, C. Borchard, and M. Wurst.

Manuscript I

Effects of rising temperature on the formation and microbial degradation of marine diatom aggregates

Judith Piontek[1], Nicole Händel[1], Gerald Langer[1], Julia Wohlers[2], Ulf Riebesell[2], Anja Engel[1]

[1] Alfred Wegener Institute for Polar and Marine Research, Am Handelshafen 12, 27570 Bremerhaven, Germany

[2] Leibniz Institute of Marine Science, IFM-Geomar, Düsternbrooker Weg 20, 24105 Kiel, Germany

ABSTRACT: Effects of elevated temperature on the formation and subsequent degradation of diatom aggregates were studied in a laboratory experiment with a natural plankton community from the Kiel Fjord (Baltic Sea). Aggregates were derived from diatom blooms that developed in indoor mesocosms at 2.5°C and 8.5°C, corresponding to the winter *in-situ* temperature of the Western Baltic Sea of today and the sea surface temperature during winter projected for the year 2100, respectively. Formation and degradation of diatom aggregates at the same two temperatures was promoted with roller tanks in the dark over a period of 11 days. Comparison of the two temperature settings revealed an enhanced aggregation potential of diatom cells at elevated temperature, which was likely induced by an increased concentration of transparent exopolymer particles (TEP). The enhanced aggregation potential led to a significantly higher proportion of particulate organic matter in aggregates at higher temperature. Moreover, elevated temperature favoured the growth of bacteria, bacterial biomass production, and the activities of sugar- and protein-degrading extracellular enzymes in aggregates. Stimulating effects of rising temperature on growth and metabolism of the bacterial community resulted in an earlier onset of aggregate degradation and silica dissolution. Remineralization of carbon in aggregates at elevated temperature was partially compensated by formation of carbon-rich TEP during dark incubation. Hence, our results suggest that increasing temperature will affect both formation and degradation of diatom aggregates. We conclude that the vertical export of organic matter through aggregates may change in the future, depending on the magnitude, and on the vertical depth penetration of warming in the ocean.

KEY WORDS: diatom aggregates, temperature, degradation, extracellular enzymes, bacterial growth, global warming

INTRODUCTION

Phytoplankton aggregates are hotspots of bacterial activity in marine systems (Alldredge & Silver 1988, Simon 2002), and comprise a variety of biological and chemical processes on small spatial and temporal scales. The formation of macroscopic phytoplankton aggregates (i.e. marine snow) has frequently been observed during phytoplankton blooms, in particular when dominated by diatoms (Smetacek 1985, Riebesell 1991, Kiørboe et al. 1996). Aggregates are main vehicles in export of organic matter from the surface ocean, and drive the sequestration of particulate organic carbon (POC) to the deep sea (Fowler & Knauer 1986, Asper 1987). The efficiency of aggregate export is controlled by a number of factors, of which the rate of aggregate formation, aggregate size, sinking velocity, and bacterial degradation activity are the most important ones. Aggregation and degradation of organic matter were separately shown to be sensitive to changing temperature. Thornton and Thake (1998) demonstrated that the formation of aggregates from nitrate-limited continuous cultures of *Skeletonema costatum* was positively correlated to temperature. The rate of bacterial aggregate degradation depends primarily on growth and metabolic activity of the associated bacterial community, and on the quality of aggregated organic matter. It has been proposed that temperature represents a principally limiting or supporting factor for microbial processes (Pomeroy & Wiebe 2001). Growth of isolated marine bacterial strains, for example, followed the Arrhenius law over a broad range of temperature (Wiebe et al. 1992, Pomeroy & Wiebe 2001). Cell-specific growth rates in natural bacterial populations were more than doubled, when temperature was increased from 10°C to 26°C. Moreover, the cell-specific respiratory CO_2-production increased within the same range of temperature by a factor of approx. 4.7 (Jiménez-Mercardo et al. 2007). Bacterial growth requires suitable organic substrates, provided by the degradation of organic matter. The initial step in organic matter degradation is the hydrolysis of high-molecular-weight compounds by

bacterial extracellular enzymes (Hoppe et al. 1993, Arnosti 2004). Enzymatically catalyzed reactions are known to show an optimum curve to temperature. Increasing temperature accelerates enzymatic reactions as long as rising temperature does not cause damage or denaturisation of proteins. For instance, Rath and Herndl (1994) showed that the activity of β-glucosidase extracted from marine snow increased until a temperature optimum of about 40°C was reached, and decreased strongly at 50°C. In their study, thermostability of β-glucosidase was improved if enzymes were associated with marine snow.

Temperature effects on the cycling of organic matter in the ocean, and the underlying mechanisms are of interest to better predict consequences of global warming for the future ocean. Since effects of rising temperature on phytoplankton aggregates can hardly be estimated by investigating single processes, we conducted an encompassing experiment that integrated temperature effects on growth and aggregation of phytoplankton cells, and on the bacterial degradation of aggregates. Winter/spring blooms occurring in the Kiel Fjord (Western Baltic Sea) were used as a suitable model system. For the Baltic Sea region, an increase in winter sea surface temperature of up to 10°C is predicted until the year 2100 (IPCC 2001). Here, we report temperature effects on the formation, biogeochemical properties, and microbial degradation of aggregates derived from natural diatom communities that were grown at present-day and at elevated temperature (+6°C).

MATERIAL AND METHODS

Experimental set-up. The experiment was conducted in the frame of the AQUASHIFT indoor mesocosm study 2006 that investigated the impact of temperature changes on the biology and biogeochemistry during winter/spring phytoplankton blooms. The general set-up of the AQUASHIFT mesocosms is described in more detail in Sommer et al. (2007).

Briefly, a natural phytoplankton community was collected from the Western Baltic Sea (Kiel Fjord) and incubated in 8 mesocosms in 4 temperature-controlled walk-in rooms. Temperatures of 2.5°C, 4.5°C, 6.5°C and 8.5°C were applied to duplicate mesocosms with a volume of 1400 litres each. Calculated from the decadal mean between 1993 and 2002, 2.5°C were chosen as *in-situ* temperature in the Kiel Fjord during winter and early spring (Sommer et al. 2007). A 12/12 hours light/dark cycle was applied. The light regime simulated the daily course of light intensities based on season-dependent database values derived from a model using astronomic formulae (Brock 1981). The maximum light intensity was 179 µmol photons m^{-2} s^{-1}. After addition of 13 µmol l^{-1} nitrate, an initial nitrate concentration of 21 µmol l^{-1} was achieved in all mesocosms. Initial phosphate concentration was 0.9 µmol l^{-1} in all mesocosms. Hence, inorganic nutrients yielded a N:P ratio of 23.3 in all mesocosms, indicating a phosphate deficiency relative to the Redfield Ratio (Redfield et al. 1963).

For the purpose of this study, aggregates were formed experimentally from particulate matter produced in the duplicate mesocosms at 2.5°C (*in-situ* temperature) and at 8.5°C. Aggregation and sedimentation of diatoms in the ocean mainly occurs after the peak of blooms (Smetacek 1985, Riebesell 1991, Kiørboe et al. 1996). Therefore, material for the aggregation experiment was collected from the mesocosms four days after the bloom peak, defined as the maximum concentration of chlorophyll *a*. The peak of the bloom in the mesocosms at 8.5°C occurred six days earlier than at 2.5°C (Wohlers et al., in prep.). The aggregation experiment was therefore conducted with a time shift of six days between the two temperature treatments.

In order to harvest sinking particulate matter, including phytoplankton cells and detrital material, organic matter that had sedimented from the water column was drawn from the bottom of the mesocosms by the use of a peristaltic pump. For each mesocosm, the

collected material was diluted with mesocosm water to obtain similar particle volumes for all incubations. The suspensions were carefully mixed and transferred into roller tanks. Organic matter of duplicate mesocosms per temperature was incubated separately. A series of five roller tanks per mesocosm was prepared, thus yielding a total of 20 tanks in four incubation series. Mean values and standard deviations presented in this study are derived from these duplicates per temperature treatment. Each roller tank had a diameter of 23 cm, and contained a volume of 5 litres. In order to promote aggregation, all tanks were placed on roller tables and were rotated with 0.5 rpm in the dark at temperatures of 2.5°C and 8.5°C, respectively (Fig. 1).

Sampling. Sampling of each incubation series was performed at t_0 and after 60, 108, 156, 204, and 252 hours. Macroscopic aggregates (>2 mm) and seawater with dispersed particulate organic matter (POM) were sampled separately after removing roller tanks from the roller table and allowing settling of aggregates to the bottom of the tank. All aggregates were then isolated with a serological pipette and pooled to an aggregate slurry. The volume of the aggregate slurry that contained all macroscopic aggregates of the roller tank was determined using a 500 ml graduated cylinder. After all aggregates were removed, the seawater surrounding the aggregates (SSW) was sampled, and its volume determined with a 1000 ml graduated cylinder. It was assumed that aggregates comprised only a relatively small fraction of the total slurry volume due to the simultaneous uptake of SSW during manual aggregate isolation. In order to calculate the amounts of particulate components in the aggregate fraction, amounts of particulate components in the SSW were subtracted from those in the slurry according to Engel et al. (2002). Hence, the proportions of particle volume (PV), particulate organic carbon (POC), nitrogen (PON) and phosporous (POP),

transparent exopolymer particles (TEP), and chlorophyll *a* (Chl *a*) were calculated as follows:

$$AGG = v(sl)*c_x(sl) - v(sl)*c_x(SSW) \quad (1)$$

where $v(sl)$ is the slurry volume, $c_x(sl)$ is the concentration of parameter x in the slurry and $c_x(SSW)$ is the concentration of parameter x in the SSW. PV and amounts of POC, PON, POP, TEP, and Chl *a* were normalized to 1 l of tank volume.

Biogeochemical analyses. The aggregate slurry and the SSW were analyzed separately. In order to produce a homogeneous suspension for subsampling, aggregate slurries were diluted in a ratio of 1:50 with 0.2 µm-filtered and autoclaved seawater, and agitated gently. For measurements of POC, PON, and POP duplicate samples of 20 ml diluted aggregate slurry and 250 ml of SSW were filtered onto precombusted GF/F-filters (Whatman), and stored at -20°C until further processing. Prior to analysis, filters were dried for 12 hours at 80°C. POC and PON were measured on a CHN-analyser (Carlo Erba NA-1500). For the analysis of POP, samples were digested with peroxy sulfate at 120°C for 30 minutes. After digestion, POP was measured as dissolved ortho-phosphate according to Koroleff (1977).

For the analysis of TEP, triplicate samples of 5-10 ml aggregate slurry and 25 ml SSW were filtered onto 0.4 µm-polycarbonate filters and stained with Alcian Blue, a cationic copper phthalocyanine dye that complexes carboxyl and half-ester sulphate reactive groups of acidic polysaccharides. Samples were stored frozen at -20°C until analysis. TEP concentrations were measured photometrically (λ = 787 nm) and expressed in xanthan equivalents per litre [Xeq. l^{-1}] (Passow & Alldredge 1995). A factor of 0.75 was assumed to convert TEP (µg Xeq.) into carbon units (TEP-C, µg C) (Engel & Passow 2001).

Samples for determination of Chl *a* were filtered onto GF/F-filters (Whatman) and stored at -20°C in the dark. Prior to analysis, filters were homogenized with an ultrasonic mixer and

pigments were extracted with 80% acetone (Strickland & Parsons 1974). Chl *a* concentration was determined by the use of a fluorometer (excitation: 480 nm, emission: 685 nm) and corrected for phaeopigments by measuring the fluorescence before and after acidification of samples with 1 N hydrochloric acid.

A Beckmann Coulter Counter (Multisizer II) equipped with a 100 µm aperture was used to determine PV of aggregates and SSW. The volume of particles between 2.8 µm and 60 µm equivalent spherical diameter was determined and summed up to PV. Prior to analysis, aggregates were broken down so efficiently that all particles were small enough to pass the aperture and their volume was subsequently detected. This was confirmed by particle size spectra of broken aggregates provided by the Coulter Counter measurements, which revealed that more than 90% of the detected particle volume was derived from particles smaller than 40 µm. Analysis was done in triplicate, each with 2 ml of sample.

Dissolved silicate (dSi) was determined in undiluted SSW according to the method of Koroleff (1977) by the use of an autoanalyzer. Ammonium molybdate reacts with dSi in seawater, generating a blue molybdate-complex. After reduction with oxalic acid, concentration can be measured photometrically.

Microbiological analyses. All microbiological analyses were performed for aggregate slurries and SSW, respectively. Rates and bacterial cell numbers were normalized to 1 ml of aggregates and SSW, respectively. For enumeration of bacteria, samples were filtered onto black 0.2 µm-polycarbonate filters (Whatman) and stained with 4'6'diamidino-2-phenolindole (DAPI) (Porter & Feig 1980). Samples were stored at -20°C. Cells were counted using an epifluorescence microscope (Axioplan, Zeiss) at 1000 fold magnification within 4 weeks after sampling. At least 1000 cells per sample were counted for statistical evaluation.

Bacterial biomass production (BBP) was determined by incorporation of ^{3}[H]-thymidine (Fuhrman & Azam 1982). Samples of 5-10 ml diluted aggregate slurry were incubated in triplicate with a saturating final concentration of 10 nM ^{3}[H]-thymidine. Samples were incubated for 90 minutes in the dark at 2.5°C and 8.5°C, respectively. After incubation, samples were poisoned with 2% formalin (final concentration) to stop growth and filtered onto 0.2 µm-polycarbonate filters (Sartorius). Filters were rinsed with ice-cold 5% trichloracetic acid and radio-assayed by liquid scintillation counting. For calculation of BBP from thymidine incorporation, a conversion factor of 2 x 10^{18} cells mol^{-1} thymidine and a carbon conversion factor of 0.3 x 10^{-6} µg C $µm^{-3}$ cell were applied (Ducklow & Carlson 1992). A mean cell volume of 0.03 $µm^3$ $cell^{-1}$ was assumed. The cumulative BBP represents the overall BBP during the 252 hours of incubation as calculated from the measured rates and the incubation time.

The activity of bacterial extracellular enzymes was measured in the diluted aggregate slurries and the SSW using fluorogenic substrate analogues (Hoppe 1983). The reaction velocities of α- and β-glucosidase, leucine-aminopeptidase, and alkaline phosphatase were determined by the use of 4-methylumbelliferyl-α-glucopyranoside, 4-methylumbelliferyl-β-glucopyranoside, L-leucine-4-methyl-7-coumarinylamide, and 4-methylumbelliferyl-phosphate, respectively. Fluorogenic substrate analogues were added to subsamples of 200 µl volume to final concentrations ranging from 0.2 µM to 1000 µmol l^{-1}. Samples were incubated in duplicate for 3 hours in the dark at 2.5°C and 8.5°C, respectively. Fluorescence was measured with a microtiter plate fluorometer (Fluoroskan Ascent, Thermo Labsystems; excitation: 355 nm, emission: 460 nm).

The velocity (V) of enzymatic hydrolysis followed Michaelis-Menten kinetics in all samples. Hence, data were fitted according to

$$V = \frac{V_{max}[S]}{K_m + [S]} \quad (2)$$

using the software SigmaPlot 9.0. Here, S is the substrate concentration [µmol l^{-1}], V_{max} is the maximum velocity of enzyme reaction (=maximum hydrolysis rate) [µmol l^{-1} h^{-1}], which is attained at saturating substrate concentration, and K_m [µmol l^{-1}] is the Michaelis constant. The Michaelis-Menten kinetic describes the single-substrate mechanism for an enzyme reaction:

$$[E] + [S] \underset{k_{-1}}{\overset{k_1}{\rightleftharpoons}} [ES] \xrightarrow{k_2} [E] + [P] \quad (3)$$

where E is the enzyme, ES the enzyme-substrate complex, P the product of the enzymatic reaction, and $k_{1, -1, 2}$ the rate constants of the individual steps. As V_{max} evaluates the catalytic step of enzymatic substrate degradation at saturating substrate concentration, it is defined by

$$V_{max} = k_2[E] \quad (4)$$

The strength of binding between enzyme and substrate molecule is given by K_m, an inverse measure of the enzyme affinity:

$$K_m = \frac{k_{-1} + k_2}{k_1} \quad (5)$$

In order to characterize the enzymatic degradation of a substrate, it is useful to apply a parameter including both, the catalytic and the substrate binding step. This is especially reasonable when dealing with a complex natural system that contains unknown concentrations of enzymes and substrates. The ratio V_{max}/K_m describes the efficiency of enzymatic substrate degradation as a function of the affinity, the catalytic capacity and the concentration of the enzyme:

$$\frac{V_{max}}{K_m} = \frac{k_1}{k_{-1} + k_2} \cdot k_2 \cdot [E] \quad (6)$$

The ratio of V_{max}/K_m is helpful to assess the enzymatic degradation of substrates at low, non-saturating concentrations.

For comparison of enzymatic activities at 2.5°C and 8.5°C an enhancement factor (I) was calculated as follows

$$I = \frac{x(8.5°C)}{x(2.5°C)} \quad (7)$$

where x is the mean value over incubation time of V_{max}, V_{max}/K_m, and cell-specific V_{max}, respectively, in aggregates and in SSW at 8.5°C and 2.5°C.

RESULTS

Bloom development in the mesocosms

In all mesocosms, the build-up and decline of phytoplankton blooms dominated by diatoms were observed. After 3 to 7 days, Chl *a* started to increase exponentially in the mesocosms at 8.5°C (elevated temperature) and 2.5°C (*in-situ* temperature). Algal growth resulted in a drawdown of nitrate and phosphate in all mesocosms. Maximum Chl *a* concentration was reached between day 11 and 19 and did not reveal significant differences between the two temperatures. After the peak, Chl *a* decreased rapidly and sedimentation of particles to the bottom of the mesocosms was observed. When organic matter was collected from the mesocosms for dark incubations in roller tanks, phosphate and nitrate were depleted in all mesocosms. The stoichiometry of suspended POM at 8.5°C and 2.5°C revealed ratios of [PON]:[POP] higher than the Redfield Ratio, indicating that algal growth was limited by phosphate-deficiency at both temperatures (Tab. 1). A detailed description of the bloom development will be presented elsewhere (Wohlers et al., in prep.).

Formation of aggregates

Total particle volume (PV) in roller tanks initially was similar between the temperature treatments yielding 43 ± 8 µl l^{-1} at 8.5°C and 33 ± 4 µl l^{-1} at 2.5°C (Fig. 2). . During the first 60 hours of incubation, aggregates formed in roller tanks at both temperatures, reaching a maximum size of approx. 5 mm in diameter. Aggregates comprised diatom species mainly of the genera *Skeletonema* and *Chaetoceros*. After 60 hours the molar ratio of Chl *a* : PON in aggregates was 2.1 ± 0.7 at 8.5°C and 3.6 ± 1.3 at 2.5°C. The proportions of total POM (=AGG + SSW) included in aggregates were significantly higher at 8.5°C than at 2.5°C ($p < 0.001$) during the whole experiment. Aggregates at 8.5°C contained between 93 and 96% of total PV, while aggregates at 2.5°C included between 48 and 61% of total PV (Fig. 2). Between 81 and 96% of total POC, PON, and POP was contained in aggregates at 8.5°C, while aggregates at 2.5°C included between 43 and 69% (Fig. 3, Tab. 2). TEP concentration in aggregates and SSW at 8.5°C was significantly higher than at 2.5°C ($p < 0.01$) (Fig. 4). At both temperatures, TEP concentration increased during dark incubation in the roller tanks. Concentration of total TEP started to increase after 156 hours to values of up to 10.5 ± 1.9 mg Xeq. l^{-1} at 8.5°C and 2.6 ± 0.6 mg Xeq. l^{-1} at 2.5°C. Thereby, the main proportion of total TEP was determined in the SSW at both temperatures. TEP concentration in aggregates increased only slightly during incubation (Fig. 4). Ratios of TEP : PV were significantly higher in aggregates at 8.5°C than at 2.5°C ($p < 0.001$). The mean ratio of TEP : PV over incubation time was 117 ± 41 µg Xeq. $µl^{-1}$ in aggregates at 8.5°C and 37.0 ± 19.1 µg Xeq. $µl^{-1}$ in aggregates at 2.5°C (Fig. 2, 4). TEP in aggregates comprised a carbon amount of up to 0.3 ± 0.06 mmol TEP-C l^{-1} at 8.5°C and 0.09 ± 0.04 mmol TEP-C l^{-1} at 2.5°C.

Microbial growth

The abundance of aggregate-associated bacteria after 60 hours of incubation was 1.8 x 10^8 ± 3.1 x 10^7 cells (ml AGG)$^{-1}$ at 8.5°C and 2.0 x 10^8 ± 5.8 x 10^7 cells (ml AGG)$^{-1}$ at 2.5°C. At the same timepoint, the bacterial abundance in SSW was one order of magnitude lower with 1.9 x 10^7 ± 0.8 x 10^7 cells (ml SSW)$^{-1}$ at 8.5°C and 0.8 x 10^7 ± 0.2 x 10^7 cells (ml SSW)$^{-1}$ at 2.5°C (Fig. 5). Bacteria showed exponential growth with μ = 0.007 ± 0.001 h^{-1} in aggregates at 8.5°C, and μ = 0.006 ± 0.003 h^{-1} in SSW at 8.5°C. In contrast, at 2.5°C bacterial cell abundance in aggregates and SSW did not increase until the end of incubation time (Fig. 5).

Cumulatively calculated BBP in aggregates was 0.72 ± 0.06 µmol carbon (ml AGG)$^{-1}$ and 0.09 ± 0.002 µmol carbon (ml AGG)$^{-1}$ at 8.5°C and 2.5°C, respectively. POC-specific BBP in aggregates at 8.5°C was about one order of magnitude higher than at 2.5°C ($p < 0.01$) (Fig. 6).

Activity of extracellular enzymes

In general, maximum hydrolysis rates (V_{max}) of alkaline phosphatase and leucine-aminopeptidase were significantly higher than those of α- and β-glucosidase in aggregates and SSW at both temperatures ($p < 0.001$) (Tab. 3, 4). Temperature effects on V_{max} were observed for sugar- and protein-degrading extracellular enzymes, where V_{max} in aggregates and SSW was higher at 8.5°C than at 2.5°C (Tab. 3, 4, Fig. 7). The differences between V_{max} at 8.5°C and at 2.5°C were significant for β-glucosidase and leucine-aminopeptidase in aggregates, and for α-glucosidase, β-glucosidase and leucine-aminopeptidase in SSW ($p < 0.05$) (Tab. 3, 4). The factor I_{Vmax} was calculated according to eq. (7) in order to compare the different tested extracellular enzymes with regard to the temperature-induced enhancement of V_{max}. A higher value of I_{Vmax} reveals that increased temperature had a

stronger impact on V_{max} of protein-degrading leucine-aminopeptidase than on V_{max} of polysaccharide-degrading α-glucosidase, β-glucosidase, and alkaline phosphatase. The temporal development of V_{max} in aggregates differed between the temperature treatments. V_{max} of β-glucosidase, leucine-aminopeptidase, and alkaline phosphatase decreased over time in aggregates at 8.5°C, but increased in aggregates at 2.5°C (Fig. 7).

A significantly higher ratio of V_{max}/K_m indicated an enhanced activity of α-glucosidase, β-glucosidase, and leucine-aminopeptidase at non-saturating substrate concentration in aggregates and SSW at 8.5°C compared to 2.5°C ($p < 0.05$) (Tab. 3, 4). This suggests an increased degradation efficiency of polysaccharides and proteins at higher temperature, even when substrate availability is low. $I_{Vmax/Km}$ was calculated according to eq. (7) to compare the temperature effects on the efficiency of the different tested extracellular enzymes. As indicated by highest $I_{Vmax/Km}$ for β-glucosidase in aggregates, increased temperature had the strongest impact on the degradation efficiency of β-glycosidic linked polysaccharides in aggregates (Tab. 3, 4).

The cell-specific V_{max} of aggregate-associated bacteria was higher than those of bacteria in SSW for all tested extracellular enzymes and at both temperatures (Tab. 5) ($p < 0.05$). $I_{cell\text{-}spec\ Vmax}$ reveals that cell-specific V_{max} of leucine-aminopeptidase in aggregates and SSW was significantly higher at 8.5°C than at 2.5°C ($p < 0.05$).

Organic matter turnover in aggregates

Aggregates at 2.5°C did not show a net loss of PV and POM at the end of incubation time. In contrast, PV (Fig. 2), POC (Fig. 3), PON, and POP (Tab. 2) decreased in aggregates at 8.5°C until the end of incubation. Aggregates at 8.5°C contained a PV of 49.0 ± 1.2 µl l^{-1} after 60 hours of incubation. PV decreased to 27.4 ± 0.6 µl l^{-1} within the next 48 hours,

equivalent to a net loss of 40 ± 4%. POC in aggregates at 8.5°C was 1.4 ± 0.2 mmol l^{-1} after aggregate formation (t = 60 hours) and decreased by 21 ± 10% until the end of incubation (Fig. 3). PON and POP in aggregates at 8.5°C were reduced by 5 ± 1% and 17 ± 1%, respectively, over the course of incubation (Tab. 2).

The molar ratios of [POC]:[PON], [POC]:[POP], and [PON]:[POP] in aggregates at 8.5°C and 2.5°C did not show a consistent trend over time. At both temperatures, ratios were clearly higher than predicted by the Redfield Ratio (Tab. 6). Ratios of [PON]:[POP] were not significantly different between the temperature treatments. In contrast, significantly lower ratios of [POC]:[PON] and [POC]:[POP] were obtained at 8.5°C than at 2.5°C ($p < 0.05$) due to higher amounts of PON and POP (Tab. 1, 2, 6). The initial concentration of dSi in SSW was below the detection limit at both temperatures. After 108 hours of incubation at 8.5°C, dSi started to increase up to a final value of 10.3 ± 1.0 µmol l^{-1}. In contrast, dSi in SSW at 2.5°C did not increase significantly until the end of incubation (Fig. 8).

DISCUSSION

The experiment was set-up to assess the effects of increasing temperature on the formation, biogeochemical properties, and degradation of diatom aggregates. Two temperature treatments were applied during bloom development, aggregation of cells, and subsequent degradation of aggregates.

Temperature effects on the formation and biogeochemical composition of aggregates

In the present study, higher temperature clearly increased the proportion of PV (Fig. 2), POC (Fig. 3), PON, and POP contained in aggregates (Tab. 2). Thus, aggregates played a larger role in the overall turnover of organic matter at elevated temperature. In the ocean,

larger proportions of POC, PON, and POP in aggregates represent a more efficient allocation of organic matter for potential export via fast particle sinking.

Because we did not investigate the aggregation process directly, we can only speculate about the potential mechanisms that were responsible for enhanced aggregate formation at higher temperature. The initial PV at elevated and *in-situ* temperature was not significantly different, so that similar collision rates between particles can be assumed for both treatments. Instead, higher TEP : PV ratios likely enhanced aggregation at elevated temperature (Fig. 2, 4), since TEP have been identified to promote aggregation by increasing the stickiness of particles (Alldredge et al. 1993, Passow et al. 1994, Engel 2000).

Transparent exopolymer particles (TEP)

TEP contain primarily polysaccharides, and are therefore carbon-rich and poor in nitrogen. The formation of TEP from dissolved sugars is an important process to convert dissolved into particulate organic carbon (Engel et al. 2004). The organic matter used in the present study contained high amounts of TEP (Fig. 4), which was related to exudation by diatoms suffering from nutrient depletion in the mesocosms (Wohlers et al., in prep.). A further increase in TEP concentration was observed during dark incubation, being significantly higher at elevated temperature than at *in-situ* temperature (Fig. 4). It seems likely that high abundance of bacteria had a substantial effect on the formation of TEP from precursors, originating from phytoplankton exudation. Bacterial degradation activity increases the proportion of deoxy sugars in extracellular polysaccharides (EPS), enhancing the hydrophobic feature of EPS and the formation of TEP (Giroldo et al. 2003). Bacteria also produce considerable amounts of exopolymers, in particular when attached to surfaces (Decho 1990). The formation of an exopolymer capsule enables marine bacteria to attach to

surfaces (Heissenberger et al. 1996). TEP can be generated by releasing polysaccharide fibrils from the capsular material. However, this process was of minor importance in our experiment. A cell-specific TEP production of 0.1 fg Xeq. $cell^{-1}$ h^{-1} was determined for coastal North Sea bacterioplankton (Stoderegger & Herndl 1999). Assuming this rate, only 0.8% and 3.6% of TEP production in aggregates at *in-situ* and elevated temperature, respectively, could be related to bacterial production.

Temperature sensitivity of bacterial growth and degradation activity

Aggregates harbour diverse and large bacterial communities, since they provide a beneficial substrate supply for bacterial growth. In accordance with previous studies (Alldredge et al. 1986, Herndl 1988, Ploug & Grossart 2000, Karner & Herndl 1992, Grossart et al. 2003), we observed an enrichment of bacteria in aggregates (Fig. 5), as well as increased cell-specific enzymatic rates of aggregate-associated bacteria (Tab. 5). It has been suggested that the acceleration of metabolic rates after attachment allows bacteria maximum benefit from substrate-replete aggregate surfaces (Grossart et al. 2007).

In the present study, rising temperature substantially increased rates of bacterial growth and degradation activity, on aggregates as well as in the SSW (Fig. 5 - 7, Tab. 3 - 5). Temperature effects on bacterial extracellular enzymes were strong enough to increase the loss of POM from aggregates, accelerating the turnover of aggregates at elevated temperature (Fig. 2, 3, Tab. 2). Extracellular enzymes are produced by bacteria to hydrolyze polymers into subunits, which can then be taken up by the cell. Their hydrolytic activity drives the solubilization of particles and is therefore crucial for the degradation of aggregates (Smith et al. 1992). Temperature effects on extracellular enzymes integrated two aspects:

(1) Rising temperature enhanced the enzymatic degradation of organic matter thermodynamically by an increase of the rate constants k_1 and k_2 given in equation (3).

(2) Aggregates at elevated temperature showed higher abundances of bacteria and therefore higher production of extracellular enzymes (Fig. 5). Starting with similar bacterial abundances at both temperatures, only aggregates and SSW at elevated temperature provided conditions beneficial for bacterial growth (Fig. 5, 6). Thus, higher enzymatic activities in aggregates at elevated temperature were supported by an increased enzyme production of a larger bacterial community.

Cell-specific rates of extracellular enzyme activity (cell-specific V_{max}) allow for a differentiation between these two aspects, since they exclude effects due to temperature-related differences in bacterial abundance. Significant differences in cell-specific V_{max} of leucine-aminopeptidase between the two temperatures indicated that temperature effects on the catalytic step of the enzymatic reaction were decisive for the increased rate of enzymatic protein hydrolysis. In contrast, cell-specific V_{max} of α- glucosidase and β-glucosidase did not reveal significant differences between the two treatments, suggesting increased enzymatic degradation of polysaccharides at elevated temperature to be primarily promoted by a larger bacterial community.

Tested extracellular enzymes revealed different sensitivities to rising temperature, leading to differences in activity ratios of polysaccharide-, protein-, and organic phosphate-degrading enzymes between the two temperatures (Tab. 3, 4, 5). However, we did not determine an effect of different activity ratios on the stoichiometry of POM. Nevertheless, different temperature sensitivities of extracellular enzymes may have changed the biochemical composition of labile organic matter in aggregates and SSW, which is highly relevant for bacterial growth, but accounts only for a minor proportion of total organic

matter. Different control mechanisms of enzyme expression further complicate the projection of degradation rates of bulk organic carbon, nitrogen, and phosphate from the magnitude of enzymatic activity. Extracellular glucosidase activity is repressed by high concentrations of the monomeric end products and therefore regulated by ambient substrate concentrations (Chróst 1991). In contrast, leucine-aminopeptidase was shown to be repressed only by specific amino acids known to be rare in seawater, e.g. histidine and phenylalanine. High protease activity at low concentration of labile substrates was found in a previous study (Christian & Karl 1998). It is assumed that a constitutively high leucine-aminopeptidase activity ensures an efficient supply with nitrogenous substrates, which are often limiting bacterial growth (Christian & Karl 1998).

The activity of extracellular enzymes in aggregates showed different temporal trends at the two temperatures. Continuously increasing enzymatic rates in aggregates at *in-situ* temperature suggest a sufficient substrate supply to bacteria until the end of incubation, supporting the assumption that aggregate degradation was temporally impeded due to lower temperature and not due to substrate limitation. Enzymatic rates in aggregates at elevated temperature decreased with time, coinciding with an exponential increase in cell numbers (Fig. 5, 7). A similar coincidence of increasing bacterial cell density and decreasing metabolic rates in aggregates was observed for glucose and leucine uptake (Azúa et al. 2007). Decreasing uptake rates were suggested to indicate a quantitative and qualitative impoverishment of organic matter in aggregates with time, an explanation that seems to be reasonable also for temporally decreasing enzymatic activity in aggregates at elevated temperature.

Degradation of particulate matter in aggregates

The flux of organic matter in aggregates and the related particle concentration both decrease continuously with depth (Martin et al. 1987, Kiørboe 2001). In the present study, aggregates at elevated temperature showed a net loss of PV (Fig. 2), POC (Fig. 3), PON, and POP (Tab. 2) during the incubation, while no net loss of PV and POM was determined from aggregates at *in-situ* temperature (Fig. 2, 3, Tab. 2). Duration of the experiment was restricted to 11 days. Eight days remained after the formation of aggregates. Thus, experimental results reflect an early phase of degradation. Increased temperature clearly enhanced the remineralization of aggregates during this early phase. As no net loss occurred from aggregates at *in-situ* temperature, acceleration of remineralization cannot be expressed in terms of a temperature-normalized factor. It must be assumed that degradation of aggregated POM at *in-situ* temperature occurs on longer time scales. Hence, our results indicate a temporal lag of at least eight days between aggregate formation and degradation at *in-situ* temperature but an immediate onset of aggregate degradation at elevated temperature. This finding is in good accordance with results from the AQUASHIFT mesocosm study 2005, where a diminished temporal lag between the peaks of primary production and bacterial production also suggested an earlier start of organic matter degradation at elevated temperature (Hoppe et al. 2008). Considering that degradation of aggregates in the ocean coincides with sinking, a significantly earlier onset of aggregate degradation at elevated temperature would lead to an enhanced remineralization of aggregated POM especially in the upper ocean.

Aggregates at elevated temperature showed a discrepancy between the net loss of POM and the net loss of PV. PV was reduced stronger than POM until the end of incubation and revealed a much lower variability between parallels (Fig. 2, 3). It should be noted that particles not detectable by the Coulter Counter, e.g. hydrated gels and particles smaller than

2.7 µm, contributed to a significant extent to the pool of POM. TEP are not quantified by the Coulter Counter, but contain organic carbon. Aggregates at elevated temperature included a TEP amount up to 5.2 mg Xeq. l^{-1} (Fig. 4). TEP can be considered as an integral part of aggregates due to the function as glue. It was therefore estimated that up to 0.3 mmol TEP-C l^{-1} were included in aggregates at elevated temperature. Thus, the carbon loss from aggregates at elevated temperature (Fig. 3) was partially compensated by new production of TEP-C (Fig. 4).

Concentration ratios of [POC]:[PON], [POC]:[POP], and [PON]:[POP] in aggregates did not reveal consistent temporal trends at both temperatures. The ratios of [POC]:[PON] and [POC]:[POP] were significantly lower in aggregates at elevated temperature due to stoichiometric differences in the sedimented organic matter collected from the mesocosms (Tab. 1, 2, 6). A positive relationship between degradation rates and the nitrogen and phosphate content of organic matter was found, when data across a broad spectrum of detritus, from unicellular algae to terrestrial macrophytes, were included in the statistical analysis. Conversely, this general relationship was not confirmed for the degradation of several distinct sorts of detritus, including debris derived from phytoplankton (Enríquez et al. 1993 and references within). It seems unlikely, that the lack of aggregate remineralization at *in-situ* temperature was due to an unsuitable stoichiometry and quality of POM in our experiment. Initial Chl *a* : PON ratios of aggregates at the two temperatures indicated a similar freshness of algal cells. We therefore assume that sufficient amounts of labile organic matter were available for bacteria at both temperatures. Hence, increased temperature can be regarded as the leading factor for an accelerated degradation at higher temperature in this short-term incubation. However, potential effects of POM stoichiometry on the degradation of aggregates on time scales exceeding the incubation period of our experiment cannot be excluded.

Decomposition of diatom cells is tightly coupled to the dissolution of silica from diatom frustules (Ragueneau et al. 2006). Concentration of dSi in the SSW at elevated temperature increased by 10 µmol l^{-1} during the last six days of incubation (Fig. 8). Increasing concentration indicated dissolution of biogenic silica (bSi). In contrast, no increase was determined at *in-situ* temperature, indicating that no dissolution of bSi occurred (Fig. 8). Chemical dissolution of bSi can start after microbial degradation of the organic layer associated with the diatom surface (Bidle & Azam 2001). It can therefore be assumed that lower abundance of bacteria (Fig. 5) and lower protease activity (Tab. 3, 4, Fig. 7) at *in-situ* temperature were not sufficient to remove the protecting outer organic layer associated with diatom frustules. The incubated natural diatom community consisted mainly of *Chaetoceros spp.* and *Skeletonema spp.* for which a Si:C ratio of about 0.1 can be assumed (Brzezinski 1985). Assuming that all POC was derived from diatoms, a concentration of approx. 14 µmol bSi l^{-1} can be estimated for the SSW at elevated temperature. Hence, dissolution of bSi from diatoms dispersed in the SSW could explain the increase in concentration quantitatively. However, following the linear initial rate approach (Greenwood et al. 2001), a bSi dissolution rate of 0.12 d^{-1} was obtained for POM at 8.5°C. This rate is three times higher than previously found in studies that were conducted at 5°C or 10°C higher temperature (Bidle & Azam 2001, Moriceau et al. 2007). It seems therefore likely that the increasing silicate concentration in the SSW at elevated temperature was substantially influenced by bSi dissolution from aggregates. Aggregates leak solutes containing high concentration of dissolved compounds (Smith et al. 1992, Kiørboe 2001). Previous studies revealed an acceleration of silica dissolution from dispersed diatoms with increasing temperature (Lewin 1961, Kamatani 1982). Results of the present study indicate a temperature-induced acceleration of bSi dissolution also from diatom aggregates.

Application of experimental results to larger scale - implications for the future ocean

Extrapolating the results of this study to natural systems bears large uncertainties. Nevertheless, manipulative laboratory experiments are a valuable tool to assess potential consequences of global change, such as ocean warming and acidification, for natural systems. Formation of large particle aggregates, and the rates of their decomposition by heterotrophic bacteria are important processes to determine the efficiency of particle export in the ocean (Fowler & Knauer 1986, Kiørboe et al. 1996, Smith et al. 1992). Our experimental results indicate that elevated temperature increases both the probability of aggregate formation and the rate of bacterial degradation of aggregated organic matter. Effects of elevated temperature on export efficiencies in the future ocean will likely depend on the relative magnitude of increased aggregation versus enhanced bacterial degradation. It is important to consider that aggregation and degradation processes in the ocean are often vertically separated. While high particle abundances required for the aggregation of POM are mostly achieved in the surface layer, bacterial degradation of sinking aggregates continues in the subsurface strata. In shallow coastal areas like the Kiel Fjord, where the surface temperature extends to the bottom, climate warming will most probably involve the whole water column. Here, temperature-enhanced organic matter degradation and the resulting acceleration of organic carbon turnover are likely to be the dominant effects of warming. In deep water bodies, the temperature increase at the surface may be disproportionately high compared to subsurface strata. Here, the enhancement of aggregate formation may predominate and increase the export of carbon, since sinking of aggregates to cooler depths may mitigate effects of ocean warming on bacterial degradation. Other factors such as phytoplankton growth, light, and nutrient availability will further affect the timing of formation and bacterial colonization of aggregates, and therewith co-determine the export efficiencies of aggregates. We therefore suppose that *in-situ* effects of warming

on the formation and degradation of phytoplankton aggregates in the ocean are of higher complexity, depending on the depth penetration of increasing ocean temperature as well as on the timing of biological processes.

Acknowledgements. This study was supported by the Helmholtz Association (HZ-NG-102) and by the German Research Foundation (DFG) (priority program 1162 AQUASHIFT, Project No. RI 598/2-1). We thank P. Breithaupt, R. Koppe, K. Walther, H. Mempel, H. Johannsen, M. Schartau, and P. Fritsche for help in sample processing, and H. Ploug for fruitful comments. Two anonymous referees are acknowledged for their suggestions on improving this publication.

LITERATURE CITED

ALLDREDGE AL, SILVER ML (1988) Characteristics, dynamics and significance of marine snow. Prog Oceanogr 20:41-82

ALLDREDGE AL, COLE JJ, CARON DA (1986). Production of heterotrophic bacteria inhabiting macroscopic aggregates (marine snow) from surface waters. Limnol Oceanogr 31:68-78

ALLDREDGE AL, PASSOW U, LOGAN BE (1993) The abundance and significance of a class of large transparent organic particles in the ocean. Deep Sea Res 40:1131-1140

ARNOSTI, C (2004) Speed bumps and barricades in the carbon cycle: substrate structural effects on carbon cycling. Mar Chem 92:263-273

ASPER VL (1987) Measuring the flux and sinking speed of marine snow aggregates. Deep Sea Res 34:1-17

AZÚA I, UNANUE M, AYO B, ARTOLOZAGA I, IRIBERRI J (2007) Influence of age of aggregates and prokaryotic abundance on glucose and leucine uptake by heterotrophic marine prokaryotes. International Microbiology 10:13-18

BIDLE KD, AZAM F (2001) Bacterial control of silicon regeneration from diatom detritus: Significance of bacterial ectohydrolases and species identity. Limnol Oceanogr 46:1606-1623

BROCK TD (1981) Calculating solar radiation for ecological studies. Ecol Model 14:1-19

BRZEZINSKI, MA (1985) The Si:C:N ratio of marine diatoms: interspecific variability and the effect of some environmental variables. J Phycol 21:347-357.

CHRISTIAN JR, KARL DM (1998) Ectoaminopeptidase specifity and regulation in antarctic marine pelagic microbial communities. Aquat Microb Ecol 15:303-310

CHRÓST RJ (1991) Environmental control of the synthesis and activity of aquatic microbial ectoenzymes. In: Chrost RJ (ed) Microbial enzymes in aquatic environments. Springer, New York, p 29-59

DECHO AW (1990) Microbial exopolymer secretion in the ocean environments: their role(s) in food webs and marine processes. Oceanogr Mar Biol Annu Rev 28:73-153

DUCKLOW HW, CARLSON CA (1992) Oceanic bacterial production. Adv Microb Ecol 12:113-181

ENGEL A (2000) The role of transparent exopolymer particles (TEP) in the increase in apparent particle stickiness (alpha) during the decline of a diatom bloom. J Plankton Res 22:485-497

ENGEL A, PASSOW U (2001) Carbon and nitrogen content of transparent exopolymer particles (TEP) in relation to their Alcian Blue adsorption. Mar Ecol Prog Ser 219:1-10

ENGEL A, MEYERHÖFER M, VON BRÖCKEL K (2002) Chemical and biological composition of suspended particles and aggregates in the Baltic Sea in summer (1999). Est Coast Shelf Sci 55:729-741

ENGEL A, THOMS S, RIEBESELL U, ROCHELLE-NEWALL E, ZONDERVAN I (2004) Polysaccharide aggregation as a potential sink of marine dissolved organic carbon. Nature 428:929-932

ENRÍQUEZ S, DUARTE CM, SAND-JENSEN K (1993) Patterns in decomposition rates among photosynthetic organisms: the importance of detritus C:N:P content. Oecologia 94:457-471

FOWLER SW, KNAUER GA (1986) Role of large particles in the transport of elements and organic compounds through the oceanic water column. Prog Oceanog 16:147-194

FURHMAN JA, AZAM F (1982) Thymidine incorporation as a measure of heterotrophic bacterioplanktion production in marine surface waters: Evaluation and field results. Mar Biol 66:109-120

GIROLDO D, VIEIRA AAH, SMESTAD PAULSEN B (2003) Relative increase of deoxy sugars during microbial degradation of an extracellular polysaccharide released by a tropical freshwater *Thalassiosira sp.* (Bacillariophyceae). J Phycol 39:1109-1115.

GREENWOOD JE, TRUESDALE VW, RENDELL AR (2001) Biogenic silica dissolution in seawater – in vitro chemical kinetics. Prog Oceanogr 48:1-23

GROSSART HP, PLOUG H (2001) Microbial degradation of organic carbon and nitrogen in diatom aggregates. Limnol Oceanogr 46:267-277

GROSSART HP, HIETANEN S, PLOUG H (2003) Microbial dynamics on diatom aggregates in Øresund, Denmark. Mar Ecol Prog Ser 249:69-78

GROSSART HP, TANG KW, KIØRBOE T, PLOUG H (2007) Comparison of cell-specific activity between free-living and attached bacteria using isolates and natural assemblages. FEMS Microbiol Lett 266:194-200

HEISSENBERGER A, LEPPARD GG, HERNDL GJ (1996) Ultrastructure of marine snow. II. Microbiological considerations. Mar Ecol Prog Ser 135:299-308

HERNDL GJ (1988) Ecology of amorphous aggregations (marine snow) in the Northern Adriatic Sea: II. Microbial density and activity in marine snow and its implication to overall pelagic processes. Mar Ecol Prog Ser 48:265-275

HOPPE HG (1983) Significance of exoenzymatic activities in the ecology of brackish water: measurements by means of methylumbelliferyl-substrates. Mar Ecol Prog Ser 11:299-308

HOPPE HG, DUCKLOW H, KARRASCH B (1993) Evidence for dependency of bacterial growth on enzymatic hydrolysis of particulate organic matter in the mesopelagic ocean. Mar Ecol Prog Ser 93:277-283

HOPPE HG, BREITHAUPT P, WALTHER K, KOPPE R, BLECK S, SOMMER U, JÜRGENS K (2008) Climate warming during winter affects the coupling between phytoplankton and bacteria during the spring bloom: Results from a mesocosm study. Aquat Microb Ecol 51: 105-115

INTERNATIONAL PANEL OF CLIMATE CHANGE (IPCC) (2001) Impacts, adaptations and vulnerability. UNEP and WHO, Climate Change 2001

JIMÉNEZ-MERCADO A, CAJAL-MEDRANO R, MASKE H (2007) Marine heterotrophic bacteria in continuous culture, the bacterial carbon growth efficiency, and mineralization of excess substrate and different temperature. Microb Ecol 54:56-64

KAMATANI A (1982) Dissolution rates of silica from diatoms decomposing at various temperatures. Mar Biol 68:91-96

KARNER M, HERNDL GJ (1992) Extracellular enzymatic activity and secondary production in free-living and marine snow associated bacteria. Mar Biol 113:341-347

KIØRBOE T (2001) Formation and fate of marine snow: small-scale processes with large-scale implications. Sci Mar 65:57-71

KIØRBOE T, HANSEN JLS, ALLDREDGE AL, JACKSON GA and 5 others (1996) Sedimentation of phytoplankton during a diatom bloom: rates and mechanisms. J Mar Res 54:1123-1148

KOROLEFF F (1977) The international intercalibration exercise for nutrient methods. International council for the exploration of the sea, Charlottenlund

LEWIN J (1961) The dissolution of silica from diatom walls. Geochim Cosmochim Acta 21:182-198

MARTIN JH, KNAUER GA, KARL DM, BROENKOW WW (1987) VERTEX: carbon cycling in the northeast Pacific. Deep Sea Res 34: 267-285

MORICEAU B, GARVEY M, RAGUENEAU O, PASSOW U (2007) Evidence for reduced biogenic silica dissolution rates in diatom aggregates. Mar Ecol Prog Ser 333:129-142

PASSOW U, ALLDREDGE AL (1995) A dye-binding assay for the spectrophotometric measurement of transparent exopolymer particles (TEP). Limnol Oceanogr 40:1326-1335

PASSOW U, ALLDREDGE AL, LOGAN BE (1994) The role of particulate carbohydrate exudates in the flocculation of diatom blooms. Deep Sea Res I 41:335-357

PLOUG H, GROSSART HP (2000) Bacterial growth and grazing on diatom aggregates: respiratory carbon turnover as a function of aggregate size and sinking velocity. Limnol Oceanogr 45:1467-1475

POMEROY L, WIEBE WJ (2001) Temperature and substrates as interactive limiting factors for marine heterotrophic bacteria. Aquat Microb Ecol 23:187-204

PORTER KG, FEIG YS (1980) The use of DAPI for identifying and counting microflora. Limnol Oceanogr 25:943-947.

RAGUENEAU O, SCHULTES S, BIDLE K, CLAQUIN P, MORICEAU B (2006) Si and C interactions in the world ocean: Importance of ecological processes and implications for the role of diatoms in the biological pump. Global Biogeochem Cycles 20: GB4S02

RATH J, HERNDL GJ (1994) Characteristics and diversity of β-D-glucosidase (EC 3.2.1.21) activity in marine snow. Appl Environ Microbiol 60:807-813

REDFIELD AC, KETCHUM BM, RICHARDS FA (1963) The influence of organism on the composition of seawater. In: Hill MN (ed) The sea. Wiley, New York, p 26-77

RIEBESELL U (1991) Particle aggregation during a diatom bloom. II. Biological aspects. Mar Ecol Prog Ser 69:281-291.

SIMON M (2002) Microbial ecology of organic aggregates in aquatic ecosystems. Aquat Microb Ecol 28:175-211

SMETACEK V (1985) Role of sinking in diatom life history cycles: ecological, evolutionary and geological significance. Mar Biol 84:239-251

SMITH DC, SIMON M, ALLDREDGE AL, AZAM F (1992) Intense hydrolytic enzyme activity on marine aggregates and implications for rapid particle dissolution. Nature 359:139-142

SOMMER U, ABERLE N, ENGEL A, HANSEN T, LENGFELLNER K, SANDOW M, WOHLERS J, ZÖLLNER E, RIEBESELL U (2007) An indoor mesocosm system to study the effect of climate change on late winter and spring succession of Baltic Sea phyto- and zooplankton. Oecologia 150:655-667

STODEREGGER KE, HERNDL GJ (1999) Production of exopolymer particles by marine bacterioplankton under contrasting turbulence conditions. Mar Ecol Prog Ser 189:9-16

STRICKLAND JDH, PARSONS TR (1974) A practical handbook of seawater analysis. Fisheries Research Board Canada, Ottawa

THORNTON DCO, THAKE B (1998) Effect of temperature on the aggregation of Skeletonema costatum (Bacillariophyceae) and the implication for carbon flux in coastal waters. Mar Ecol Prog Ser 174: 223-231

WIEBE WJ, SHELDON WM JR, POMEROY LR (1992) Bacterial growth in the cold: evidence for an enhanced substrate requirement. Appl Environ Microbiol 58:359-364

TABLES

Table 1: Concentration of inorganic nutrients (n.d.: not detectable) and elemental stoichiometry of suspended POM in the mesocosms at 8.5°C and 2.5°C at the start of the aggregation experiment. Mean values ± SD of duplicate mesocosms per temperature.

	8.5°C	**2.5°C**
inorganic nutrients		
nitrate [µmol l^{-1}]	n.d.	n.d.
phosphate [µmol l^{-1}]	0.07 ± 0.02	0.03 ± 0.01
stoichiometery of POM		
[POC]:[PON]	10.0 ± 2.4	16.6 ± 2.1
[PON]:[POP]	32.6 ± 5.8	29.5 ± 0.2

Table 2: PON and POP in aggregates at the time of aggregate formation (60 h) and at the end of the experiment (252 h) ([µmol l^{-1}], [% of total]), and loss from aggregates until the end of incubation [%]. Mean values ± SD of duplicate incubations at 8.5°C and 2.5°C.

	8.5°C		**2.5°C**	
	PON	**POP**	**PON**	**POP**
60 hours				
[µmol l^{-1}]	116 ± 18	3.9 ± 1.0	28 ± 3	1.0 ± 0.0
[% of total]	91 ± 2	89 ± 2	59 ± 12	58 ± 7
252 hours				
[µmol l^{-1}]	110 ± 16	3.2 ± 0.8	38 ± 11	1.4 ± 0.4
[% of total]	84 ± 3	78 ± 0	62 ± 8	60 ± 3
loss [%]	5 ± 1	17 ± 1	-	-

Table 3: Activity of extracellular enzymes associated with aggregates. Mean values over time ± SD of duplicate incubations per temperature. $I_{V\max}$ and $I_{V\max/Km}$ were calculated according to eq. (7). Asterisks indicate significant differences between temperature treatments ($p < 0.05$).

	V_{max} [nmol (ml AGG)$^{-1}$ h^{-1}]		$I_{V\max}$	V_{max}/K_m [h^{-1}]		$I_{V\max/Km}$
	8.5°C	**2.5°C**		**8.5°C**	**2.5°C**	
α-glucosidase	7.0 ± 1.5	4.5 ± 0.15	1.6	0.20 ± 0.02	0.05 ± 0.01	4.0*
β-glucosidase	21.0 ± 1.3	5.0 ± 0.10	4.2*	0.65 ± 0.13	0.05 ± 0.01	13.0*
leucine-aminopeptidase	386 ± 62	66.5 ± 4.0	5.8*	9.0 ± 1.0	3.0 ± 0.20	3.0*
alkaline phosphatase	221 ± 14	169 ± 37	1.3	108 ± 21.0	118 ± 0.20	0.9

Table 4: Activity of extracellular enzymes in the SSW. Mean values over time ± SD of duplicate incubations per temperature. $I_{V\max}$ and $I_{V\max/Km}$ were calculated according to eq. (7). Asterisks indicate significant differences between temperature treatments ($p < 0.05$).

	V_{max} [nmol l^{-1} h^{-1}]		$I_{V\max}$	V_{max}/K_m [h^{-1}]		$I_{V\max/Km}$
	8.5°C	**2.5°C**		**8.5°C**	**2.5°C**	
α-glucosidase	180 ± 50	106 ± 14	1.6*	0.008 ± 0.0004	0.002 ± 0.0004	4.0*
β-glucosidase	320 ± 0.060	171 ± 46	1.9*	0.006 ± 0.0025	0.002 ± 0.0017	3.0*
leucine-aminopeptidase	7400 ± 2020	1250 ± 149	5.9*	0.089 ± 0.020	0.040 ± 0.0010	2.2
alkaline phosphatase	2400 ± 1850	1500 ± 127	1.6	1.58 ± 0.750	1.55 ± 0.34	1.0

Table 5: Cell-specific potential hydrolysis rates (cell-spec V_{max}) in AGG and SSW. Mean values over time ± SD of duplicate incubations per temperature. $I_{cell\text{-}spec\ Vmax}$ was calculated according to eq. (7). Asterisks indicate significant differences between temperature treatments ($p < 0.05$).

	AGG V_{max} **[amol cell^{-1} h^{-1}]**			**SSW** V_{max} **[amol cell^{-1} h^{-1}]**		
	8.5°C	**2.5°C**	$I_{cell\text{-}spec\ Vmax}$	**8.5°C**	**2.5°C**	$I_{cell\text{-}spec\ Vmax}$
α-glucosidase	33 ± 21	57 ± 15	0.6	9 ± 1	10 ± 1	0.9
β-glucosidase	95 ± 29	61 ± 30	1.6	19 ± 8	15 ± 3	1.3
leucine-aminopeptidase	1717 ± 532	521 ± 23	3.3*	387 ± 96	101 ± 342	3.8*
alkaline phosphatase	1081 ± 672	1220 ± 516	0.89	131 ± 69	125 ± 42	1.0

Table 6: Molar elemental ratios of POM in aggregates at 8.5°C and 2.5°C. Mean values over time ± SD of duplicate incubations per temperature.

	[POC]:[PON]	**[POC]:[POP]**	**[PON]:[POP]**
8.5°C	11.4 ± 2.0	349 ± 56	30.2 ± 5.2
2.5°C	20.2 ± 2.1	536 ± 87	26.8 ± 4.8

FIGURE CAPTIONS

Figure 1: Scheme of experimental set-up and sampling. See text for explanation.

Figure 2: Total amounts of PV (=AGG + SSW) and proportions in AGG at 2.5°C and 8.5°C. Mean values ± SD of duplicate incubations per temperature.
(▲ total PV at 8.5°C, ● PV in aggregates at 8.5°C, △ total PV at 2.5°C, ○ PV in aggregates at 2.5°C)

Figure 3: Total amounts of POC (= AGG + SSW) and proportion in AGG at 2.5°C and 8.5°C. Mean values ± SD of duplicate incubations per temperature.
(▲ total POC at 8.5°C, ● POC in aggregates at 8.5°C, △ total POC at 2.5°C, ○ POC in aggregates at 2.5°C)

Figure 4: Amounts of total TEP (= AGG + SSW) and proportion in AGG at 2.5 °C (*in-situ* temperature) and 8.5 °C. Mean values ± SD of duplicate incubations per temperature.
(▲ total TEP at 8.5°C, ● TEP in aggregates at 8.5°C, △ total TEP at 2.5°C, ○ TEP in aggregates at 2.5°C)

Figure 5: Bacterial cell numbers in aggregates and SSW at 2.5°C and 8.5°C. Fitted curves show nonlinear regression with $N_t=N_0*e^{\mu t}$, where N_0 is the initial cell number, μ the growth rate constant and t the time. Mean values ± SD of duplicate incubations per temperature.
(● 8.5°C, ○ 2.5°C)

Figure 6: Temporal development of BBP normalized to POC amounts in aggregates at 2.5°C and 8.5°C. Mean values ± SD of duplicate incubations per temperature.
(● 8.5°C, ○ 2.5°C)

Figure 7: V_{max} of α-glucosidase, β-glucosidase, and leucine-aminopeptidase in aggregates and SSW at 8.5°C and 2.5°C. Mean values ± SD of duplicate incubations per temperature.
(● α-glucosidase at 8.5°C, ■ β-glucosidase at 8.5°C, ▲ leucine-aminopeptidase at 8.5°C, ○ α-glucosidase at 2.5°C, □ β-glucosidase at 2.5°C, △ leucine-aminopeptidase at 2.5°C)

Figure 8: Time course of dissolved silicate concentration (dSi) in the SSW at 2.5 °C and 8.5 °C. Mean values ± SD of duplicate incubations per temperature.
(● 8.5°C, ○ 2.5°C)

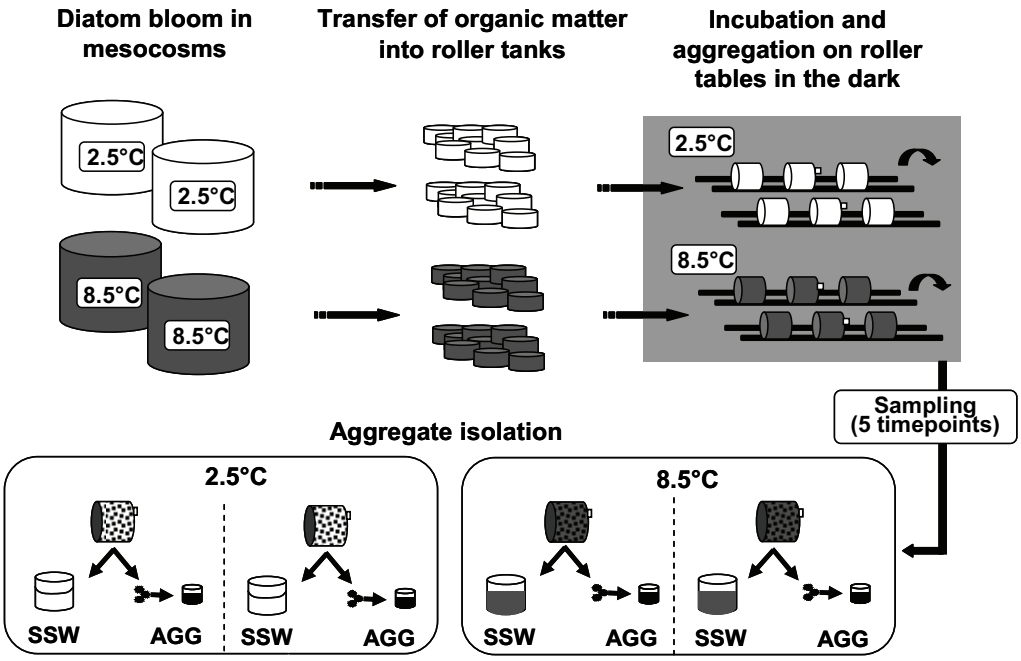
Diatom bloom in mesocosms
Transfer of organic matter into roller tanks
Incubation and aggregation on roller tables in the dark
2.5°C
2.5°C
8.5°C
8.5°C
2.5°C
8.5°C
Sampling (5 timepoints)
Aggregate isolation
2.5°C
8.5°C
SSW
AGG
SSW
AGG
SSW
AGG
SSW
AGG

Figure 1

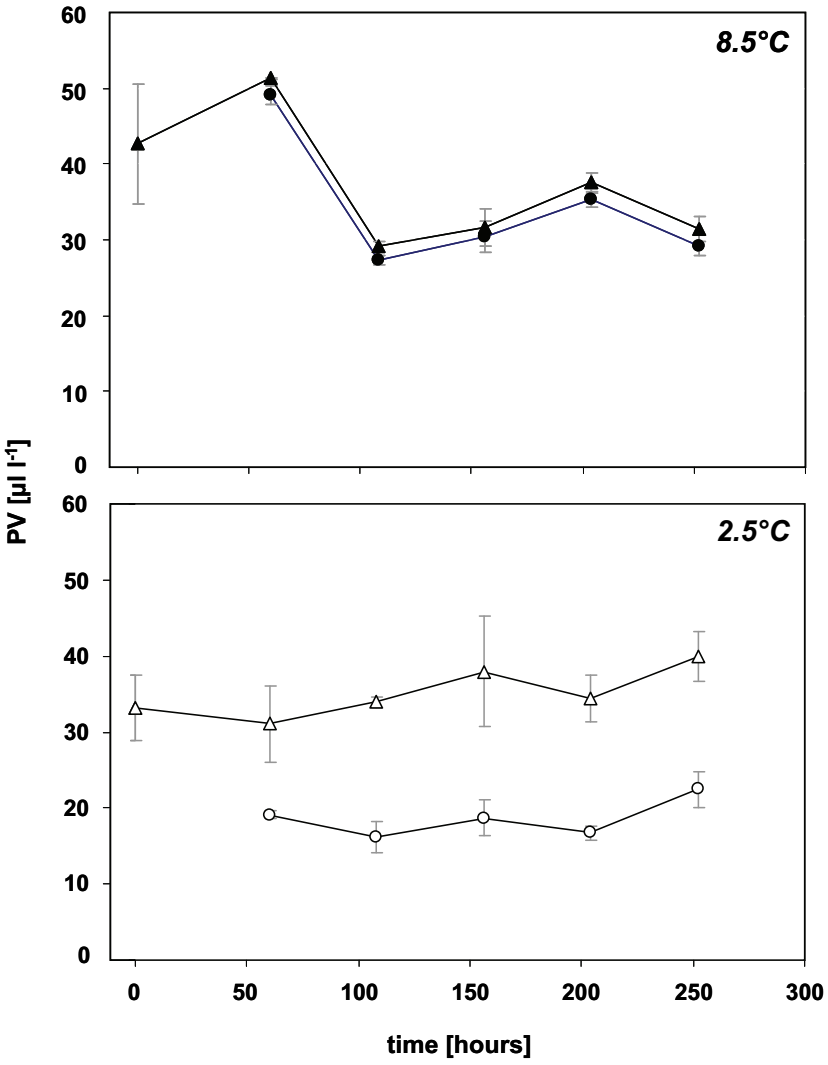
8.5°C
2.5°C
PV [µl l-1]
time [hours]
0
10
20
30
40
50
60
0
50
100
150
200
250
300

Figure 2

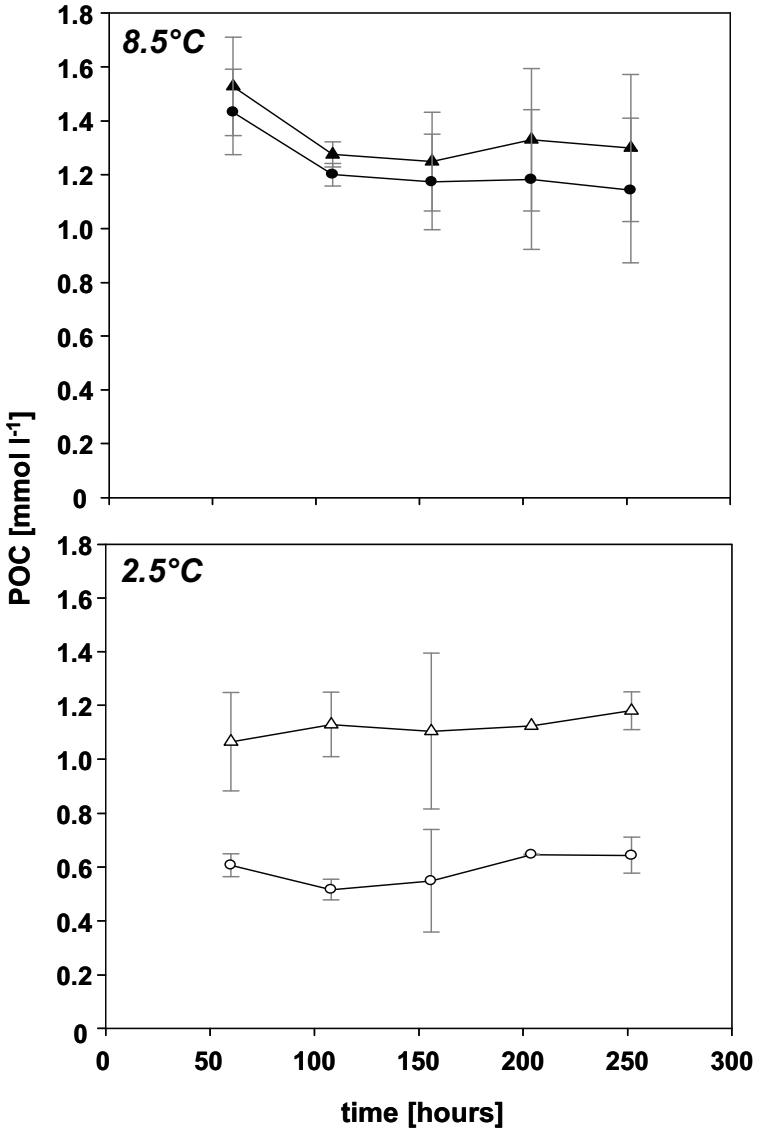
8.5°C
2.5°C
POC [mmol l-1]
time [hours]
0
0.2
0.4
0.6
0.8
1.0
1.2
1.4
1.6
1.8
0
50
100
150
200
250
300

Figure 3

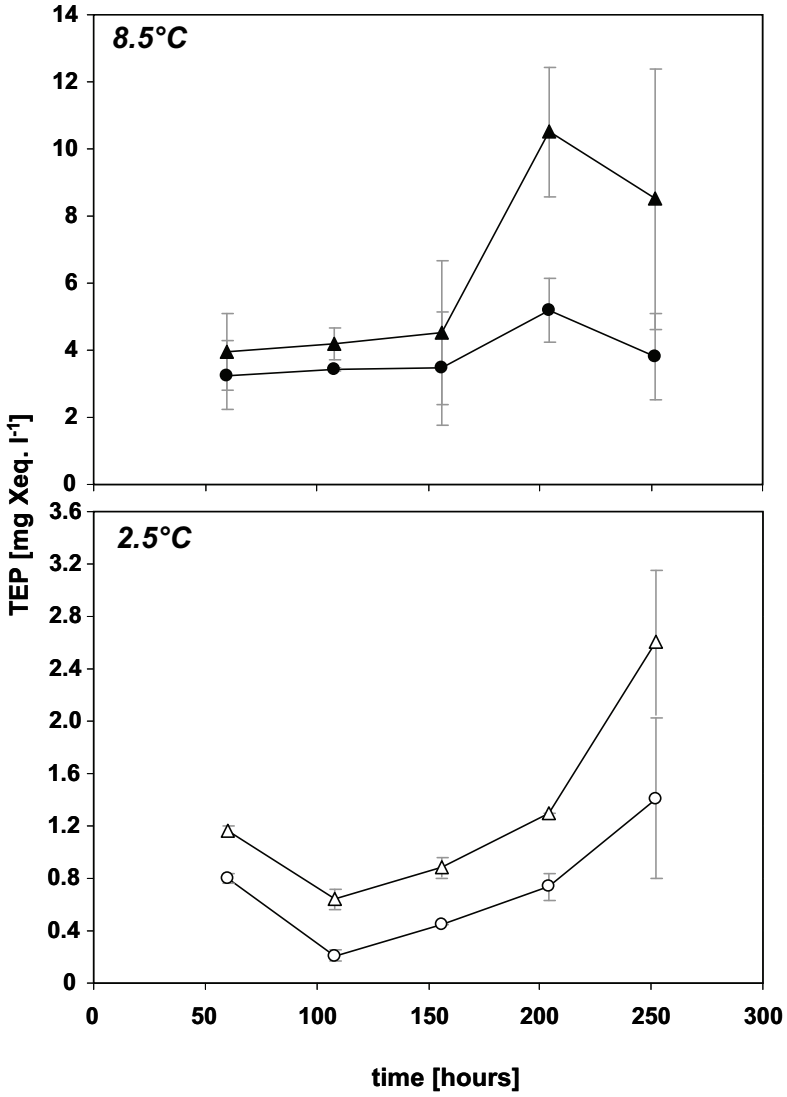
8.5°C
2.5°C
TEP [mg Xeq. l-1]
time [hours]
0
2
4
6
8
10
12
14
0.4
0.8
1.2
1.6
2.0
2.4
2.8
3.2
3.6
50
100
150
200
250
300

Figure 4

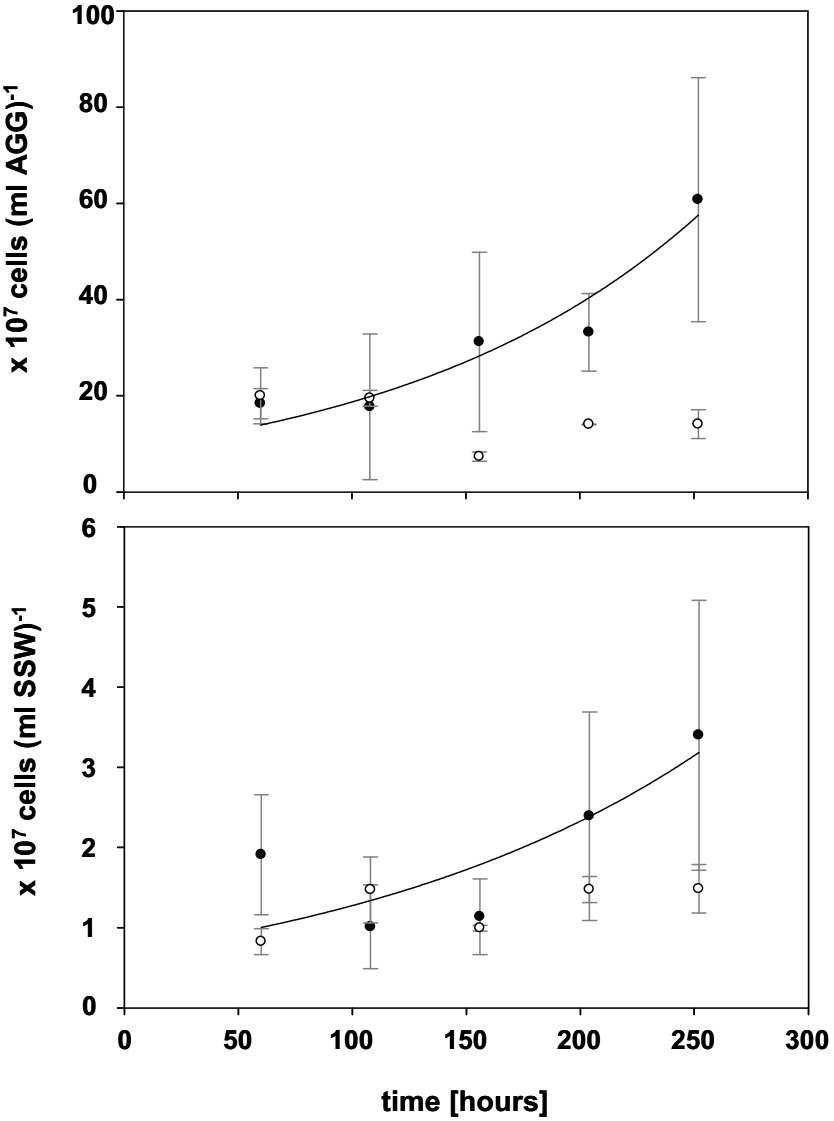
x 10^7 cells (ml AGG)^-1
100
80
60
40
20
0
x 10^7 cells (ml SSW)^-1
6
5
4
3
2
1
0
0
50
100
150
200
250
300
time [hours]

Figure 5

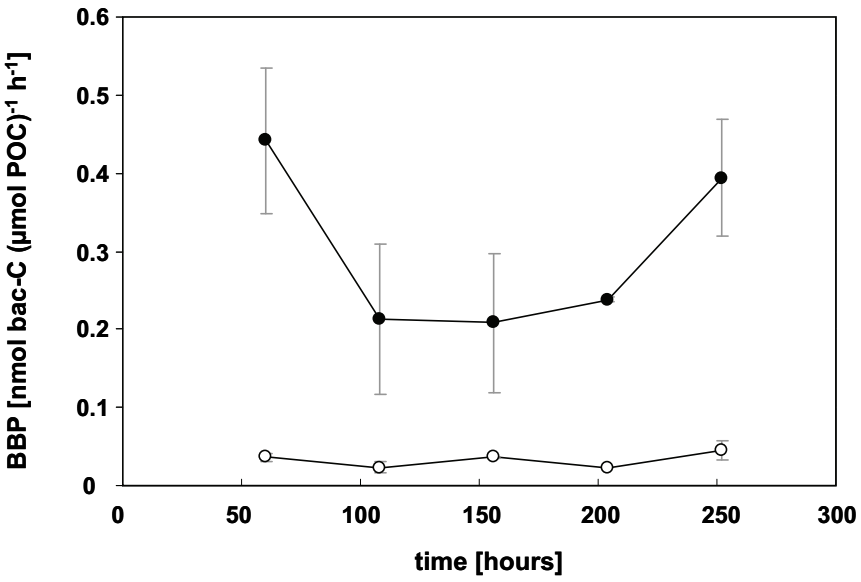
BBP [nmol bac-C (µmol POC)-1 h-1]
0.6
0.5
0.4
0.3
0.2
0.1
0
0
50
100
150
200
250
300
time [hours]

Figure 6

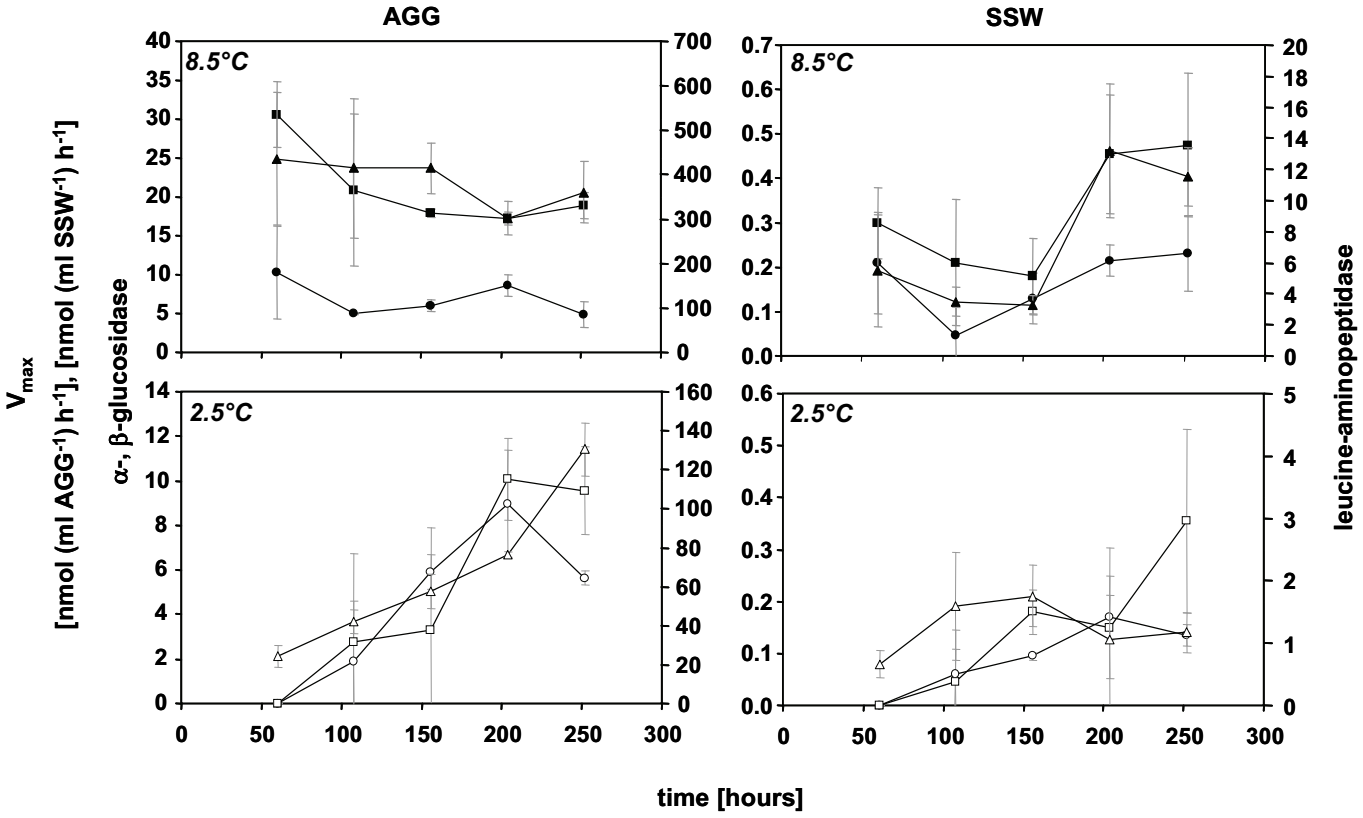
AGG
SSW
8.5°C
2.5°C
V_{max}
[nmol (ml AGG^{-1}) h^{-1}], [nmol (ml SSW^{-1}) h^{-1}]
α-, β-glucosidase
leucine-aminopeptidase
time [hours]

Figure 7

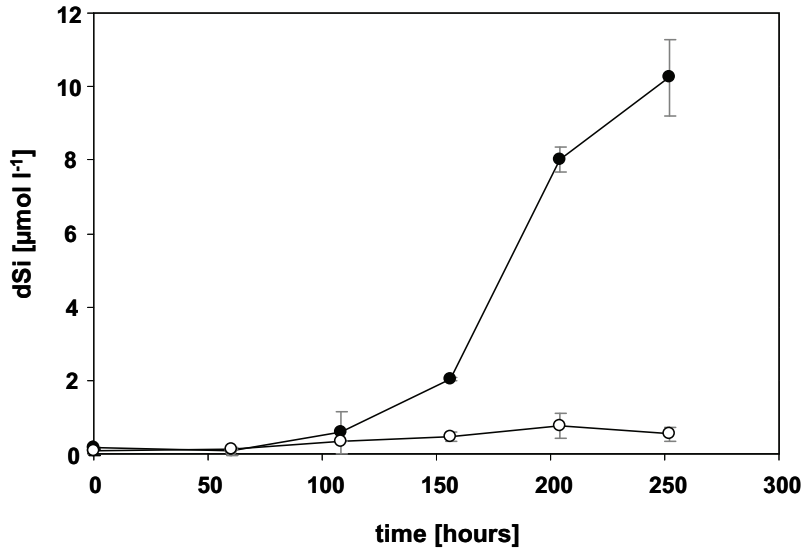

Figure 8

Manuscript II

Abundance and size distribution of transparent exopolymer particles (TEP) in a coccolithophorid bloom in the northern Bay of Biscay (June 2006)

Jérôme Harlay [a], Caroline de Bodt [a], Anja Engel [b], Sandra Jansen [b], Quentin d'Hoop [a], Judith Piontek [b], Nicolas van Oostende [c], Steve Groom [d], Koen Sabbe [c] and Lei Chou [a]

[a] Université Libre de Bruxelles (ULB), Brussels, Belgium

[b] Alfred Wegener Institute for Polar and Marine Research (AWI), Bremerhaven, Germany

[c] Ghent University, Ghent, Belgium

[d] Plymouth Marine Laboratory (PML), Plymouth, United Kingdom

Abstract

The distribution of transparent exopolymer particles (TEP) was investigated during a coccolithophorid bloom in the northern Bay of Biscay (North Atlantic Ocean) in early June 2006. MODIS chlorophyll-a (Chl-a) and reflectance images before and during the cruise were used to localize areas of important biological activity and high reflectance (HR). TEP profiles along the continental margin, determined using microscopic (TEP_{micro}) and colorimetric (TEP_{color}) methods, showed abundant (6.1×10^6 to 4.4×10^7 L^{-1}) and relatively small particles (0.5 µm - 20 µm), leading to a low total volume fraction (0.05 to 2.2 ppm) of TEP_{micro} and similar vertical profiles of TEP_{color}. Estimates of carbon content in TEP (TEP-C) derived from the microscopic approach yielded surface concentration of 1.50 µmol C L^{-1}. The contribution of TEP-C to particulate organic carbon (POC) was estimated to be 12 % (molar C ratio) during this survey. Our results suggest that TEP formation is a probable first step to rapid and efficient export of carbon during declining coccolithophorid blooms.

Keywords:

TEP, carbon, coccolithophores, North Atlantic Ocean

1. Introduction

During the last 15 years, many field studies have pointed out the importance of exopolymer substances (EPS) in natural aquatic systems (Passow, 2002; Wotton, 2004). A large fraction of EPS consists of carbohydrates that are released during and after phytoplankton blooms (Myklestad, 1995). Due to their physico-chemical characteristics, EPS are able to stick to each other, and form networks of fibrils (Leppard, 1995) or colloids (Kepkay, 1994), and are thereby transferred from the dissolved to the particulate organic matter pool. Transparent exopolymer particles (TEP) merge the two properties of being 1) retained onto 0.4 µm membrane filters and 2) being stainable by Alcian Blue, a specific dye for acidic ($-COO^-$) and/or sulphated ($-O-SO_3^-$) reactive groups of carbohydrates (Alldredge *et al*., 1993). Several studies indicate that TEP are natural constituents of the bulk particulate matter in marine (Passow and Alldredge, 1995b; Mari and Kiorboe, 1996; Krembs and Engel, 2001; Garcia *et al.*, 2002; Engel, 2004; Brussaard *et al.*, 2005; Radic *et al.*, 2005; Shackelford and Cowen, 2006; Prieto *et al.*, 2006; Sugimoto *et al.*, 2007) and freshwater (Logan *et al.*, 1995; Grossart *et al.*, 1997; Berman and Viner-Mozzini, 2001; Arruda-Fatibello *et al.*, 2004) ecosystems. Most of the field sites, where TEP have been described so far, were dominated by diatoms, dinoflagellates or cyanobacteria.

However, nutrient-induced blooms of *Emiliania huxleyi* in mesocosms suggested that coccolithophores could also be responsible for high concentrations of TEP (Engel *et al.*, 2004). The dynamics of such an induced *E. huxleyi* bloom may be extrapolated to the field to some extent. As described in this mesocosm study, phytoplankton blooms start with an exponential phase during which cell division occurs under nutrient-replete conditions (Delille *et al*., 2005; Engel *et al.*, 2005). The exhaustion of nutrients coincides with the beginning of the stationary phase. Cell division is then considerably reduced while large amounts of coccoliths are still produced by the coccolithophores. During the stationary phase, the cells

are generally covered by several layers of coccoliths and the distal ones are released into the water column when new ones are produced (Paasche, 2002). This phase is often associated with the decay of the bloom, when high abundance of *Emiliania huxleyi* coincides with those of viruses, enhancing viral infection and bloom termination (Catsberg *et al.*, 2001; Jacquet *et al.*, 2002). The persistence of coccolithophorid blooms after nutrient exhaustion is haphazard and patchy in natural environments. The release of large amounts of coccoliths, in particular by *Emiliania huxleyi* (Paasche, 2002), modifies the optical properties of surface seawater, and leads to high reflectance (HR) patches that can be observed by remote sensing (GREPMA, 1988; Holligan *et al.*, 1983; Holligan *et al*, 1993a; Brown and Yoder, 1994).

Excess carbon production compared to what is expected according to the Redfield's stoichiometry was pointed out in phytoplankton blooms during mesocosm experiments (Engel *et al*., 2002; Delille *et al.*, 2005; Engel *et al.*, 2005). Using a modelling approach based on mesocosm observations, a link was established between the excess of dissolved inorganic carbon (DIC) uptake (termed carbon over-consumption) and the rapid formation of TEP-C through dissolved organic carbon (DOC) exudation by phytoplankton after nutrient exhaustion (Schartau *et al.*, 2007). Thus, in the stationary phase, carbon cycling is uncoupled from nutrient availability because of continuous production and release of organic carbon by the cells. Because TEP have high C:N ratios (Mari, 1999; Engel and Passow, 2001; Mari *et al.*, 2001), they are thought to contribute to particulate organic carbon (POC) rather than to the particulate nitrogen pool and can therefore increase C:N ratios of the particulate organic matter (POM).

This study investigated the contribution of coccolithophores to the TEP production, the pattern of TEP concentrations and size distribution during a coccolithophorid bloom in the northern Bay of Biscay (North Atlantic Ocean, early June 2006). Chemical and biological parameters as well as remote sensing images are included in order to better describe

phytoplankton bloom dynamics. Here, we present TEP profiles at different stations in the northern Bay of Biscay and estimate the contribution of TEP to POC.

2. Materials and methods

2.1. Study site and field sampling

The continental shelf of the northern Bay of Biscay is located south of Ireland and west of France, where a steep slope separates the abyssal plain from the continental plateau (Fig. 1). Samples were collected between 31 May and 9 June 2006. Images from the NASA Moderate Resolution Imaging Spectroradiometer (MODIS) instrument on-board the Aqua platform were processed in near-real time and sent via e-mail to the research vessel. Chlorophyll-a (Chl-a) concentration was computed using the MODIS OC3 band switching algorithm (see O'Reilly *et al.*, 1998). False colour composites were produced from the 443 nm, 490 nm and 551 nm channels displayed as the red, green and blue components of a colour image. These reflectance images show the approximate "colour of the ocean" and the magnitude of coccolithophore scattering as blue-white areas (Holligan *et al.*, 1983). The Chl-a images revealed two zones in terms of phytoplankton biomass (Fig. 1a). In the western zone, Chl-a was low, while in the eastern part corresponding to the continental shelf and margins, Chl-a levels were higher, indicating enhanced biological activity. HR was mainly observed inshore of the 200 m isobath, the bathymetric boundary between the open ocean and the continental plateau (Fig. 1b), except south of 48.3 N where HR extended over the slope.

Sampling stations (Fig. 1) were located at the continental margin over the continental shelf (stations 1, 4, 7 and 8) and along the shelf break, situated at about 500 m (stations 2 and 5) and 1200 m depth (stations 3 and 6). A HR patch was localized by remote sensing at stations

4, 5, 7, 8 and was sampled with adjacent stations (Fig. 1b). The cruise was split in two legs (first leg: 3 days, second leg: 4 days). During the second leg some stations (1 and 4) were revisited after 9 and 6 days as referred to as stations 1bis and 4bis, respectively.

A Seabird CTD system, equipped with a 12 Niskin bottles (10 L) rosette sampler, was used to determine depth profiles of temperature and salinity, and to collect seawater for chemical and biological analyses. At each station, water was collected in the morning at 3 m, 10 m, 20 m, 40 m, 60 m, 80 m, 100 m and 150 m depths. Some additional depths (30 m, 50 m and 120 m) were also sampled in the surface layer for some stations. All samples were processed onboard immediately after sampling.

2.2. Chlorophyll-a (Chl-a) and diagnostic pigments

The concentration of Chl-a was determined from 250 ml seawater filtered onto glass fibre filters (Whatman GF/F) under low vacuum, wrapped in aluminium foil and stored at -20°C until analysis. Pigment extraction was realized in 10 ml of 90% acetone. Filters were kept overnight in the dark at -20°C and were centrifuged for 10 minutes at 5000 rpm at 4°C prior to measurement. Chl-a concentration was determined fluorimetrically (Shimatzu RF-1501 spectrofluorophotometer), together with total phaeophytin concentration after acidification (HCl, 0.1N), according to Yentsch and Menzel (1963).

Separation of the algal pigments was performed using a high performance liquid chromatographic (HPLC) method based on Wright and Jeffrey (1997). Between 0.5 and 3.5 L of seawater were filtered through glass fiber filters (Whatmann GF/F). The filters were stored in liquid nitrogen onboard until analysis. Extraction of the pigments was performed in a 90 % aquaeous aceton solution. Standard pigment mixtures were run together with the samples to allow identification and quantification of the detected pigment peaks in the chromatogram.

The analysis of the diagnostic pigments for coccolithophores (19'-hexanoyloxyfucoxanthin, HexaFx) and diatoms (fucoxanthin, Fx) allowed the computation of the HexaFx:Fx ratio to assess the relative contribution of coccolithophores to the phytoplankton pool (Barlow *et al.*, 1993, 1998). Higher values of this ratio indicates the higher the contribution of coccolithophores in the phytoplankton pool.

2.3. Dissolved Phosphorus

Dissolved phosphate concentration was measured colorimetrically after filtration through a 0.4 µm Nuclepore filter, using the molybdate blue method described in Grasshoff *et al.* (1983). The detection limit is 10 nM using a 10-cm optical cell.

2.4. Particulate organic carbon (POC)

Seawater (200 ml to 2000 ml) was filtered through precombusted (4 hours, 500°C) GF/F filters. The samples were stored at -20°C until analysis. Within three months after the cruise, the filters were dried overnight at 50°C prior to analysis. POC was determined using a Fisons NA-1500 elemental analyser after carbonate removal from the filters by HCl fumes overnight. Four to five standards of certified reference stream sediment (STSD-2) from the Geological Survey of Canada, together with 3-4 blank filters were used for the calibration. POC has been sampled down to 80 m for stations 4 and 4b, 100 m for station 1, 120 m for station 1bis, 150 m for stations 7 and 8 and down to 540 m for station 2 (of which only the uppermost 150 m are presented). No data were obtained for 30 m, 40 m and 60 m at station 1 because of technical problems during the analysis of this parameter.

2.5. Transparent exopolymer particles (TEP)

2.5.1. Colorimetric determination of TEP (TEP_{color})

Triplicates of 5-250 ml each were filtered (<200 mbar) onto 25 mm Nuclepore membrane filters (0.4 µm pore size) for the colorimetric determination of TEP (TEP_{color}), according to Passow and Alldredge (1995a). The filters were stained with 0.5 ml Alcian Blue (Alldredge *et al.*, 1993) and stored frozen at -20°C and analysed within 6 weeks. Prior to spectrophotometric analysis (787 nm in a 1 cm path-length cell), the filters were soaked for 2 hours in 80 % H_2SO_4. Light absorbance was corrected for the adsorption of Alcian Blue on blank filters. TEP_{color} is given in relative units, i.e. in % of the highest absorbance at each station (Tab. 1).

2.5.2. Microscopic determination of TEP size spectrum

Microscopic analysis of TEP was conducted after Engel (2009). Therefore, 5 to 200 ml of seawater were filtered (<200 mbar) onto 0.4 µm Nuclepore filters within 1 hour after sampling and stained with 0.5 ml Alcian Blue (pH 2.5) (Alldredge *et al.*, 1993). The filters were prepared in duplicate, placed onto semi-permanent TEP slides (CytoClear) and stored frozen at -20 °C until analysis. TEP slides were transferred to a compound light microscope and screened by a digital AxioCam HRc camera (Zeiss) with a 200-400-x magnification. About 30 pictures per filter were randomly taken in a cross section. The composite pictures were split into red, green and blue components (RGB Split) using the image analysis program WCIF ImageJ (a public domain program developed at the US National Institute of Health - http://www.uhnresearch.ca/facilities/wcif/fdownload.html- courtesy of Wayne Rasband, National Institute of Mental Health, Bethesda, Maryland, USA). The red segment accentuates the blue stained TEP and was used for further analysis. TEP with an area larger than 0.2 μm^2

were enumerated and sized for individual area and major cross section. The equivalent spherical diameter (ESD) was calculated for individual particles from area measurements, leading to a range of [0.5 to 80 μm (ESD)].

TEP were classified according to their ESD into 20 logarithmic size classes (Mari and Burd, 1998). TEP size distributions were described using a power law of the type $dN/d(d_p) = kd_p^{\delta}$, where *dN* is the number of particles per unit volume in the size range d_p to $\lfloor d_p + d(d_p) \rfloor$. The constant, *k*, depends on the concentration of particles and the spectral slope, δ (with $\delta<0$) describes the size distribution. Both constants were derived from regressions of $\log\lfloor dN/d(d_p) \rfloor$ versus $\log\lfloor d_p \rfloor$. δ is related to the slope of the cumulative size distribution $N = ad_p^{\beta}$ by $\delta=\beta+1$. Spectral slopes were used to describe the TEP size distribution; an increase in δ being due to an increase of the fraction of large TEP. The volume concentration is defined, here, as the mean volume of the particles that belong to a size class in the sample; changes of this quantity indicate some changes in the dynamics of particles, due to aggregation/disaggregation processes.

2.5.3. Estimation of TEP carbon concentration (TEP-C)

TEP-C content (TEP-C_{micro}, μM) was assessed by the microscopic approach assuming hat the volume of TEP is proportional to r^D, where r is the equivalent spherical radius in μm, and D the fractal dimension associated to the size distribution of particles. Therefore TEP-C_{micro} was determined from TEP size spectra according to Mari (1999). For each sample, D was deduced from the spectral slope, δ, according to the semi-empirical relationship (Burd and Jackson, unpublished data, as referred in Mari and Burd, 1998)

$$D = (64 - \delta) / 26.2 \qquad \text{(eq. 1)}$$

Thus, TEP-C_{micro} was derived from the histogram distribution, according to:

$$TEP - C_{micro} = \frac{a}{12} \sum_i n_i r_i^D \,, \qquad \text{(eq. 2)}$$

where n_i is the concentration of TEP in the size class i and r_i the mean equivalent spherical radius of this size class. The constant, a = 0.25×10^{-6} µg C was determined by Mari (1999).

3. Results

3.1. Hydrography

Vertical distributions of temperature revealed that sea-surface temperatures ranged between 13.0 and 14.0°C during the first leg (stations 1 to 5) and increased up to 14.9°C during the second leg (stations 6, 7, 8, 4bis and 1bis) (Fig. 2). They also shows that the upper water column over the continental shelf can be divided into 3 distinct parts: (i) a thin surface mixed layer of 10 m, (ii) an intermediate layer displaying a strong vertical gradient, and (iii) a homogeneous cold deep layer below 60 m (11.4°C).

The smaller temperature gradient on the continental slope suggests input of a cold, deeper water mass in the upper 25-35 m, which corresponds to the photic zone (see below). This induced a mixing of the upper layer of the water column. Between the two legs, warming of the surface layer deepened the vertical temperature gradient down to 50 m depth at the stations 1bis and 4bis. Salinity stayed within a narrow range of 35.5 - 35.6 down to 800 m depth at the deepest station 6 (data not shown).

Dissolved phosphate concentration was in average 0.49 ± 0.04 µM (average ± standard deviation; n = 7) at 150 m depth, while PO_4 was depleted in surface waters (Fig. 2). Compared to the slope, the continental shelf was more PO_4 depleted, and the concentrations in the upper 10 m ranged between 0.01 and 0.05 µM. Higher surface concentrations of

phosphate were observed for the shelf-break (0.08 - 0.16 μM), where the surface layer only occasionally fell below 0.05 μM (station 6) during the second leg (Fig. 2).

3.2. Chlorophyll-a and reflectance

Satellite images showed surface Chl-a concentrations (Fig. 1a and 1c) and several HR patches (Fig. 1b and 1d) distributed inshore of the 200 m isobath, the bathymetric boundary between the open ocean and the continental shelf of the northern Bay of Biscay, in June 2006. The comparison of MODIS (Fig. 1a and 1c) and reflectance (Fig. 1b and 1d) images revealed changes in phytoplankton biomass in the southern HR patch (stations 4, 7 and 8) between the two legs. An overall decline in surface Chl-a concentration was observed between the two periods at the revisited stations. At stations 4bis, 7 and 8 this decline was associated with an increase in reflectance.

Sea-surface Chl-a concentration ranged between 0.5 and 2.0 μg L^{-1} (Fig. 3). The highest concentration was determined at station 2, where the concentration in the photic zone (ranging between 25 and 37 m depth based on light measurements) exceeded 1.5 μg L^{-1}. The vertical profiles over the continental shelf showed higher Chl-a concentration at intermediate depth situated between 20 and 40 m, which decreased strongly down to 80 m. At stations 1bis and 4bis, 9 days and 6 days respectively after the initial visit, Chl-a concentration in surface waters decreased respectively by 0.6 and 0.2 μg L^{-1}. As inferred from Chl-a concentration and pigment composition (Fig. 3), the mixed phytoplankton community was dominated by coccolithophores at stations 1, 2 and 3.

3.3. POC

The highest concentrations of POC were observed within the upper 20 m of the water column, ranging between 10 and 15 µM and reaching up to 25 µM at station 7 (Fig. 4). Concentrations were lower than 2.5 µM below 20 m depth, except for station 1 where 7.7 µM were determined few meters above the sea-bottom, which may be linked to resuspension of sediments. At station 4bis, POC concentration in the water column was significantly lower than at other stations. No significant difference in POC concentration was observed between station 1 and 1bis.

3.4. Concentration and size distribution of TEP

3.4.1. TEP_{color}

The vertical profiles of relative TEP_{color} absorbance exhibited strong variations, achieving maximum values (100 %) in the surface or subsurface layer (Fig. 5). A general decrease of absorbance was observed from surface to depth, showing similar vertical distribution patterns as Chl-a and POC. The lowest absorbance (normalised for 1 L of seawater) was observed in the deepest samples, and ranged between 9% and 14.5% below 150 m (not shown). In contrast, the upper 40 m exhibited more variable values.

3.4.2. Concentration and size distribution of TEP_{micro}

The microscopic determination of TEP allowed for their enumeration and classification into size classes, based on their equivalent spherical diameter (ESD). The size frequency distribution of TEP showed a dominance (>90%) of particles smaller than 20 µm (ESD) in surface waters. Figure 6 is a three-dimensional representation of the vertical distribution of TEP_{micro} volume concentration (in $\mu m^3\ ml^{-1}\ \mu m^{-1}$) as a function of the size of particles in the

water column. The larger particles ranged between 20 and 30 µm and were abundant in the upper part of the water column. Their concentration strongly decreased with depth to become insignificant below 80 m. The coincidence of abundant large and small particles in the first 30 meters (i.e. the upper mixed layer) can be considered as the result of the assembly of lager particles from smaller ones in the aggregation process. Therefore, the snapshot of this station 8 likely represents the different steps of the formation of TEP from their small precursors, formed by coagulation of phytoplankton exudates, to larger particles formed by the aggregation of the bulk colloidal material.

In accordance with the distribution of TEP_{color}, TEP_{micro} abundance was higher in surface waters, down to 40 m depth, ranging between 2.1×10^3 ml^{-1} and 43.7×10^3 ml^{-1} at stations 2 and 1, respectively (Fig. 7). At greater depth the distribution was relatively uniform and in the lower range of surface abundances. In the HR patch (stations 4, 7 and 8), TEP_{micro} exhibited concentrations in the range of 3.3×10^3 ml^{-1} to 20.2×10^3 ml^{-1}. An overall 2-fold increase of TEP_{micro}, in association with a decrease of Chl-a concentration after 6 days, was observed at the revisited stations 4bis, where concentrations ranged between 6.7×10^3 ml^{-1} and 20.2×10^3 ml^{-1}. However, such an increase in TEP concentration was not observed after 9 days at stations 1 and 1bis, despite a similar decrease of Chl-a concentration.

A power law relationship fitted the size distributions of TEP very well in all cases ($r^2 > 0.9$) as shown in Figure 8. The size distribution can be described by spectral slope, δ, with less negative values indicating an increase with the fraction of large particles and, potentially, TEP aggregation. In the top 40 m, δ values ranged between -3 and -2 (Fig. 9). The increase of δ in the surface layer at the re-visited station 1bis suggests that aggregation of TEP has taken place after an elapse of time of 9 days. On the contrary, a decrease of δ was observed between station 4 and 4bis. Together with an increase of total TEP abundance, this could be

attributed to the production of smaller TEP. The fractal dimension, D, of TEP was deduced from δ, and ranged between 2.51 and 2.56.

3.4.3. TEP-C estimates

Surface concentration of TEP-C_{micro} ranged between 0.44 µmol C L^{-1} and 5.25 µmol C L^{-1} at station 4bis and 1, showing higher concentrations above the thermocline (Fig. 4). Except station 1, TEP-C_{micro} concentrations in the photic zone were found to be below 2.00 µmol C L^{-1}. At greater depths, 0.75 µmol C L^{-1} was an upper limit for TEP-C_{micro} at all stations, except station 1, where the resuspension of sediment was probably responsible for higher TEP-C estimates close to the bottom. Low variability in TEP-C was observed at the revisited stations (1bis and 4bis).

4. Discussion

4.1. Relationship between bloom development and biological parameters

Based on remote sensing images (Fig. 1), vertical profiles of nutrients (Fig. 2) and Chl-a (Fig. 3), the coccolithophorid bloom investigated in our study can be split into two distinctive regions: (i) a southern part associated with higher Chl-a and lower reflectance where coccolithophores were in the initial stage of the bloom (stations 1, 2, 3 and 6), and (ii) a northern part where increased reflectance rather suggested that the coccolithophorid bloom had reached a stationary phase (stations 4, 5, 7 and 8).

The surface waters of the study area were characterized by the formation of a seasonal thermocline at 50 m depth on the continental shelf and a general warming by 1°C during the course of the cruise (10 days). Over the shelf-break (stations 2, 3 and 5), the temperature

below the thermocline decreased continuously with depth, suggesting the mixing of the upper layer with a deep cold nutrient-rich water mass. A significant (r^2=0.82, n=96, $p<0.0001$) correlation was observed between phosphate consumption and temperature, indicating a strong control of hydrodynamics on phytoplankton activity (Wollast and Chou, 2001). The northern Bay of Biscay is characterized by intermittent inputs of nutrient-rich deep water to the photic layer promoted by internal waves (Huthnance *et al.*, 2001), enhancing and sustaining localized biological activity in spring (Joint *et al.*, 2001). In the Bay of Biscay, two diatom blooms usually occur during phytoplankton succession in spring and fall but diatoms remain in the phytoplanktonic community along the spring bloom (Joint *et al.*, 2001). Prymnesiophytes, to which coccolithophores belong, are an important component of the phytoplankton community in this area, especially in spring, and persist at low densities over the whole annual cycle (Joint *et al.*, 2001). The accumulation of coccoliths, the minute calcite discs produced by this species, modifies the optical properties of surface seawater leading to high reflectance so that high reflectance are traditionally associated to coccolithophorid blooms (Balch *et al.*, 1996). The spatial distribution of localized HR patches on satellite images (Figure 1b and 1d) suggested the development of a coccolithophore-dominated bloom during our study, as reported by Holligan *et al.* (1983, 1993), the GREPMA (1988), and Brown and Yoder (1994) in the North Atlantic. The most common species that is known to produce such important blooms is *E. huxleyi* (Brown and Yoder, 1994).

Surface distributions of Chl-a and PO_4 suggest that phytoplankton production has led to inorganic phosphate depletion in surface waters. Dissolved silicates (data not shown) remained below 2 µM in surface waters, probably due to the uptake of this nutrient by diatoms (Egge and Aksnes, 1992). Such a situation likely triggers coccolithophores at the period of high irradiance (Tyrrell and Merico, 2004), whose requirements for inorganic

phosphorus are relatively low, due to their reliance on alkaline phosphatase allowing them to use organic phosphorus (Riegman *et al.*, 2000).

4.2. TEP concentrations observed in the field

Microscopic enumeration and sizing of TEP_{micro} (Table 1) showed abundant (6.13×10^3 ml^{-1} to 4.4×10^4 ml^{-1}), relatively small particles (0.5 μm - 20 μm ESD) leading to a low total volume concentration of TEP (0.05 - 2.2 ppm) (not shown). The fractal scaling of TEP (D), deduced from the spectral slope (eq. 1), was close to the value of 2.55 proposed by Mari and Burd (1998) for naturally occurring TEP. These concentrations agreed with previous estimates (0.76 - 4.1 ppm) in the NE Atlantic mixed layer (Engel, 2004) and were in the lower range (3-310 ppm) of earlier observations in a coastal diatom bloom of the Baltic Sea (Mari and Burd, 1998). Small variations of the spectral slope (δ) with depth and between stations suggest only minor changes in the size distribution of particles. Hence, TEP aggregation can hardly be assessed from size distributions in this study. Together with the observed increase in total TEP_{micro} abundance at revisited stations, the dominance of small particles may rather point towards TEP production at the time of our study, than to massive aggregation, as it may occur in later phases of phytoplankton blooms. Concentrations of TEP_{color} in coastal regions range from <100 μg Xeq L^{-1} to 3000 μg Xeq L^{-1} (Passow, 2002 and citations within). For an open ocean transect in the NE Atlantic surface water TEP_{color} concentration ranged from 40 to 120 μg Xeq L^{-1} in the top 20 m (Engel, 2004), and vertical patterns of TEP distribution were similar to those reported on Figure 5. The upper and lower boundaries of TEP-C concentration provided by Engel (2004) lead to estimates between 30 and 89 μg C L^{-1}, and are thus in agreement with our values determined by TEP-C_{micro} (Fig. 4). Previous measurements conducted in the study area in June 2004 revealed TEP_{color}

concentrations similar to those determined by Engel (2004) (up to 120 µg Xeq L^{-1}) and averaged TEP-C_{color} of 29.0 ± 4.2 µg C L^{-1} (mean ± confidence interval at 95 %, n = 54) in the surface layer (Harlay *et al.*, in prep).

TEP-C_{micro} concentrations above 20 µg C L^{-1} were determined in samples exhibiting various degrees of coccolithophorid dominance, based on the HexaFx:Fx ratio of diagnostic pigments (Fig. 3). At stations 2 and 3, where HexaFx:Fx ratio was high, TEP-C_{micro} did not exceed 10 µg C L^{-1}. Hence, no particular trend in relation with TEP-C_{micro} estimates in the phytoplankton assemblage could be assessed from coccolithophorid dominance at the time of our survey. We hypothesize that the history of water masses in terms of phytoplankton activity and the taxonomic composition of phytoplankton assemblages in the different patches investigated are responsible for this pattern.

4.3. Contribution of TEP-C to POC

The relative contribution of the TEP-C to POC was estimated for each depth by the molar ratio of TEP-C_{micro} to POC in the water column that ranged between 1.5 and 68 %. TEP-C_{micro} accounted for 12 % of POC in the photic zone and was slightly lower than our estimate for the photic zone in the same area during an earlier cruise to this study site (June 2004), where 26 ± 4 % was observed (TEP-C_{color}:POC, mean ± confidence interval at 95 %, n = 31) (Harlay *et al.*, in prep). The contribution of TEP-C to POC during this coccolithophorid bloom is in the range reported in previous studies, which indicated a contribution of TEP-C to POC ranging between 17 % and 54 % (Mari, 1999; Engel and Passow, 2001; Engel, 2002). Statistically, no significant changes were detected after 9 days at station 1.

4.4. TEP production and carbon cycling

The decoupling from inorganic nutrient of carbon production by carbon over-consumption (Engel *et al.*, 2002; Schartau *et al.*, 2007) suggests that the flux of particulate carbon might be enhanced when TEP is produced, rendering coccolithophores good candidates for the export and sequestration of carbon. Several studies have shown that the balance between TEP and solid particles, such as cells, co-determines the efficiency of particle coagulation and formation of macroscopic aggregates (Logan *et al.*, 1995; Engel, 2000; Kahl *et al.*, 2008). Particle aggregates are a major vehicle for organic matter export to the deep ocean. Coccolithophores potentially enhance the efficiency of organic matter export through the addition of mineral ballast (François *et al.*, 2002; Klaas and Archer, 2002). Hence, TEP production during coccolithophorid blooms may control aggregate formation and enhance organic matter export (De la Rocha and Passow, 2007). The deposition of gelatinous detritus mixed with *E. huxleyi* at the seafloor has been described by Cadée (1985) for the North Sea. Based on the sinking velocity of coccoliths and coccospheres, Holligan *et al.* (1993b) estimated the time required for the coccolithophore optical signature to disappear from satellite images to be > 200 d in the North Sea. However, the effective life-time of coccolithophorid blooms does not exceed 40 d after the optical signature appears (Holligan *et al.,* 1993b). The persistence of coccolithophores in waters depleted in nutrients for 3 to 6 weeks and the potential production of up to 400 coccoliths per cell with a mean delay of 2-3 hours per coccolith (Linschooten *et al.*, 1991; Fernandez *et al.*, 1993) suggest that cells remain active for several weeks after the onset of the bloom. If carbon over-consumption can be applied to coccolithophorid physiology, one can suspect that the significance of coccolithophores in carbon cycling, at least the bloom-forming species *E. huxleyi*, has been under-evaluated. The *E. huxleyi* blooms could result in massive aggregation events that wash out the surface waters from detritus and particles.

Our survey did probably not cover any massive aggregation phase of the coccolithophorid bloom because of the small size of TEP. Therefore, the contribution of TEP in coccolithophore aggregates to the vertical export was not quantified in this study. However, the deposition of gelatinous detritus over the continental slope of the Bay of Biscay has been found to occur later in the summer (de Wilde *et al.*, 1998: McCave *et al.*, 2001). Pigment analysis and scanning electron microscopy of particulate samples in late August 1995 showed that coccolithophores were the major contributors to this mass deposition (de Wilde *et al.*, 1998). The carbon content of the deposited mucus layer represented 250 mmol C m^{-2} and covered an area of 50 000 km² (de Wilde *et al.*, 1998), comparable to the 65 000 km² surface area of a coccolithophorid bloom at the continental margin of the Gulf of Biscay observed in June 2006. Since specific pigments are well preserved together with the carbonates, this detrital mass deposition indicates a tight coupling of particulate matter export and surface production of coccolithophores. The production of TEP observed during the present study could constitute the first step within the process of coccolithophore aggregation, sedimentation and sea floor deposition in the Bay of Biscay.

5. Conclusions

The present study shows agreement between the vertical distribution of TEP determined with the microscopic (this study) and the colorimetric (Engel, 2004; Harlay *et al.*, in prep) approaches. The estimates of TEP-C obtained with the microscopic approach are comparable to those previously obtained with the colorimetric one in the Bay of Biscay (coccolithophorid bloom in June 2004, Harlay *et al.*, in prep) and during an offshore transect at the same latitude in the NE Atlantic Ocean (Engel, 2004). High absorbance of particles issued from the area where coccolithophores occurred, or had occurred in the past history of the water mass,

has been pointed out. We suggest that during coccolithophorid blooms, the production of TEP is also occuring, as already determined for other phytoplankton groups (Passow, 2002) as a possible consequence of carbon over-consumption by this taxon. The implication of those particles into the seasonal cycling of carbon is enhanced by the physical properties of the water column. The formation of aggregates potentially contributes, through the ballast of aggregates with biogenic calcite, to efficient and rapid export of carbon out of the photic layer and important deposition over the seafloor. Carbon over-consumption by phytoplankton and the subsequent transformation of the cellular releases into TEP (Schartau *et al.*, 2007) accounts for an additional sink for carbon sequestration in coccolithophorid blooms, where the efficiency of the carbon pump may not be limited to the production of biomass, as computed from variations in Chl-a concentration (e.g. Iglesias-Rodriguez *et al.*, 2002). However, such a mechanism has been neglected in carbon inventories because of the complexity of the study of gel phases in marine environments. The significance of gel particles in the global carbon cycle may have been underestimated, so far, and improvement in the description of these processes is required to better constrain this flux as well as the development of techniques to estimate the coupling between the surface and the seafloor.

Further effort is then needed to increase the reproducibility of both approaches for estimating TEP-C. The microscopic approach, less sensitive to coccolithophorid density and changes in TEP stainability, provided a reliable estimate of the carbon content of TEP during this study. However, its use as a routine method for TEP determination during multidisciplinary studies is often discarded against the colorimetric technique that requires less man-time and expertise. However, highly coloured TEP do not necessarily reflect high TEP-C (TEP-C_{micro}:POC of 12 %) but suggest different chemical properties of their constituents. Improvement of the methods is a particular challenge for studying possible changes in polysaccharides chemical composition of TEP in aging-bloom situations (polysaccharide

diagenesis) or to directly determine TEP-C in the field, since conversion factors obtained from phytoplankton blooms can only give rough estimates in peculiar conditions.

Acknowledgements

The authors would like to thank the officers and crewmembers of the RV Belgica for their logistic support on board the ship during the survey conducted in the northern Bay of Biscay. Joan Backers, Jean-Pierre De Blauw and Gregory Deschepper of the Unit of the North Sea Mathematical Models (Brussels/Oostende, Belgium) are acknowledged for their support in data acquisition during the cruise. This study was financed by the Belgian Federal Science Policy Office in the framework of the PEACE project (contract no. SD/CS/03A/B) and by the Helmholtz Association (contract no. HZ-NG-102). C. De Bodt was supported by a PhD grant from the EU FP6 IP CarboOcean project (contract no. 511176–2). N. Van Oostende received a PhD grant from the Institute for the Promotion of Innovation through Science and Technology in Flanders (IWT-Vlaanderen). This is also a contribution to the EU FP6 European Network of Excellence EUR–OCEANS (contract no. 511106-2) and a Belgian input to the SOLAS international research initiative.

References

ALLDREDGE A. L., PASSOW U., AND LOGAN B. E. (1993) The abundance and significance of a class of large, transparent organic particles in the ocean. *Deep Sea Research Part I: Oceanographic Research Papers* **40**, 1131-1140.

BALCH W. M., KILPATRICK K. A., HOLLIGAN P., HARBOUR D., AND FERNANDEZ E. (1996) The 1991 coccolithophore bloom in the central North Atlantic.2. Relating optics to coccolith concentration. *Limnology and Oceanography* **41**, 1684-1696.

BARLOW R. G., MANTOURA R. F. C., CUMMINGS D. G., POND D. W., AND HARRIS R. P. (1998) Evolution of phytoplankton pigments in mesocosm experiments. *Estuarine, Coastal and Shelf Science* **46**, 15-22.

BARLOW R. G., MANTOURA R. F. C., GOUGH M. A., AND FILEMAN T. W. (1993) Pigment signatures of the phytoplankton composition in the northeastern Atlantic during the 1990 spring bloom. *Deep Sea Research Part II: Topical Studies in Oceanography* **40**, 459-477.

BERMAN T. AND VINER-MOZZINI Y. (2001) Abundance and characteristics of polysaccharide and proteinaceous particles in Lake Kinneret. *Aquatic Microbial Ecology* **24**, 255-264.

BROWN C. W. AND YODER J. A. (1994) Coccolithophorid blooms in the global ocean. *Journal of Geophysical Research* **99**, 7467-7482.

BRUSSAARD C. P. D., KUIPERS B., AND VELDHUIS M. J. W. (2005) A mesocosm study of *Phaeocystis globosa* population dynamics: I. Regulatory role of viruses in bloom control. *Harmful Algae* **4**, 859-874.

CADÉE G. C. (1985) Macroaggregates of *Emiliana huxleyi* in sediment traps. *Marine Ecology-Progress Series* **24**, 193-196.

CATSBERG T., LARSEN A., SANDAA R. A., BRUSSAARD C. P. D., EGGE J. K., HELDAL M., THYRHAUG R., VAN HANNEN E. J., AND BRATBAK G. (2001) Microbial population dynamics and diversity during a bloom of the marine coccolithophorid *Emiliania huxleyi* (Haptophyta). *Marine Ecology-Progress Series* **221**, 39-43.

DE LA ROCHA C. L. AND PASSOW U. (2007) Factors influencing the sinking of POC and the efficiency of the biological carbon pump. *Deep Sea Research Part II: Topical Studies in Oceanography* **54**, 639-658.

DE WILDE P. A. W. J., DUINEVELD G. C. A., BERGHUIS E. M., LAVALEYE M. S. S., AND KOK A. (1998) Late-summer mass deposition of gelatinous phytodetritus along the slope of the N.W. European Continental Margin. *Progress in Oceanography* **42**, 165-187.

DELILLE B., HARLAY J., ZONDERVAN I., JACQUET S., CHOU L., WOLLAST R., BELLERBY R. G. J., FRANKIGNOULLE M., BORGES A. V., RIEBESELL U., AND GATTUSO J.-P. (2005) Response of primary production and calcification to changes of pCO_2 during experimental blooms of the coccolithophorid *Emiliania huxleyi*. *Global Biogeochemical Cycles* **19**, GB2023.

EGGE J. K. AND AKSNES D. L. (1992) Silica as regulating nutrient in phytoplankton competition. *Marine Ecology-Progress Series* **83**, 281-289.

ENGEL A. (2000) The role of transparent exopolymer particles (TEP) in the increase in apparent particle stickiness ( ) during the decline of a diatom bloom. *Journal of Plankton Research* **22**, 485-497.

ENGEL A. (2002) Direct relationship between CO_2 uptake and transparent exopolymer particles production in natural phytoplankton. *Journal of Plankton Research* **24**, 49-53.

ENGEL A. (2004) Distribution of transparent exopolymer particles (TEP) in the northeast Atlantic Ocean and their potential significance for aggregation processes. *Deep Sea Research Part I: Oceanographic Research Papers* **51**, 83-92.

ENGEL, A. (2009) Marine Gel Particles, Practical Guidelines for the Analysis of Seawater, Wurl. O. (ed.), CRC Press, Taylor and Francis Group, Boca Rayton, Florida, USA, *in press*.

ENGEL A., DELILLE B., JACQUET S., RIEBESELL U., ROCHELLE-NEWALL E., TERBRUGGEN A., AND ZONDERVAN I. (2004) Transparent exopolymer particles and dissolved organic carbon production by *Emiliania huxleyi* exposed to different CO_2 concentrations: a mesocosm experiment. *Aquatic Microbial Ecology* **34**, 93-104.

ENGEL A., GOLDTHWAIT S., PASSOW U., AND ALLDREDGE A. L. (2002) Temporal decoupling of carbon and nitrogen dynamics in a mesocosm diatom bloom. *Limnology and Oceanography* **47**, 753-761.

ENGEL A. AND PASSOW U. (2001) Carbon and nitrogen content of transparent exopolymer particles (TEP) in relation to their Alcian Blue adsorption. *Marine Ecology-Progress Series* **219**, 1-10.

ENGEL A., ZONDERVAN I., AERTS K., BENTHIEN A., CHOU L., DELILLE B., GATTUSO J.-P., HARLAY J., HEEMANN C., HOFFMANN L., JACQUET S., NEJSTGAARD J., PIZAY M.-D., ROCHELLE-NEWALL E., SCHNEIDER U., TERBRUEGGEN A., AND RIEBESELL U. (2005) Testing the direct effects of CO_2 concentration on marine phytoplankton: A mesocosm experiment with the coccolithophorid *Emiliania huxleyi*. *Limnology and Oceanography* **50**, 493-507.

FERNÁNDEZ E., BOYD P. W., HOLLIGAN P. M., AND HARBOUR D. S. (1993) Production of organic and inorganic carbon within a large-scale coccolithophore bloom in the northeast Atlantic Ocean. *Marine Ecology-Progress Series.* **97**, 271-285.

FRANÇOIS R., HONJO S., KIRSHFIELD R., AND MANGANINI S. (2002) Factors controlling the flux of organic carbon to the bathypelagic zone of the ocean. *Global Biogeochemical Cycles* **16**, 1-20.

GARCIA C. M., PRIETO L., ECHEVARRIA F., GARCIA-LAFUENTE J., RUIZ J., RUIZ J., AND RUBIN J. P. (2002) Hydrodynamics and the spatial distribution of plankton and TEP in the Gulf of Cadiz (SW Iberian Peninsula). *Journal of Plankton Research* **24**, 817-833.

GRASSHOFF K., EHRHARDT M., AND KREMLING K. (1983) *Methods of seawater analysis*. Verlag Chemie.

GREPMA (1988). Satellite (AVHRR:NOAA-9) and ship studies of a coccolithophorid bloom in the western English Channel. (Viollier, M., Sournia, A., Birrien, M.-J., Chrétiennot-Dinet, P., Le Borgne, P., Le Corre, P., Morin, P., and Olry, J. P.) *Marine Nature* **1**(1), 1-14.

GROSSART H.-P., SIMON M., AND LOGAN B. E. (1997) Formation of macroscopic organic aggregates (Lake snow) in a large lake: The significance of transparent exopolymer particles, phytoplankton, and zooplankton. *Limnology and Oceanography* **42**, 1651-1659.

HOLLIGAN P. M., FERNÁNDEZ E., AIKEN W., BALCH W. M., BOYD P. W., BURKILL P. H., FINCH M., GROOM S. B., MALIN G., MULLER K., PURDIE D. A., ROBINSON C., TREES C. C., TURNER S. M., AND VAN DER WAL P. (1993a) A biogeochemical study of the coccolithophore, *Emiliania huxleyi*, in the North Atlantic. *Global Biogeochemical Cycles* **7**, 879-900.

HOLLIGAN P. M., GROOM S. B., AND HARBOUR D. S. (1993b) What controls the distribution of the coccolithophore *Emiliania huxleyi* in the North Sea? *Fisheries Oceanography* **2**, 175-183.

HOLLIGAN P. M., VIOLLIER M., HARBOUR D. S., CAMUS P., AND CHAMPAGNE-PHILIPPE M. (1983) Satellite and ship studies of coccolithophore production along a continental shelf edge. *Naure* **304**, 339-342.

HUTHNANCE J. M., COELHO H., GRIFFITHS C. R., KNIGHT P. J., REES A. P., SINHA B., VANGRIESHEIM A., WHITE M., AND CHATWIN P. G. (2001) Physical structures, advection and mixing in the region of Goban spur. *Deep Sea Research Part II: Topical Studies in Oceanography* **48**, 2979-3021.

IGLESIAS-RODRIGUEZ M. D., BROWN C. W., DONEY S. C., KLEYPAS J., KOLBER D. D., AND KOLBER Z. (2002) Representing key phytoplankton functional groups in ocean carbon cycle models: Coccolithophorids. *Global Biogeochemical Cycles*, doi:10.1029/2001GB001454.

JACQUET S., HELDAL M., IGLESIAS-RODRIGUEZ M. D., LARSEN A., WILSON W., AND BRATBAK G. (2002) Flow cytometric analysis of an *Emiliania huxleyi* bloom terminated by viral infection. *Aquatic Microbial Ecology* **27**, 111-124.

JOINT I., WOLLAST R., CHOU L., BATTEN S., ELSKENS M., EDWARDS E., HIRST A., BURKILL P. H., GROOM S., GIBB S., MILLER A., HYDES D. J., DEHAIRS F., ANTIA A. N., BARLOW R., REES A., POMROY A., BROCKMANN U., CIMMINGS D., LAMPITT R., LOIJENS M., MANTOURA F., MILLER P., RAABE T., ALVAREZ-SALGADO X., STELFOX C., AND WOOLFENDEN J. (2001) Pelagic production at the Celtic Sea shelf break. *Deep Sea Research Part II: Topical Studies in Oceanography* **48**, 3049-3081.

KAHL L. A., VARDI A., AND SCHOFIELD O. (2008) Effects of phytoplankton physiology on export flux. *Marine Ecology-Progress Series* **354**, 3-19.

KLAAS C. M. AND ARCHER D. E. (2002) Association of sinking organic matter with various types of mineral ballast in the deep sea: Implications for the Rain Ratio. *Global Biogeochemical Cycles* **16**, doi: 10.1029/2001GB001765.

KEPKAY P. E. (1994) Particle aggregation and the biological reactivity of colloids. *Marine Ecology-Progress Series* **109**, 293-304.

KREMBS C. AND ENGEL A. (2001) Abundance and variability of microorganisms and transparent exopolymeric particles across the ice-water interface of melting first year sea ice in the Laptev Sea (Arctic). *Marine Biology* **138**, 173-185.

LEPPARD G. G. (1995) The characterization of algal and microbial mucilages and their aggregates in aquatic ecosystems. *Science of the Total Environment* **165**, 103-131.

LINSCHOOTEN C., VAN BLEIJSWIJK J. D. L., VAN EMBURG P. R., DE VRIND J. P. M., KEMPERS E. S., WESTBROEK P., AND DE VRIND-DE JONG E. W. (1991) Role of light-dark cycle and medium composition on the production of coccoliths by *Emiliania huxleyi* (Haptophyceae). *J Phycol* **27**, 82-86.

LOGAN B. E., PASSOW U., ALLDREDGE A. L., GROSSART H.-P., AND SIMON M. (1995) Rapid formation and sedimentation of large aggregates is predictable from coagulation rates (half-lives) of transparent exopolymer particles (TEP). *Deep Sea Research Part II: Topical Studies in Oceanography* **42**, 203-214.

MARI X. (1999) Carbon content and C:N ratio of transparent exopolymeric particles (TEP) produced by bubbling exudates of diatoms. *Marine Ecology-Progress Series* **183**, 59-71.

MARI X., BEAUVAIS S., LEMEE R., AND PEDROTTI M. L. (2001) Non-Redfield C : N ratio of transparent exopolymeric particles in the northwestern Mediterranean Sea. *Limnology and Oceanography* **46**, 1831-1836.

MARI X. AND BURD A. (1998) Seasonal size spectra of transparent exopolymeric particles (TEP) in a coastal sea and comparision with those predicted using coagulation theory. *Marine Ecology-Progress Series* **163**, 63-76.

MARI X. AND KIORBOE T. (1996) Abundance, size distribution and bacterial colonization of transparent exopolymeric particles (TEP) during spring in the Kattegat. *Journal of Plankton Research* **18**, 969-986.

MCCAVE I. N., HALL I. R., ANTIA A. N., CHOU L., DEHAIRS F., LAMPITT R. S., THOMSEN L., VAN WEERING T. C. E., AND WOLLAST R. (2001) Distribution, composition and flux of particulate material over the European margin at 47°-50°N. *Deep Sea Research Part II: Topical Studies in Oceanography* **48**, 3107-3139.

MYKLESTAD S. M. (1995) Release of extracellular products by phytoplankton with special emphasis on polysaccharides. *Science of the Total Environment* **165**, 155-164.

O'REILLY J.E., MARITORENA S., MITCHELL B.G., SIEGEL D.A., CARDER K.L., GARVER S.A., KAHRU M., AND MCCLAIN C. (1998) Ocean color chlorophyll algorithms for SeaWiFS *Journal of Geophysical Research-Oceans*, **103**, 24937-24953.

PAASCHE E. (2002) A review of the coccolithophorid *Emiliania huxleyi* (Prymnesiophyceae), with particular reference to growth, coccolith formation, and calcification-photosynthesis interactions. *Phycol.* **40**, 503-529.

PASSOW U. (2002) Transparent exopolymer particles (TEP) in aquatic environments. *Progress in Oceanography* **55**, 287-333.

PASSOW U. AND ALLDREDGE A. L. (1995a) A dye-binding assay for the spectrophotometric measurement of transparent exopolymer particles (TEP). *Limnology Oceanography* **40**, 1326-1335.

PASSOW U. AND ALLDREDGE A. L. (1995b) Aggregation of a diatom bloom in a mesocosm: The role of transparent exopolymer particles (TEP). *Deep Sea Research Part II: Topical Studies in Oceanography* **42**, 99-109.

PRIETO L., NAVARRO G., COZAR A., ECHEVARRIA F., AND GARCIA C. M. (2006) Distribution of TEP in the euphotic and upper mesopelagic zones of the southern Iberian coasts. *Deep Sea Research Part II: Topical Studies in Oceanography* **53**, 1314-1328.

RADIC T., KRAUS R., FUKS D., RADIC J., AND PECAR O. (2005) Transparent exopolymeric particles' distribution in the northern Adriatic and their relation to microphytoplankton biomass and composition. *Science of the Total Environment* **353**, 151-161.

RIEGMAN R., STOLTE W., NOODERLOOS A. A. M., AND SLEZAK D. (2000) Nutrient uptake and alkaline phosphatase (ec 3:1:3:1) activity of *Emiliania huxleyi* (prymnesiophyceae) during growth under N and P limitation in continuous cultures. *Journal of Phycology* **36**, 87-96.

SCHARTAU M., ENGEL A., SCHRÖTER J., THOMS S., VÖLKER C., AND WOLF-GLADROW D. (2007) Modelling carbon overconsumption and the formation of extracellular particulate organic carbon. *Biogeosciences Discussions* **4**, 13-67.

SHACKELFORD R. AND COWEN J. P. (2006) Transparent exopolymer particles (TEP) as a component of hydrothermal plume particle dynamics. *Deep Sea Research Part I: Oceanographic Research Papers* **53**, 1677-1694.

SUGIMOTO K., FUKUDA H., BAKI M. A., AND KOIKE I. (2007) Bacterial contributions to formation of transparent exopolymer particles (TEP) and seasonal trends in coastal waters of Sagami Bay, Japan. *Aquatic Microbial Ecology* **46**, 31-41.

TYRRELL T. AND MERICO A. (2004) *Emiliania huxleyi*: bloom observations and the conditions that induce them. In *Coccolithophores. From molecular Processes to global Impact* (ed. H. R. Thierstein and J. R. Young). pp. 75-97. Springer.

WOLLAST R. AND CHOU L. (2001) Ocean Margin EXchange in the Northern Gulf of Biscay: OMEX I. An introduction. *Deep Sea Research Part II: Topical Studies in Oceanography* **48**, 2971-2978.

WOTTON R. (2004) The ubiquity and many roles of exopolymers (EPS) in aquatic systems. *Scientia Marina* **68**, 13-21.

WRIGHT S.W. AND JEFFREY S.W. (1997) High-resolution HPLC system for chlorophylls and carotenoids of marine phytoplankton. in *Phytoplankton pigments in oceanography*. 327-341. (eds.) S.W. Jeffrey, R.F.C. Mantoura and S.W. Wright (UNESCO Publishing)

YENTSCH C. S. AND MENZEL D. W. (1963) A method for the determination of phytoplankton chlorophyll and phaeophytin by fluorescence. *Deep Sea Research and Oceanographic Abstracts* **10**, 221-231.

Tables

Table 1: Maximum values in the upper 160 m of some parameters described for each station referred by station number and their sampling date. The thickness of the photic zone refers to the depth at which 1% of the incoming PAR is measured ($Z_{1\%}$). Chl-a_{max} [µg L^{-1}] and POC_{max} [µmol L^{-1}] represent the highest levels of Chl-a and POC per profile. The values of the maximum of absorbance at each station (normalized per liter of seawater) are quoted as TEP_{color} [Abs] for the colorimetric determination of TEP (TEP_{color}). The following columns present the maxima of total area [µm² ml^{-1}], abundance [ml^{-1}] and carbon content estimate [µmol C L^{-1}] of the TEP_{micro}.

(*) stations located within the HR patch

(n.d.) parameter not determined

(Table 1)

Stations	Date	$Z_{1\%}$	Chl-a max	POC max	TEP_{color} [Abs]	area TEP_{micro}	abund. TEP_{micro}	$TEP\text{-}C_{micro}$
		m	µg L^{-1}	µmol L^{-1}	per L of SW	µm² ml^{-1}	ml^{-1}	µmol C L^{-1}
1	2006-05-31	30	1.49	11.7	4.10	11.6	$43.71x10^3$	5.25
1bis	2006-06-09	37	0.89	17.3	21.72	4.9	$15.40x10^3$	2.05
2	2006-06-01	31	2.01	14.8	31.67	2.8	$9.67x10^3$	1.57
3	2006-06-01		1.47	n.d.	7.55	3.2	$6.86x10^3$	0.78
4	2006-06-01	26	1.46	16.0	1.79	3.2	$6.23x10^3$	1.63
4bis*	2006-06-08	27	1.33	11.2	8.17	24.1	$2.02x10^3$	2.42
5	2006-06-02		1.3	n.d.	1.41	n.d.	n.d.	n.d.
6	2006-06-07		1.62	n.d.	14.93	n.d.	n.d.	n.d.
7*	2006-06-07	26	1.43	24.6	4.93	37.3	$18.92x10^3$	1.85
8*	2006-06-06	34	0.8	14.6	2.10	11.3	$6.13x10^3$	0.68

Figure Captions

Figure 1: Locations of the sampling stations along the 200 m (stations 1, 4, 5 and 8) and 2000 m (stations 3 and 6) isobaths superimposed on MODIS images of Chl-a (left) and Reflectance (right) satellite images on the 1st of June 2006 (a, b) and on the 5th of June 2006 (c, d) in the northern Bay of Biscay. The Chl-a concentrations are graphically represented by the gradient from violet to red (with units mg Chl-a m^{-3}). The high reflectance patches are represented by the brighter blue-white areas on the reflectance images.

Figure 2: Vertical profiles of temperature and phosphate concentration (PO4) in the upper 160 m over the continental shelf (stations 1, 1bis, 4, 4bis, 7 and 8) and over the slope (stations 2, 3, 5 and 6). Grey symbols represent the revisited stations; PO_4 concentrations were similar at the revisited stations 1bis and 4bis (superposed dots). For this figure and the following ones, the organization of the stations on the chart follows the geographic localization of the stations (stations 8, 7, 4 and 1 are located on the shelf and stations 5, 2, 6 and 3 are located on the slope), as represented in the inner box showing station names and the bathymetry of the area.

Figure 3: Vertical profiles of chlorophyll-a (Chl-a) concentration [$\mu g\ L^{-1}$] (black dots) and relative contribution of the coccolithophorid biomass (crosses), as represented by the ratio of the diagnostic pigments for coccolithophores (19'-hexanoyloxyfucoxanthin, HexaFx) and diatoms (fucoxanthin, Fx) on the lower scale. Station 5 was not sampled for diagnostic pigments concentrations. Grey symbols represent the revisited stations (1bis and 4bis).

Figure 4: Particulate organic carbon (POC) concentration [µmol C L^{-1}] (black dots) and TEP-C_{micro} estimates [µmol C L^{-1}]. Grey symbols represent the revisited stations (1bis and 4bis). Stations 3, 5 and 6 were not sampled for POC; station 3 and 5 were not sampled for TEP-C.

Figure 5: TEP_{color} expressed in % of relative absorbance compared to the maximum absorbance obtained for each station. Grey symbols represent the values at the revisited stations 4bis and 1bis.

Figure 6: Variation with depth (m) of TEP_{micro} volume concentration [μm^3 ml^{-1} μm^{-1}] per size class (equivalent spherical diameter (ESD) in µm) at station 8. The volume concentration was calculated on the assumption of the spherical shape of particles and represents the mean volume of the particles in a given size class, in one ml of the sample.

Figure 7: Abundance of TEP_{micro} [$\times 10^3$ ml^{-1}] of seawater. Stations 5 and 6 were not sampled for this parameter. Grey symbols represent the values at the revisited stations 4bis and 1bis.

Figure 8: Differential TEP size distribution at Station 1 (10 m) and the spectral slope (δ) fitted to the data by a linear regression (r^2=0.99) over the size spectrum of particles represented by the mean equivalent spherical diameter in the size class (ESD in µm). The Y-intercept of the regression line corresponds to Log k.

Figure 9: Spectral slope (δ) of the TEP_{micro} size distributions. An increase of δ corresponds to an increase of the fraction of large TEP_{micro}. Grey symbols represent the values at the revisited stations 4bis and 1bis. Stations 5 and 6 were not sampled for this parameter.

Figures

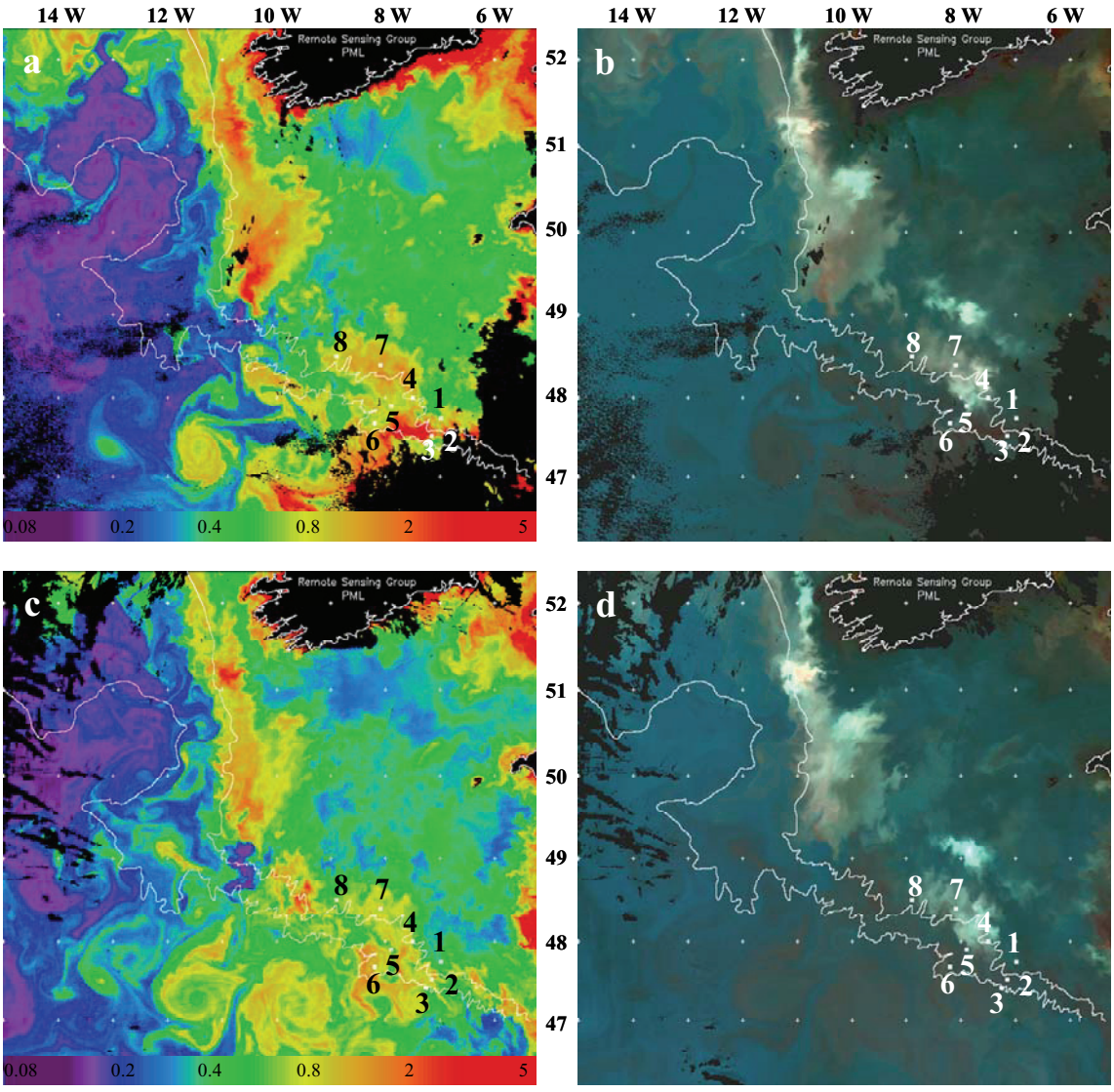

Figure 1

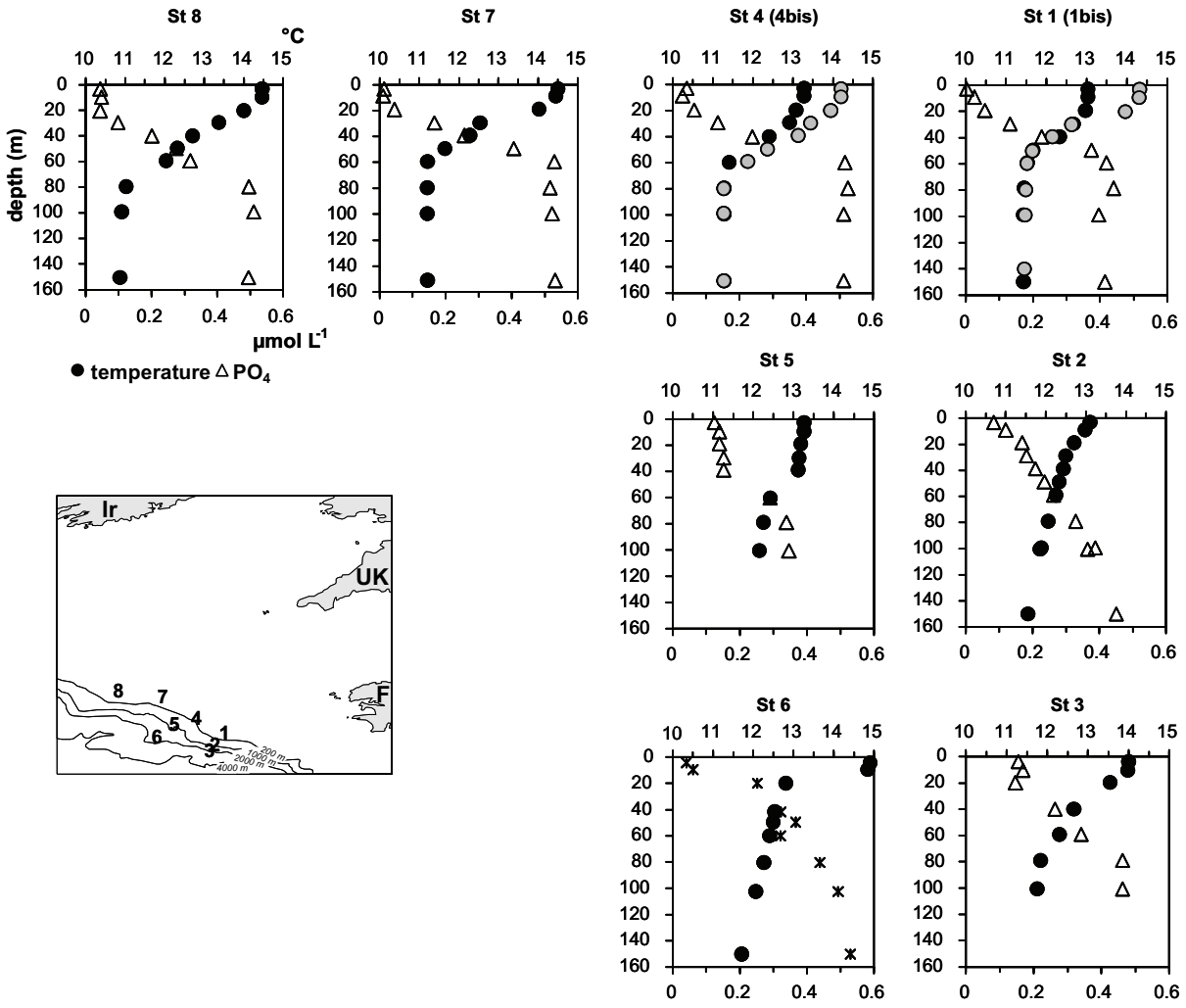
St 8
St 7
St 4 (4bis)
St 1 (1bis)
St 5
St 2
St 6
St 3
°C
depth (m)
µmol L-1
● temperature △ PO4
Ir
UK
F
8
7
4
5
6
1
2
3
1000 m
2000 m
4000 m

Figure 2

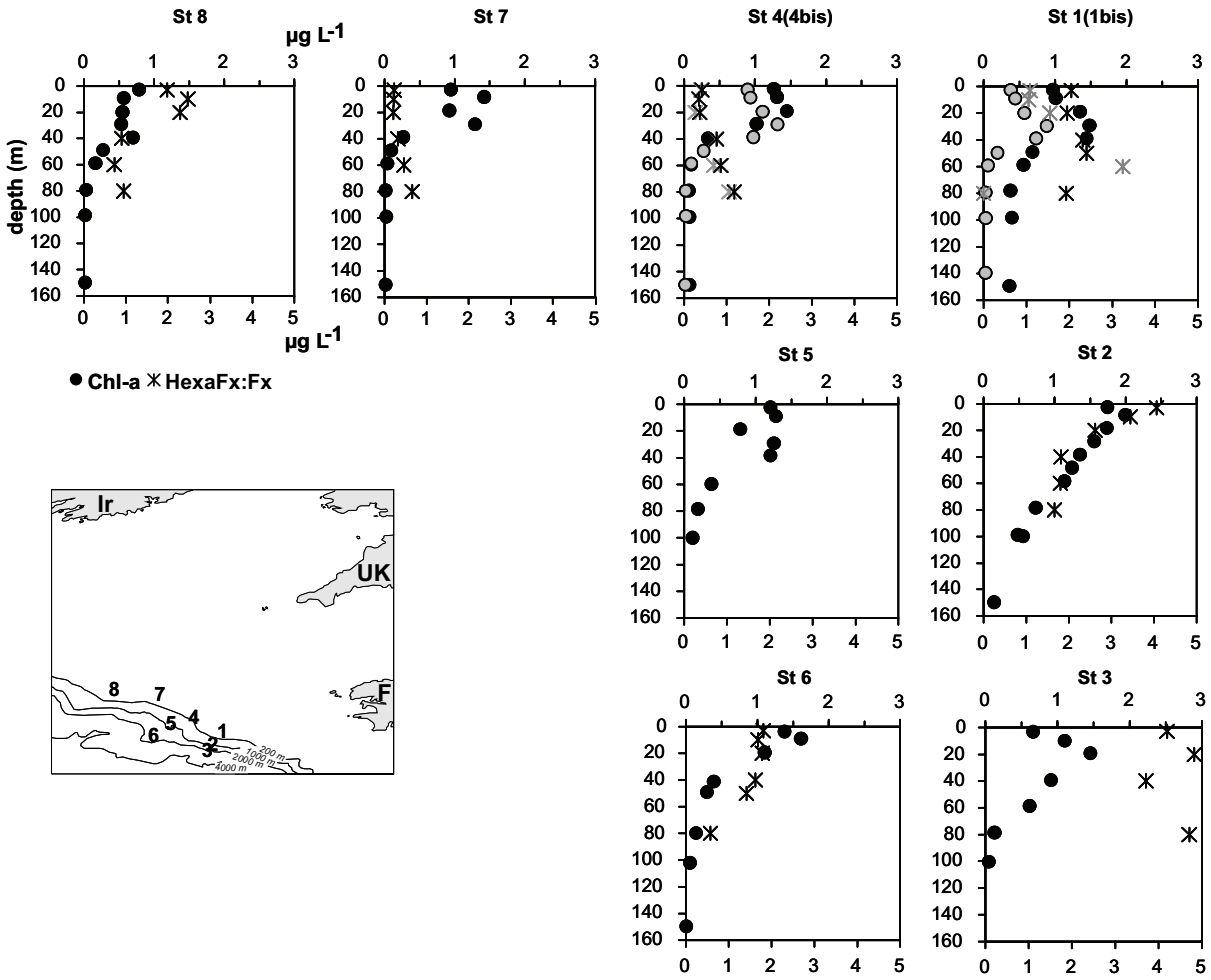
St 8
St 7
St 4(4bis)
St 1(1bis)
St 5
St 2
St 6
St 3
µg L-1
depth (m)
Chl-a HexaFx:Fx
Ir
UK
F
8
7
5
4
6
1
3
2
1000 m
2000 m
4000 m

Figure 3

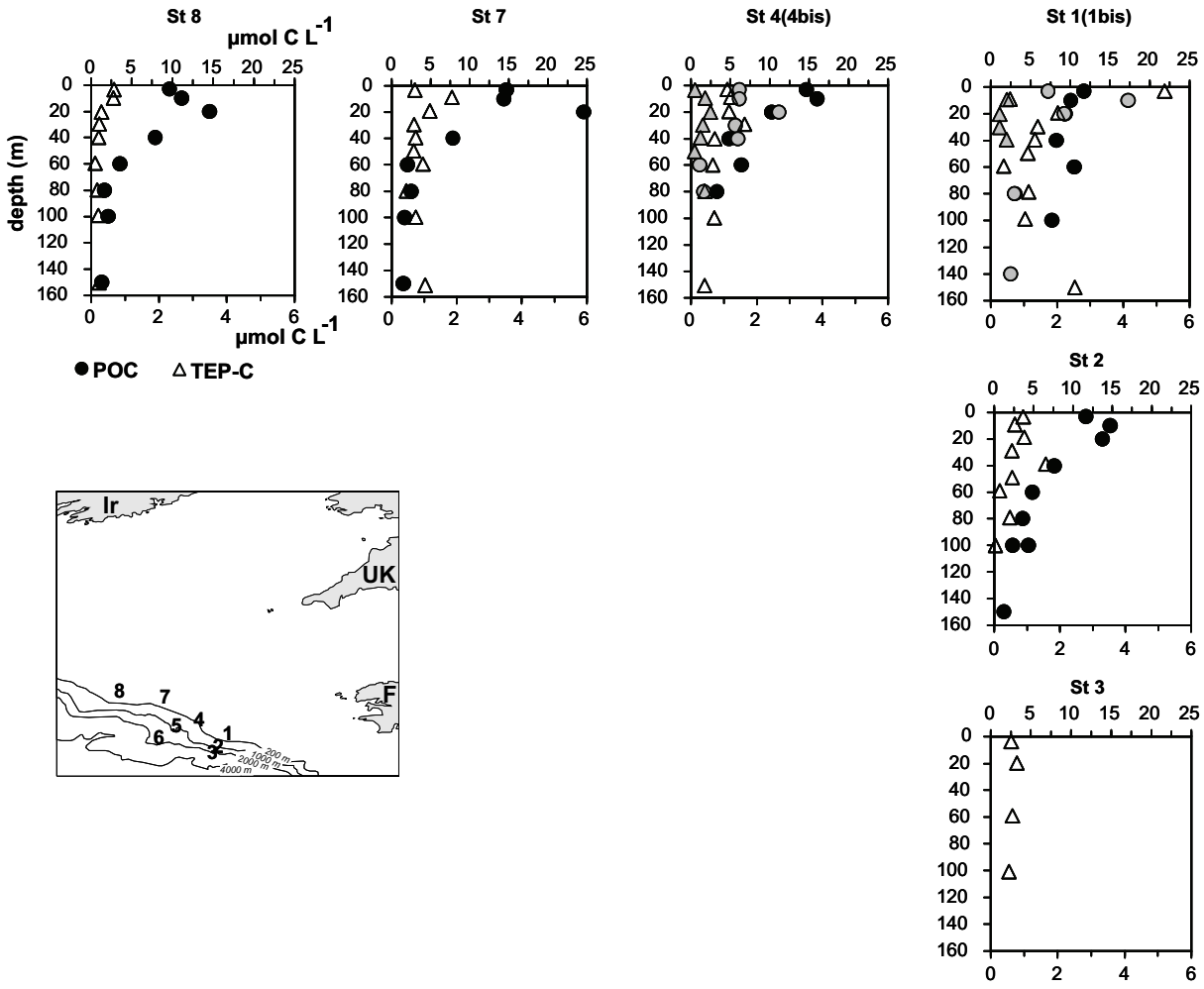
St 8
St 7
St 4(4bis)
St 1(1bis)
St 2
St 3
µmol C L-1
depth (m)
POC
TEP-C
Ir
UK
F
8
7
6
5
4
3
2
1
200 m
1000 m
2000 m
4000 m

Figure 4

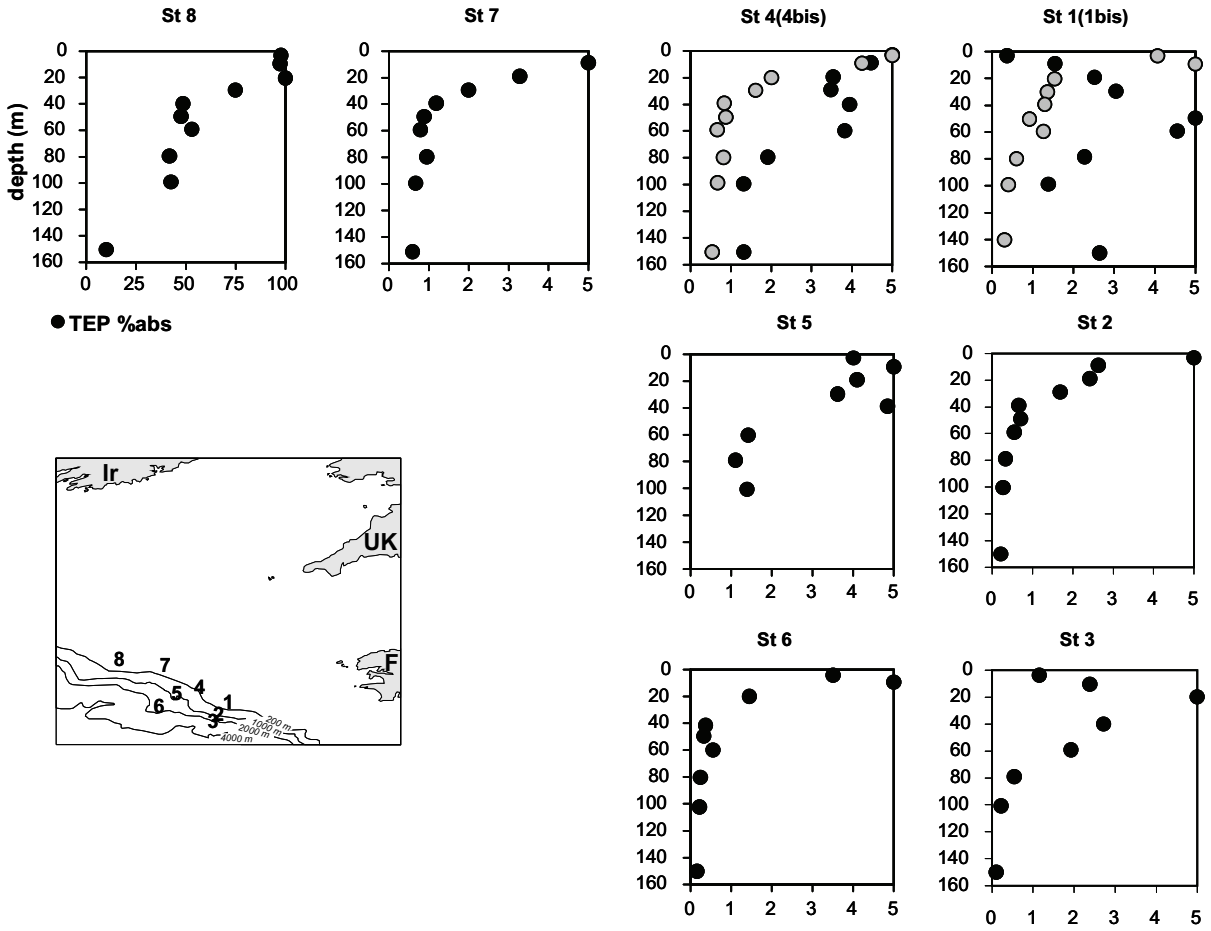
St 8
St 7
St 4(4bis)
St 1(1bis)
St 5
St 2
St 6
St 3
depth (m)
TEP %abs
Ir
UK
F
8
7
4
5
1
6
2
3
200 m
1000 m
2000 m
4000 m

Figure 5

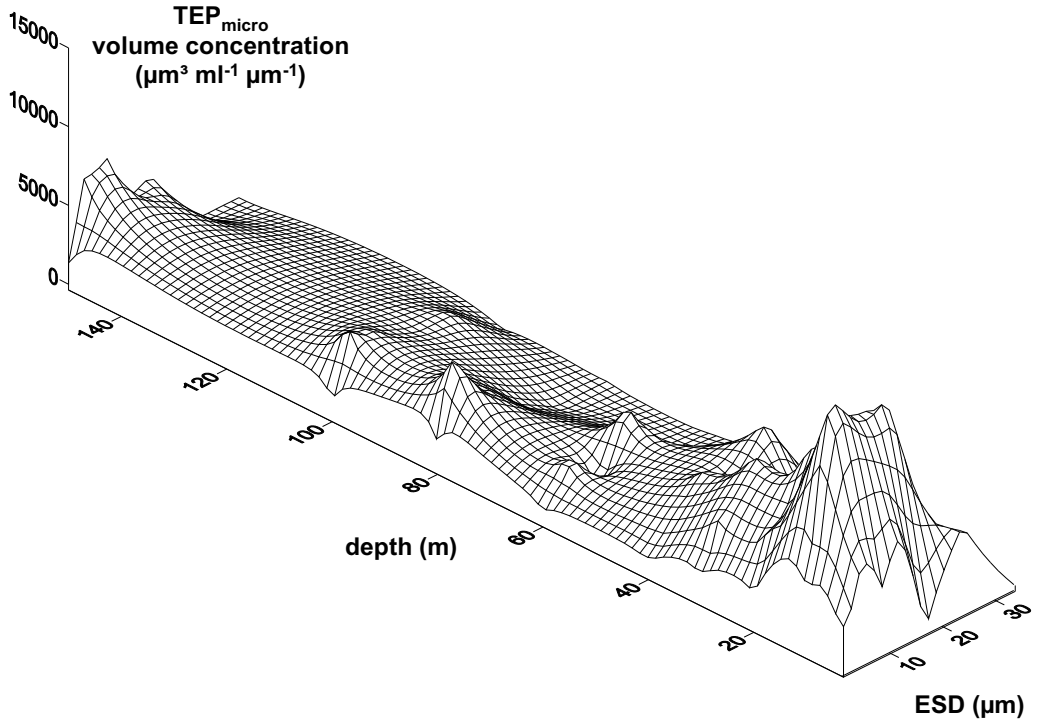
TEP micro
volume concentration
(µm³ ml-1 µm-1)
15000
10000
5000
0
140
120
100
80
60
40
20
depth (m)
10
20
30
ESD (µm)

Figure 6

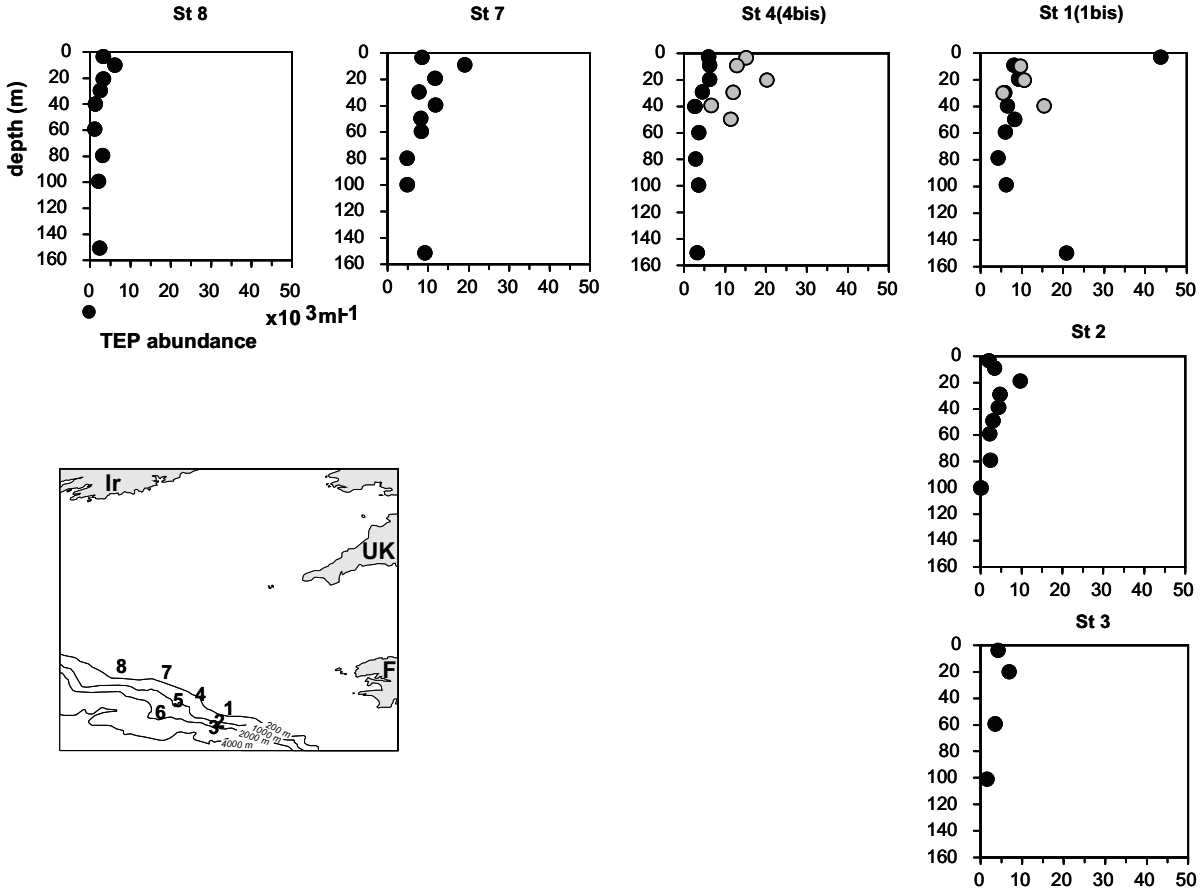
St 8
St 7
St 4(4bis)
St 1(1bis)
St 2
St 3
depth (m)
TEP abundance
x10 3ml-1
Ir
UK
F
8
7
6
5
4
3
2
1
200 m
1000 m
2000 m
4000 m

Figure 7

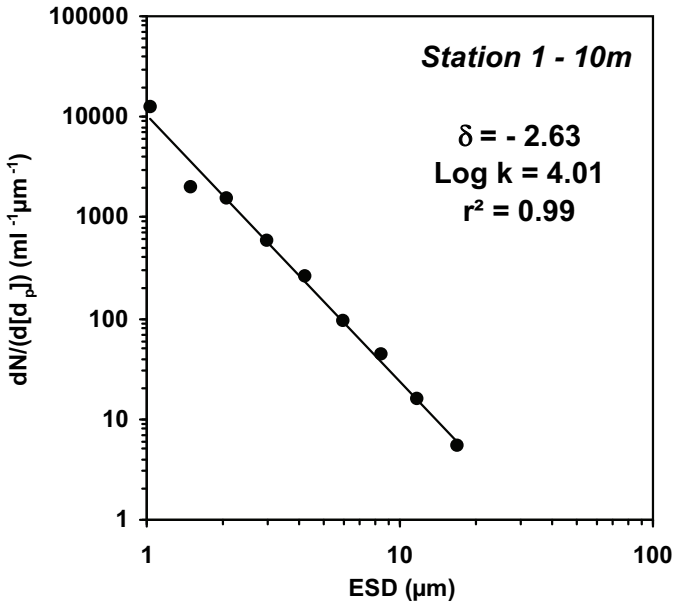
Station 1 - 10m
δ = - 2.63
Log k = 4.01
r² = 0.99
dN/(d[d_pl]) (ml⁻¹µm⁻¹)
ESD (µm)
100000
10000
1000
100
10
1
1
10
100

Figure 8

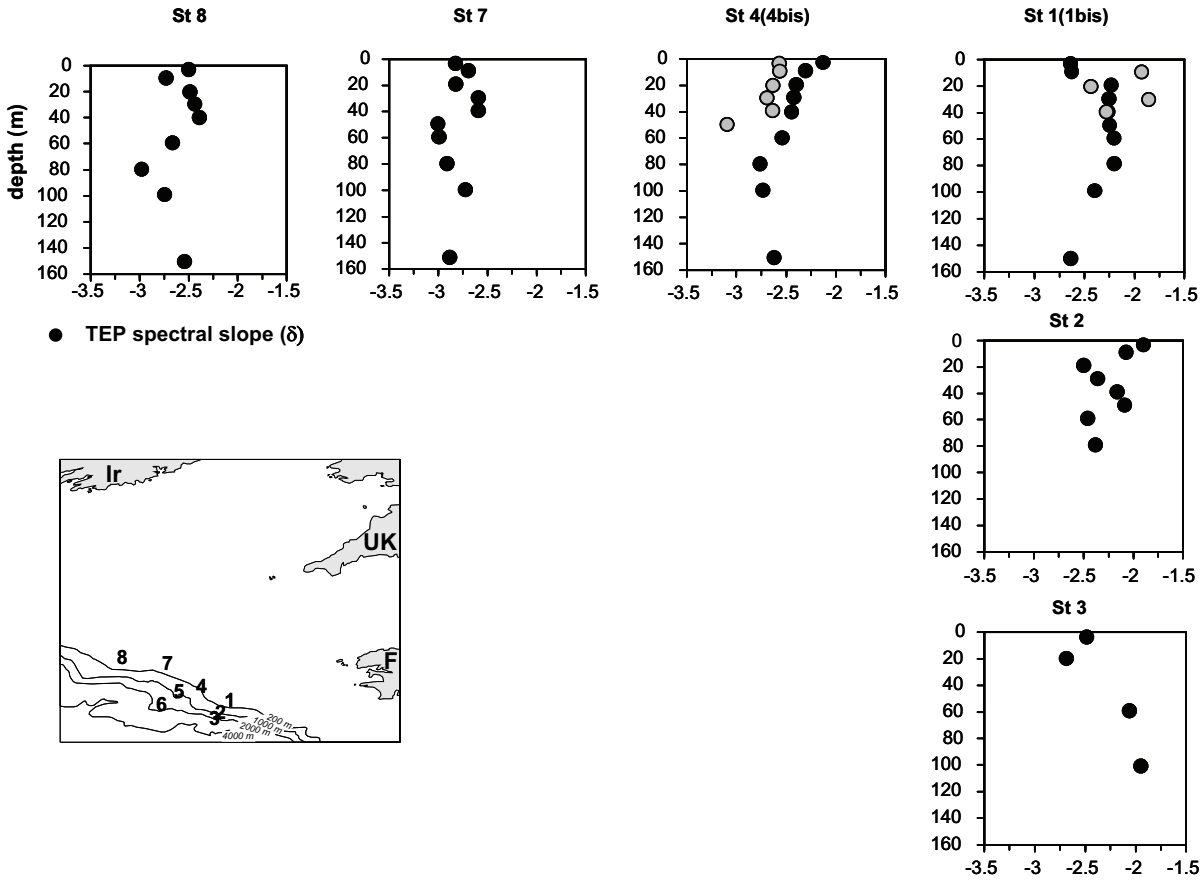
St 8
St 7
St 4(4bis)
St 1(1bis)
St 2
St 3
depth (m)
0
20
40
60
80
100
120
140
160
-3.5
-3
-2.5
-2
-1.5
TEP spectral slope (δ)
Ir
UK
F
8
7
6
5
4
3
2
1
200 m
1000 m
2000 m
4000 m

Figure 9

Manuscript III

The bacterial utilization of polysaccharides derived from *Emiliania huxleyi* and the impact of ocean acidification

Judith Piontek, Nicole Händel, Corinna Borchard, Mirko Lunau, Anja Engel

Alfred Wegener Institute for Polar and Marine Research, Am Handelshafen 12, 27570 Bremerhaven, Germany

ABSTRACT: The bacterial utilization of polysaccharides is an important process controlling the cycling of reactive organic carbon in the ocean. We examined the enzymatic polysaccharide breakdown and the subsequent assimilation of polysaccharide-derived carbon by natural bacterioplankton communities in a field study conducted in the northern Bay of Biscay and in a laboratory experiment. Bacterioplankton production in the Bay of Biscay was co-determined by the efficiency of enzymatic polysaccharide degradation and by the assimilation of glucose monomers, revealing that polysaccharide-derived carbon substantially contributed to the bacterial carbon demand. In the laboratory experiment, polysaccharides were derived from cultures of the coccolithophore *Emiliania huxleyi*, the most abundant phytoplankton species at the field site. Combined glucose was preferentially degraded, so that other neutral sugars and uronic acids were relatively enriched in polysaccharides during incubation. The assimilation of glucose derived from polysaccharide hydrolysis supported a substantial fraction of bacterial production. Polysaccharide-rich transparent exopolymer particles (TEP) produced by *Emiliania huxleyi* provided an accessible carbon source for bacteria. Incubation at elevated seawater pCO_2 resulted in higher rates of bacterial polysaccharide turnover induced by increased activities of extracellular glucosidases, suggesting effects of ocean acidification to accelerate the bacterial cycling of polysaccharides.

KEY WORDS: carbohydrates, extracellular enzymes, TEP, pH, Bay of Biscay, carbon cycle

INTRODUCTION

Carbohydrates are a major component of reactive organic carbon in the ocean, existing in dissolved, colloidal, and particulate form (Cowie & Hedges 1984, Wakeham et al. 1997, Benner 2002). A number of studies revealed the outstanding importance of dissolved free glucose in seawater for bacterial growth (Rich et al. 1996, Skoog et al. 1999, Kirchman et al. 2001). Glucose monomers support up to 45% of bacterial production in the open ocean, although the concentration is usually below 150 nmol l^{-1} (Rich et al. 1996, Kirchman et al. 2001). Glucose is also the most abundant neutral sugar in polysaccharides, whose concentration is frequently more than ten times higher than that of free monosaccharides (Borch & Kirchman 1997, Skoog & Benner 1997, Kirchman et al. 2001). However, the efficiency of polysaccharide turnover by marine bacterioplankton and the relevance of polysaccharide-derived carbon for bacterial growth are largely unexplored. The high molecular weight of polysaccharides requires the extracellular cleavage by hydrolytic enzymes prior to bacterial uptake of mono- and oligosaccharides (Arnosti 2000, 2004). The efficiency of extracellular enzymatic reactions, the energy demand for enzyme production, and the genetic capability for synthesis of suitable extracellular enzymes are complex factors controlling the bacterial polymer breakdown (Martinez et al. 1996, Arrieta & Herndl 2002). The efficiency of the bacterial utilization of carbon derived from polysaccharides is determined by the coupling between enzymatic polysaccharide hydrolysis and uptake of low-molecular-weight hydrolysates. Since the rate constants of extracellular enzyme activity are usually lower than those of substrate uptake, the hydrolysis of polymers by extracellular enzymes is often referred to as the rate-limiting step in bacterial remineralization of organic matter (Hoppe et al. 1988, Chróst 1991). On the other hand, it was shown that only a small fraction of particle hydrolysates provided by extracellular enzyme activity is taken up by the particle-associated bacterial community, suggesting the enzymatic degradation of high-

molecular-weight organic matter to occur partly decoupled from bacterial metabolism and growth (Smith et al. 1992). Therefore, explaining the bacterial polysaccharide turnover in the ocean requires studies that consider the enzymatic polysaccharide hydrolysis, the subsequent assimilation of mono- and oligosaccharides, and related changes in polysaccharide concentration and composition.

Currently, decreasing ocean pH induced by rising CO_2 in the atmosphere is together with warming the pre-eminent large-scale change in marine systems, spreading out from surface to depth (Houghton et al. 2001, Caldeira & Wickett 2003, Sabine et al. 2004, Parry et al. 2007). Changes in carbonate chemistry and pH of seawater have recently been shown to affect the autotrophic carbon consumption of phytoplankton, implying significant effects on the marine carbon cycle (Riebesell et al. 2007, Arrigo 2007). Bacteria are the main consumers of organic carbon in the ocean, representing an important compartment of the marine carbon cycle (Azam 1998, Sherr & Sherr 2000). About 50% of primary production is channelled via the microbial loop, entering marine food webs after bacterial reworking (Azam 1998). However, potential effects of rising CO_2 and correspondingly decreasing ocean pH on bacteria are currently not considered. Effects of decreasing ocean pH on polysaccharide degradation need to be investigated, since changes in the bacterial carbon supply can affect the functioning of bacterioplankton communities in marine pelagic ecosystems.

Here, we present results of a field campaign conducted in the Gulf of Biscay and of a laboratory experiment investigating the bacterial cycling of polysaccharides produced from monospecific cultures of *Emiliania huxleyi*. In the laboratory experiment, emphasis was put on the investigation of pH effects by comparing an unmodified treatment with a treatment simulating pH conditions projected for the ocean in a high-CO_2 world.

MATERIAL AND METHODS

Field sampling

Field data on the bacterial turnover of polysaccharides were collected during a campaign in the northern Bay of Biscay, south of Ireland and west of France. Six stations located along the shelf break between 47° 07' 83" N, 6° 92' 01" E and 51° 34' 42" N, 10° 49' 95" E were sampled between 10th and 16th of May, 2007 (Fig. 1). Stations 8 and 5 were revisited on 21st and 22nd of May, 2007 and then referred to as stations 8*bis* and 5*bis*, respectively. Seawater samples were collected with a CTD system equipped with a rosette sampler.

Laboratory experiment (*EhuxLAB*)

The experiment *EhuxLAB* was set up to investigate the bacterial degradation of polysaccharides derived from cultures of *Emiliania huxleyi* (strain PML B92/11). Two monospecific cultures of *Emiliania huxleyi* were grown in a chemostat system at 14°C under continuous aeration with CO_2-air mixtures of 380 µatm and 750 µatm CO_2, respectively, at a nutrient-limiting flow rate of 0.1 d^{-1} (Borchard et al., in prep.). A light intensity of 300 µmol photons m^{-2} s^{-1} was applied in a light/dark cycle of 16/8 hours. The flow was stopped after 12 days and both cultures were inoculated with a natural North Sea bacterioplankton assemblage. Cultures inoculated with bacteria were incubated in the dark at 14°C for 14 days. The aeration with defined CO_2-air-mixtures was continued until the end of the experiment, leading to a pH of 7.9 ± 0.04 at 380 µatm CO_2 and of 7.7 ± 0.08 at 750 µatm CO_2. Incubations were sampled immediately after inoculation (day 0), and after 2, 4, 7, and 14 days of dark incubation.

Microbiological analyses

Rates of bacterial extracellular enzyme activity, glucose uptake, and biomass production were determined in field samples of 5 m and 40 m depth and in *EhuxLAB*.

The reaction velocity of the polysaccharide-degrading extracellular enzymes α-glucosidase and β-glucosidase was determined using substrate analogues labelled with the fluorescent marker 4-methylumbelliferone (MUF) (Hoppe 1983). Subsamples of 200 µl were incubated with MUF-α-glucopyranosid and MUF-β-glucopyranosid at a final concentration of 1 µmol l^{-1}. Fluorescence was measured with a plate reader (FLUOstar OPTIMA, BMG Labtech) immediately after addition of the substrate analogue and after 3 hours of dark incubation at 14°C. Analysis of triplicate subsamples revealed a mean standard deviation of 5% for α-glucosidase and β-glucosidase activity. Calibration was carried out with MUF standard solutions adjusted to different pH levels. Rate constants for α- and β-glucosidase activity were calculated assuming a linear relationship between non-saturating substrate concentrations and enzymatic reaction velocities according to Michaelis-Menten kinetics.

The bacterial uptake of glucose was estimated from the assimilation of [^{3}H]-glucose. Samples of 10 ml volume were incubated with [^{3}H]-glucose at a final concentration of 10 nmol l^{-1} in the dark at 14°C for 1 to 2 hours, depending on the bacterial activity. Incubations were stopped by the addition of formalin at a final concentration of 4%. Formalin-killed controls were run for each sampling. Samples were further processed according to the microcentrifuge method as described by Smith and Azam (1992). Briefly, subsamples of 2 ml were centrifuged at approx. 1400 rpm for 20 minutes to obtain a cell pellet that was washed with ice-cold 5% trichloroacetic acid. The supernatant was carefully removed and scintillation cocktail (Ultima Gold AB, Perkin Elmer) was added. Samples were then radio-assayed by liquid scintillation counting. Analysis of triplicate subsamples revealed a mean standard deviation of 5%. Rate constants for glucose uptake were calculated assuming a linear relationship between non-saturating substrate concentration and the uptake velocity according to Michaelis-Menten kinetics.

Bacterial biomass production (BBP) was estimated from incorporation rates of radiolabelled leucine assessed by liquid scintillation counting. The radiotracer (field sampling: [^{14}C]-leucine, *EhuxLAB:* [^{3}H]-leucine) was added to samples of 10 ml volume at a saturating final concentration of 10 nmol l^{-1}. Samples were incubated at 14°C in the dark. Incubation time ranged from 45 minutes to 2 hours, depending on the bacterial activity. After incubation, samples were poisoned with formalin at a final concentration of 4% to stop bacterial growth. Formalin-killed controls were run for each sampling. Samples were further processed according to Smith and Azam (1992) as briefly described above. The mean standard deviation of triplicate subsamples was 3%. Rates of leucine incorporation were converted into BBP applying the factors of 1.15 x 10^{17} cells mol^{-1} leucine incorporated (Kirchman 1992) and 20 fg carbon cell^{-1} (Lee & Fuhrman 1987).

Bacterial cell numbers were determined by the use of a flow cytometer (FACSCalibur, Beckton Dickinson) in *EhuxLAB*. Samples were preserved with glutardialdehyde (2% final concentration) and stored at -20°C until analysis. Prior to analysis, samples were stained with SybrGreen I (Invitrogen), a nucleic acid-binding dye. Bacterial abundances were determined after visual inspection of the dot plot of SSC vs. FL1 and manual gating of the bacterial subpopulation. Fluorescent latex beads were used to normalize the counted events, revealing a standard deviation of 1%.

Since standard deviations of analytical replicates for all microbiological parameters did not exceed 5%, they were not included in figures.

Chemical analyses

Concentration and composition of total combined carbohydrates were analyzed in the surface sample of station 2 (Fig. 1) and in *EhuxLAB*. Samples for carbohydrate analysis were transferred into precombusted glas vials and stored at -20°C. Prior to analysis, samples were

desalted by the use of a 1 kDa dialysis membrane that simultaneously separated polysaccharides from mono- and oligosaccharides (Engel & Händel submitted). Dissolved and particulate polysaccharides were hydrolyzed with hydrochloric acid at a final concentration of 0.8 mol l^{-1} for 20 hours at 100°C. Analysis was carried out by ion chromatography (HPAEC-PAD, Dionex). The mean standard deviation of duplicate analysis of individual neutral and acidic sugars was below 2%. Duplicate analysis of glucosamine revealed a standard deviation of 5%.

Concentration of transparent exopolymer particles (TEP) was determined in *EhuxLAB*. Samples of 4 - 5 ml were filtered onto 0.4 µm-polycarbonate filters and stained with Alcian Blue, a dye that binds to acidic polysaccharides. Samples were stored at -20°C until analysis. TEP concentration was measured photometrically in triplicate subsamples and expressed in xanthan equivalents according to Passow & Alldredge (1995). A factor of 0.033 was assumed to convert xanthan equivalents (µg Xeq. l^{-1}) into carbon units (TEP-C, µmol C l^{-1}) (Engel et al. 2004). The mean standard deviation of triplicate subsamples was 19%. Coccoliths of *Emiliania huxleyi* are coated by acidic polysaccharides (CP) that are stained by Alcian Blue and contribute to TEP concentration (Fig. 2). The Alcian Blue adsorption of *Emiliania huxleyi* cells can be estimated according to Engel et al. (2004) with

CP (pmol C) = 0.085 x (cell number of *Emiliania huxleyi*) (1).

Concentration of particulate organic carbon (POC) was determined in *EhuxLAB*. Samples of 60 - 100 ml were filtered onto combusted GF/F filters and stored at -20°C. Prior to analysis, filters were dried at 80°C for 24 hours and acidified with 1 M hydrochloric acid to remove inorganic carbon. Samples were measured on an elemental analyzer (EuroEA, Euro Vector). Duplicate subsamples revealed a mean standard deviation of 13%. In *EhuxLAB*, samples for dissolved organic carbon (DOC) were collected in precombusted glas ampoules after filtration

through precombusted GF/F filters. Samples were acidified with 100 µl of 85% phosphoric acid and stored at 4°C in the dark until analysis. Samples were analyzed using the high-temperature combustion method (TOC analyzer, Shimadzu) (Quian & Mopper 1996). The concentration of total organic carbon (TOC) represents the sum concentration of POC and DOC.

The standard deviations of analytical replicates of TEP and POC were higher than 5%; therefore, standard deviations were added to figures.

RESULTS

Bacterial polysaccharide turnover in the Bay of Biscay (May 2007)

Surface samples and subsurface samples of 40 m depth were collected along a transect in the northern Bay of Biscay in May 2007 (Fig. 1). Sea surface temperature (SST) ranged from 12.2 to 13.5°C. Temperature in 40 m depth was 0.2 - 1.1°C lower than SST. SeaWIF satellite images revealed low chlorophyll *a* concentrations of up to 0.8 µg l^{-1} along the transect.

Activity of α- and β-glucosidase was detected in all samples except subsurface samples of stations 5*bis* and 8*bis*, revealing extracellular cleavage of polysaccharides by bacterioplankton along the transect. No significant difference was observed between rate constants of α- and β-glucosidase or between glucosidase activity at the surface and in 40 m depth. The enzymatic polysaccharide breakdown was directly related to bacterial glucose uptake, when rate constants of α- and β-glucosidase did not exceed 0.0075 d^{-1} and 0.020 d^{-1}, respectively (α-glucosidase: $r^2 = 0.66$, $p = 0.027$, $n = 7$; β-glucosidase: $r^2 = 0.65$, $p = 0.002$, $n = 12$) (Fig. 3). Rate constants of bacterial glucose uptake ranged between 0.009 d^{-1} and 0.062 d^{-1}, and were significantly higher than those of α-glucosidase ($p < 0.001$) and β-glucosidase ($p = 0.003$).

Uptake rate constants were positively correlated with BBP along the transect ($r^2 = 0.63$, $p < 0.001$, $n = 16$) (Fig. 4), indicating a direct relationship between glucose assimilation and biomass production of bacterioplankon.

Concentration and composition of polysaccharides

The natural phytoplankton community at station 2 in the Bay of Biscay (Fig. 1) was dominated by *Emiliania huxleyi* as observed by microscopic inspection. Phytoplankton cells, which were partly contained in fecal pellets and microaggregates (Fig. 5), can be regarded as main source of particulate and dissolved polysaccharides that comprised in total 5.3 µmol C l^{-1} (Tab. 1).

Polysaccharides in *EhuxLAB* were produced from monospecific continuous cultures of *Emiliania huxleyi* grown at 380 µatm and 750 µatm CO_2, respectively. The abundance of *Emiliania huxleyi* was 3.2 x 10^5 cells ml^{-1} at 380 µatm CO_2 and 4.0 x 10^5 cells ml^{-1} at 750 µatm CO_2 at the time when cultures were inoculated with bacteria. *Emiliania huxleyi* cells provided a POC concentration of 780 µmol l^{-1} and 900 µmol l^{-1} at 380 µatm and 750 µatm CO_2, respectively. Despite this low variability in cell abundance and POC concentration between the two CO_2 treatments, polysaccharide concentration in the two cultures differed substantially. Dissolved and particulate polysaccharides accounted for 64.8 µmol C l^{-1} in the culture grown at 380 µatm CO_2, while total polysaccharide concentration in the culture at 750 µatm CO_2 doubled. Polysaccharides accounted for 5.9% and 10.6% of total organic carbon at 380 µatm and 750 µatm CO_2, respectively (Tab. 1).

The composition of polysaccharides in cultures of *EhuxLAB* and at station 2 in the Bay of Biscay was of high similarity (Tab. 1). Glucose was by far the most abundant neutral sugar in polysaccharides of both the monospecific *Emiliania huxleyi* cultures and the field sample, accounting for 57% to 72% of combined sugars. Other quantitatively important neutral sugars

in polysaccharides were galactose in *EhuxLAB* and galactose and mannose/xylose in the field sample. The sum concentration of the deoxy sugars fucose and rhamnose accounted initially for 5% in both cultures of *EhuxLAB* and for 7% in the field sample. Proportions of uronic acids, including the acidic sugars glucuronic acid and galacturonic acid, ranged from 7 to 10%.

Bacterial turnover of combined glucose in *EhuxLAB*

The concentration of combined glucose decreased exponentially in both CO_2 treatments of *EhuxLAB*, yielding rate constants of 0.53 ± 0.11 ($p = 0.004$) at 380 µatm CO_2 and of 0.76 ± 0.12 ($p < 0.001$) at 750 µatm CO_2 (Fig. 6). The loss rate of combined glucose was 3 times higher at 750 µatm than at 380 µatm CO_2 during the first two days of incubation (Tab. 2). A loss of 6.3 and 16.5 µmol combined glucose l^{-1} was determined at 380 µatm and 750 µatm CO_2, respectively, at the end of incubation. The sum concentration of other neutral sugars did not decrease until the end of incubation in both treatments (Fig. 6).

Maximum bacterial cell numbers of 6.4 x 10^6 cells ml^{-1} at 380 µatm CO_2 and of 6.0 x 10^6 cells ml^{-1} at 750 µatm CO_2 were achieved during the first 4 days of incubation. Thereafter, bacterial abundances decreased strongly in both treatments. No significant difference between bacterial cell numbers at 380 µatm and 750 µatm CO_2 was determined. Also BBP at 380 µatm and at 750 µatm CO_2 was not significantly different (Fig. 7). Maximum BBP of 100 nmol C l^{-1} h^{-1} and 96 nmol C l^{-1} h^{-1} at 380 µatm and 750 µatm CO_2, respectively, was determined on day 2. BBP decreased strongly after day 4 in accordance with decreasing bacterial cell numbers (Fig. 7).

The higher loss of combined glucose at 750 µatm CO_2 relative to 380 µatm CO_2 coincided with significantly higher rate constants of extracellular α- and β-glucosidase activity ($p = 0.017$) (Tab. 2, Fig. 8), revealing an enhanced enzymatic hydrolysis of polysaccharides in the

high-CO_2 treatment. However, calculating the loss of combined glucose from enzymatic rates underestimates the actual loss determined by ion chromatography at 380 µatm CO_2 and overestimates the actual loss between day 2 and 4 at 750 µatm CO_2 (Tab. 2).

In contrast to polysaccharide-degrading extracellular enzymes, no difference between glucose uptake rate constants at 380 µatm and 750 µatm CO_2 could be determined (Tab. 2, Fig. 8), indicating that the efficiency of hydrolysate uptake was similar in both treatments. Between 2.3% and 3.4% of glucose monosaccharides provided by extracellular glucosidase activity was assimilated in both treatments, showing that the vast majority of hydrolysates remained in the pool of dissolved organic matter. The assimilation of glucose monosaccharides derived from the hydrolysis of combined glucose was almost 5 times higher at 750 µatm CO_2 than at 380 µatm CO_2 during the first two days due to a higher concentration of hydrolysates and a slightly higher uptake rate constant (Tab. 2). Despite this difference in glucose assimilation, BBP in the two treatments was similar (Fig. 7). Hence, glucose derived from the hydrolysis of polysaccharides accounted for up to 68% of carbon produced by bacteria at 750 µatm CO_2, but only for up to 16% at 380 µatm CO_2 (Tab. 2).

Degradation of bulk organic carbon and transparent exopolymer particles (TEP) in *EhuxLAB*

The initial concentration of TOC was 1190 ± 36 µmol l^{-1} and 1220 ± 40 µmol l^{-1} at 380 µatm and 750 µatm CO_2, respectively. TOC decreased exponentially with a rate constant of 0.06 ± 0.02 ($p = 0.04$) at 380 µatm CO_2, while the loss of TOC at 750 µatm CO_2 did not follow a first-order exponential decay. A TOC loss of 580 µmol l^{-1} and 507 µmol l^{-1} was determined at the end of incubation at 380 µatm and 750 µatm CO_2, respectively.

TEP in *Emiliania huxleyi* cultures of *EhuxLAB* contained 59.2 µmol C l^{-1} at 380 µatm CO_2 and 84.4 µmol C l^{-1} at 750 µatm CO_2 (Fig. 10). The initial TEP concentration decreased

exponentially during incubation with rate constants of 0.11 ± 0.01 ($p = 0.003$) at 380 µatm CO_2 and 0.11 ± 0.02 ($p = 0.01$) at 750 µatm CO_2 (Fig. 10). TEP accounted in average for 7 ± 1 % and 8 ± 2 % of POC at 380 µatm and 750 µatm CO_2, respectively. Changes in TEP were directly related to changes in POC, with Δ [POC]/[TEP] equal to 12.5 ± 2.4 and 11.9 ± 3.9 at 380 µatm and 750 µatm CO_2, respectively (Fig. 11). Measurements of TEP concentration included coccolith polysaccharides (CP) associated with *Emiliania huxleyi* that were also stained by Alcian Blue (Fig. 2). The concentration of CP can be estimated according to eq. (1). CP accounted for up to 42% of TEP concentration at 380 µatm CO_2 and for up to 50% at 750 µatm CO_2. The initial CP concentration of 23.9 µmol C l^{-1} at 380 µatm CO_2 and 31.1 µmol C l^{-1} at 750 µatm CO_2 decreased to 1.1 µmol C l^{-1} and 2.3 µmol C l^{-1}, respectively, at the end of incubation.

Changes of polysaccharide composition during degradation in *EhuxLAB*

A selective loss of combined glucose during degradation was determined in both CO_2 treatments (Fig. 6, Tab. 1, 3). The proportion of glucose decreased from initially 67% at 380 µatm CO_2 and 72% at 750 µatm CO_2 to 18% and 15%, respectively. Other neutral sugars have been enriched in polysaccharides during incubation. Proportions of glucose, galactose, and mannose+xylose were similar at the end of incubation in both treatments. The ratio of [deoxy sugars + uronic acids] : [glucose] in polysaccharides increased in both treatments, and was up to 10 and 13 times higher than initially during incubation at 380 µatm and 750 µatm CO_2, respectively (Fig. 12). The amino sugar glucosamine, a major component of bacterial cell walls, could not be detected at the beginning of dark incubation. The glucosamine concentration increased during incubation up to 87 nmol l^{-1} and 58 nmol l^{-1} at 380 µatm ($r^2 = 0.98$, $p = 0.004$) and 750 µatm CO_2 ($r^2 = 0.92$, $p = 0.08$), respectively (Fig. 13).

DISCUSSION

Bacterial cycling of polysaccharides and related carbon fluxes

Bacterial production in the open ocean is largely supported by the small pool of organic low-molecular-weight compounds that can be directly assimilated by marine bacterioplankton (Fuhrman & Ferguson 1986, Jorgensen et al. 1993, Rich et al. 1996, Kirchman et al. 2001). Our study revealed that bacterioplankton production in the Bay of Biscay was also significantly related to the bacterial capacity of polysaccharide turnover that is determined by the efficiency of extracellular enzymatic hydrolysis and subsequent hydrolysate assimilation (Fig. 3, 4). The *in-situ* polysaccharide composition was of high similarity to that of polysaccharides derived from monospecific cultures of *Emiliania huxleyi* (Tab. 1), indicating that biomass and exudates of *Emiliania huxleyi*, the most abundant phytoplankton species along the transect, were a relevant polysaccharide source in the Gulf of Biscay. Combined glucose contained more than 50% of carbon in polysaccharides, and was preferentially degraded relative to other combined neutral sugars by extracellular enzymes in *EhuxLAB* (Tab. 1-3, Fig. 6). The concurrent bacterial hydrolysate assimilation contributed substantially to the bacterial carbon supply during incubation (Tab. 2). Thus, combined glucose provided a labile carbon source for bacteria and its utilization potentially co-determined bacterioplankton dynamics in the Gulf of Biscay.

The enzymatic particle dissolution decoupled from bacterial hydrolysate consumption generates considerable amounts of dissolved organic matter, and is therefore a relevant process for large-scale transfer of organic matter from the particulate to the dissolved phase (Smith et al. 1992, 1995). Uptake rate constants in *EhuxLAB* revealed that the vast majority of glucose derived from enzymatic polysaccharide breakdown was not simultaneously assimilated by bacteria, suggesting a substantial accumulation of hydrolysates during incubation (Tab. 2, Fig. 8). Highest glucosidase activities in the Gulf of Biscay were not

directly related to glucose uptake, so that polysaccharide breakdown at high rates was not balanced by an increasing bacterial glucose utilization (Fig. 3). Thus, the cycling of polysaccharides did not only provide bacterial nutrition, but also had a large impact on the quality of reactive organic carbon.

The impact of pH on the bacterial turnover of combined glucose

The bacterial degradation of polysaccharides in *EhuxLAB* was substantially accelerated at elevated CO_2 concentration of 750 µatm, representing the CO_2 conditions of the near future (Houghton et al. 2001, Parry et al. 2007). The loss of combined glucose was significantly higher at 750 µatm than at 380 µatm CO_2 due to significantly higher rates of extracellular glucosidase activity (Tab. 2, Fig. 6, 9). The activity of enzymes in general and that of extracellular enzymes in aquatic environments in particular are known to depend on pH. The elevated CO_2 concentration of 750 µatm CO_2 decreased seawater pH relative to the incubation at 380 µatm CO_2 by 0.2 units. Extracellular enzymes are directly exposed to the ambient pH and in contrast to intracellular enzymes not buffered by the cytosol. Therefore, higher rates of polysaccharide degradation at 750 µatm CO_2 were likely induced by effects of lowered pH on the activity of bacterial extracellular glucosidases. Bacterial cell numbers were not significantly different between the two CO_2 treatments, revealing the similar abundance of enzyme producers (Fig. 7). Nevertheless, it cannot be excluded that the cell-specific production of α- and β-glucosidase in the high-CO_2 treatment was increased in response to higher concentrations of combined glucose provided by the *Emiliania huxleyi* culture grown at 750 µatm CO_2 (Tab. 1). Hence, effects of elevated CO_2 on the polysaccharide production of *Emiliania huxleyi*, serving as substrates for bacterial metabolism and growth, would in turn evoke higher bacterial degradation rates.

The loss of combined glucose calculated from enzymatic rates does not always exactly match with the loss determined by chemical analysis with ion chromatography (Tab. 2). A potential reason for mismatch is the activity of endoglucanases. Extracellular endoglucanase activity cleaves bonds within the polysaccharide, releasing carbohydrates >1 kDa. However, analysis by ion chromatography detected only the loss of carbohydrates <1kDa, driven by the activity of extracellular exoglucanases that hydrolyze bonds in terminal position. Furthermore, exudation by *Emiliania huxleyi* during the initial phase of dark incubation may have reduced the net loss of polysaccharides determined by ion chromatography.

The enhanced hydrolysis of combined glucose at elevated CO_2 concentration induced a cascading effect on the bacterial cycling of polysaccharides. Higher rates of polysaccharide hydrolysis at 750 µatm CO_2 provided a higher concentration of glucose available for uptake. Rate constants of glucose uptake did not reveal a significant difference between the two CO_2 treatments (Fig. 8, Tab. 2). Consequently, a higher amount of glucose was assimilated per time in the high-CO_2 treatment due to higher hydrolysate concentrations. Since BBP did not differ between the two treatments (Fig. 7), glucose released from polysaccharides supported a higher percentage of BBP at 750 µatm than at 380 µatm CO_2 (Tab. 2). Assuming a glucose growth efficiency of 0.4 (Rich et al. 1996) for both CO_2 treatments, the amount of remineralized combined glucose can be estimated. Accordingly, 1.4 µmol carbon l^{-1} and 4.8 µmol carbon l^{-1} derived from hydrolysis of combined glucose was respired at 380 µatm and 750 µatm CO_2, respectively, during incubation, thus revealing that carbon derived from combined glucose was remineralized more than three times faster at elevated CO_2. However, polysaccharides comprised only a minor proportion of TOC in *EhuxLAB* (Tab. 1, 3), and the turnover of polysaccharide derived carbon was quantitatively not relevant for total carbon remineralisation (Fig. 9). Nevertheless, the accelerated remineralization of polysaccharides at

elevated CO_2 concentration suggests that turnover rates of organic carbon with high proportions of carbohydrates may substantially increase in the future ocean.

Effects of bacterial degradation activity on the composition of polysaccharides derived from *Emiliania huxleyi*

Bacterial degradation activity altered the polysaccharide composition in *EhuxLAB* in two ways. Firstly, the selective degradation of combined glucose relatively enriched other combined sugars, in particular galactose, glucuronic acid, and galacturonic acid (Tab.1, 3, Fig. 6). Secondly, bacteria produced specific sugars as component of their biomass. The amino sugar glucosamine that is enriched in bacterial cell walls was not detectable at the beginning of *EhuxLAB*, but its concentration increased linearly until the end of incubation (Fig. 13). Also a relative increase in deoxy sugars was indicative of bacteria as carbohydrate source, since bacterial biomass is enriched in fucose and rhamnose (Tab. 1, 3) (Ogier et al. 2001). The lability of combined glucose and the increasing proportion of carbohydrates derived from bacterial biomass both are in good accordance with previous studies investigating the degradation of particulate and dissolved polysaccharides collected in different oceanic regions (Cowie & Hedges 1984, Tanoue & Handa 1987, Hernes et al. 1996, Amon et al. 2001). A significant effect of elevated CO_2 on compositional changes of polysaccharides during bacterial degradation could not be determined.

Bacterial degradation activity increased the proportion of surface-active sugars in polysaccharides derived from *Emiliania huxleyi* (Tab. 1, 3, Fig. 12). The deoxy sugars fucose and rhamnose are hydrophic due to the methyl group at the sixth carbon atom. Uronic acids confer a negative charge to the polysaccharide, increasing its reactivity (Decho 1990). Both components were shown to increase the stickiness of surfaces and to enhance the coagulation

of exopolymers (Giroldo et al. 2003, Vieira et al. 2008), implying an increasing aggregation potential of organic matter derived from *Emiliania huxleyi* with proceeding degradation.

Bacterial utilization of TEP derived from *Emiliania huxleyi*

Carbon in TEP accounted for approx. 10% of POC in monospecific cultures of *Emiliania huxleyi*, and represented a relevant pool of organic carbon in *EhuxLAB* (Fig. 10). TEP formation is closely related to phytoplankton exudation that provides extracellular polysaccharides, the precursors of TEP (Chin et al. 1998, Passow 2002). Factors controlling the bacterial breakdown of extracelluar polysaccharides are complex, including the molecular size and chemical composition of polysaccharides and algal-bacterial interactions (Bell et al. 1974, Jensen 1983). TEP were shown to accumulate during the decline of coccolithophore-dominated blooms (Engel et al. 2004 a, b), and were considered as recalcitrant to bacterial degradation (Nanninga et al. 1996). In this study, TEP concentration in *EhuxLAB* decreased exponentially during incubation, demonstrating that polysaccharides in TEP were subject to bacterial degradation (Fig. 10). Correspondingly, a decrease in concentrations of combined uronic acids that are abundant in TEP was determined (Tab. 1, 3). No significant effect of elevated CO_2 on TEP degradation was observed. The decrease of TEP was directly related to the decrease of POC in both CO_2 treatments (Fig. 11), revealing that TEP were degraded as efficiently as carbon derived from biomass of *Emiliania huxleyi*. A selective loss of TEP relative to POC derived from *Emiliania huxleyi* was found in a previous study (Engel et al., in press). Hence, polysaccharides in TEP derived from *Emiliania huxleyi* are accessible for bacterial utilization. Since TEP was not separated from other fractions of organic matter in *EhuxLAB*, it cannot be evaluated explicitly whether carbohydrates derived from TEP degradation were subsequently metabolized by bacteria or remained in the dissolved pool of organic matter.

Conclusions

Polysaccharides collected in the Bay of Biscay and derived from monospecific cultures of *Emiliania huxleyi* were dominated by combined glucose, and contributed substantially to the bacterial carbon supply. The polysaccharide composition was altered during degradation by the selective bacterial turnover of combined glucose and the coinciding bacterial production of carbohydrates. The bacterial assemblage was able to degrade efficiently polysaccharide-rich TEP produced from *Emiliania huxleyi*, decreasing the concentration of combined uronic acids. Turnover rates of combined glucose at elevated CO_2 concentration, representing near-future CO_2 conditions, were significantly higher than at present-day CO_2 concentration due to higher activities of polysaccharide-degrading bacterial extracellular enzymes. Hence, this study suggests that polysaccharides derived from biomass and exudates of *Emiliania huxleyi* provide a labile carbon source to bacterioplankton that will potentially be utilized at higher rate in the future high-CO_2 ocean.

REFERENCES

AMON RMW, FITZNAR HP, BENNER R (2001) Linkages among the bioreactivity, chemical composition, and diagenetic state of marine dissolved organic matter. Limnol Oceanogr 46:287-297

ARNOSTI C (2000) Substrate specificity in polysaccharide hydrolysis: Contrasts between bottom water and sediments. Limnol Oceanogr 45:1112-1119

ARNOSTI C (2004) Speed bumps and barricades in the carbon cycle: substrate structural effects on carbon cycling. Mar Chem 92:263-273

ARRIETA JM, HERNDL GI (2002) Changes in bacterial beta-glucosidase diversity during a coastal phytoplankton bloom. Limnol Oceanogr 47:594-599

ARRIGO KR (2007) Carbon cycle - Marine manipulations. Nature 450:491-492

AZAM F (1998) Microbial control of oceanic carbon flux: The plot thickens. Science 280:694-696

BELL WH, LANG JM, MITCHELL R (1974) Selective stimulation of marine bacteria by algal extracellular products. Limnol Oceanogr 19:833-839

BENNER R (2002) Chemical Composition and Reactivity. In: Hansell DA, Carlson CA (eds) Biogeochemistry of Marine Dissolved Organic Matter. (Elsevier Science, Orlando)

BORCH NH, KIRCHMAN DL (1997) Concentration and composition of dissolved combined neutral sugars (polysaccharides) in seawater determined by HPLC-PAD. Mar Chem 57:85-95

CHIN W, ORELLANA M, VERDUGO P (1998) Spontaneous assembly of marine dissolved organic matter into polymer gels. Nature 391:568-572

CALDEIRA K, WICKETT ME (2003) Anthropogenic carbon and ocean pH. Nature 425:365-365

CHRÓST RJ (1991) Environmental control of the synthesis and activity of aquatic microbial ectoenzymes. In: Chróst RJ (ed) Microbial enzymes in aquatic environments (Springer Verlag, Heidelberg)

COWIE GL, HEDGES JI (1984) Carbohydrate Sources in a coastal marine environment. Geochim Cosmochim Acta 48:2075-2087

DECHO AW (1990) Microbial exopolymer secretions in ocean environments: their role(s) in food webs and marine processes. Oceanogr Mar Biol Annu Rev 28:73-153

ENGEL A, THOMS S, RIEBESELL U, ROCHELLE-NEWALL E, ZONDERVAN I (2004a) Polysaccharide aggregation as a potential sink of marine dissolved organic carbon. Nature 428:929-932

ENGEL A, DELILLE B, JACQUET S, RIEBESELL U, ROCHELLE-NEWALL E, TERBRUGGEN A, ZONDERVAN I (2004b) Transparent exopolymer particles and dissolved organic carbon production by *Emiliania huxleyi* exposed to different CO2 concentrations: a mesocosm experiment. Aquat Microb Ecol 34:93-104

ENGEL A, HÄNDEL N (submitted) Simultaneous determination of the neutral-, amino-, and acidic sugar composition of polysaccharides in seawater using High Performance Anion Exchange Chromatography with Pulsed Amperometric Detection

ENGEL A, ABRAMSON L, SZLOSEK J, LIU Z, STEWART G, HIRSCHBERG D, LEE C (in press) Investigating the effect of ballasting $CaCO_3$ in *Emiliania huxleyi*: II. Decomposition of particulate organic matter

FUHRMAN JA, FERGUSON RL (1986) Nanomolar concentrations and rapid turnover of dissolved free amino acids in seawater: agreement between chemical and microbiological measurements. Mar Ecol Prog Ser 33:237-242

GIROLDO D, VIEIRA AAH, PAULSEN BS (2003) Relative increase of deoxy sugars during microbial degradation of an extracellular polysaccharide released by a tropical freshwater Thalassiosira sp (Bacillariophyceae). J Phycol 39:1109-1115

HERNES PJ, HEDGES JI, PETERSON ML, WAKEHAM SG, LEE C (1996) Neutral carbohydrate geochemistry of particulate material in the central equatorial Pacific. Deep-Sea Res Part II 43:1181-1204

HOPPE HG (1983) Significance of Exoenzymatic Activities in the Ecology of Brackish Water - Measurements by Means of Methylumbelliferyl-Substrates. Mar Ecol Prog Ser 11:299-308

HOPPE HG, KIM SJ, GOCKE K (1988) Microbial decomposition in aquatic environments: combined process of extracellular enzyme activity and substrate uptake. Appl Environm Microbiol 54(3): 784-790

HOUGHTON JT, DING Y, GRIGGS DJ, NOGUER M, VAN DER LINDEN PJ, DAI X, MASKELL K, JOHNSON CA (2001) Climate Change 2001: The Scientific Basis: Contribution of Working Group I to the Third Assessment Report of the Intergovernmental Panel of Climate Change, (Cambridge University Press)

JORGENSEN NOG, KROER N, COFFIN RB, YANG XH, LEE C (1993) Dissolved free amino-acids, combined amino-acids, and DNA as sources of carbon and nitrogen to marine bacteria. Mar Ecol Prog Ser 98:135-148

KIRCHMAN DL (1992) Incorporation of thymidine and leucine in the subarctic Pacific: application to estimating bacterial production. Mar Ecol Prog Ser 82:301-309

KIRCHMAN DL, MEON B, DUCKLOW HW, CARLSON CA, HANSELL DA, STEWARD GF (2001) Glucose fluxes and concentrations of dissolved combined neutral sugars (polysaccharides) in the Ross Sea and Polar Front Zone, Antarctica. Deep-Sea Res Part II 48:4179-4197

LEE S, FUHRMAN JA (1987) Relationships between biovolume and biomass of naturally derived marine bacterioplankton. Appl Environ Microbiol 53:1298-1303

MARTINEZ J, SMITH DC, STEWARD GF, AZAM F (1996) Variability in ectohydrolytic enzyme activities of pelagic marine bacteria and its significance for substrate processing in the sea. Aquat Microb Ecol 10:223-230

OGIER S, DISNAR JR, ALBERIC P, BOURDIER G (2001) Neutral carbohydrate geochemistry of particulate material (trap and core sediments) in an eutrophic lake (Aydat, France). Org Geochem 32:151-162

PARRY M, CANZIANI O, PALUTIKOF J, VAN DER LINDEN PJ, HANSON C (2007) Climate Change 2007: Impact, Adaption and Vulnerability: Contribution of Working Group II to the Fourth Assessment Report of the Intergovernmental Panel of Climate Change, (Cambridge University Press)

PASSOW U (2002) Production of transparent exopolymer particles (TEP) by phyto- and bacterioplankton. Mar Ecol Prog Ser 236:1-12

PASSOW U, ALLDREDGE AL (1995) A dye-binding assay for the spectrophotometric measurement of transparent exopolymer particles (TEP). Limnol Oceanogr 40:1326-1335

QIAN J, MOPPER K (1996) Automated high-performance, high-temperature combustion total organic carbon analyser. Anal Chem 68:3090-3097

RICH JH, DUCKLOW HW, KIRCHMAN DL (1996) Concentrations and uptake of neutral monosaccharides along 140 degrees W in the equatorial Pacific: Contribution of glucose to heterotrophic bacterial activity and the DOM flux. Limnol Oceanogr 41:595-604

RIEBESELL U, SCHULZ KG, BELLERBY RGJ, BOTROS M, FRITSCHE P, MEYERHOFER M, NEILL C, NONDAL G, OSCHLIES A, WOHLERS J, ZÖLLNER E (2007) Enhanced biological carbon consumption in a high CO2 ocean. Nature 450:545-U10

SABINE CL, FEELY RA, GRUBER N, KEY RM, LEE K, BULLISTER JL, WANNINKHOF R, WONG CS, WALLACE DWR, TILBROOK B, MILLERO FJ, PENG TH, KOZYR A, ONO T, RIOS AF (2004) The oceanic sink for anthropogenic CO2. Science 305:367-371

SHERR E, SHERR B (2000) Marine Microbes: An Overview. In: Kirchman DL (ed) Microbial Ecology of the Ocean. (Wiley-Liss, Inc., New York)

SKOOG A, BENNER R (1997) Aldoses in various size fractions of marine organic matter: Implications for carbon cycling. Limnol Oceanogr 42:1803-1813

SKOOG A, BIDDANDA B, BENNER R (1999) Bacterial utilization of dissolved glucose in the upper water column of the Gulf of Mexico. Limnol Oceanogr 44, 1625-1633

SMITH DC, AZAM F (1992) A simple, economical method for measuring bacterial protein synthesis in seawater using ^{3}H-leucine. Mar Microb Food Webs 6:1007-114

SMITH DC, SIMON M, ALLDREDGE AL, AZAM F (1992) Intense hydrolytic enzyme-activity on marine aggregates and implications for rapid particle dissolution. Nature 359:139-142

SMITH DC, STEWART GF, LONG RA, AZAM F(1995) Bacterial mediation of carbon fluxes during a diatom bloom in a mesocosm. Deep Sea Res II 42:75-97

TANOUE E, HANDA N (1987) Monosaccharide composition of marine particles and sediments from the Bering Sea and Northern North Pacific. Oceanol Acta 10:91-99

VIEIRA AAH, ORTOLANO PIC, GIROLDO D, PAULSEN BS (2008) Role of hydrophobic extracellular polysaccharide of *Aulacoseira granulata* (Bacillariophyceae) on aggregate formation in a turbulent and hypereutrophic reservoir. Limnol Oceanogr 53:1887-1899

WAKEHAM SG, LEE C, HEDGES JI, HERNES PJ, PETERSON ML (1997) Molecular indicators of diagenetic status in marine organic matter. Geochim Cosmochim Acta 61:5363-5369

TABLES

Table 1. Initial concentration (nmol l^{-1}) and relative abundance (%) of neutral and acidic sugars in polysaccharides derived from monospecific *Emiliania huxleyi* cultures in *EhuxLAB* and from a natural phyotplankton community in the Gulf of Biscay (n.d. = not determined, OC = organic carbon, TOC = total organic carbon).

	EhuxLAB				**Gulf of Biscay, station 2 (surface)**	
	380 µatm CO_2		**750 µatm CO_2**			
	nmol l^{-1}	%	nmol l^{-1}	%	nmol l^{-1}	%
glucose	**7290**	**67**	**17416**	**72**	**514**	**57**
galactose	1210	11	1975	8	131	15
arabinose	337	3	410	2	7	1
mannose+ xylose	525	5	610	3	115	13
fucose	265	2	383	2	38	4
rhamnose	369	3	765	3	24	3
Σ deoxy sugars	**634**	**5**	**1148**	**5**	**62**	**7**
glucoronic acid	270	3	362	2	9	1
galacturonic acid	637	6	1989	8	51	6
Σ uronic acids	**907**	**9**	**2351**	**10**	**60**	**7**
OC in polysaccharides						
[µmol carbon l^{-1}]	**64.8**		**142.8**		**5.3**	
[% of TOC]	**5.9**		**10.6**		**n.d.**	

Table 2. The bacterial turnover of combined glucose in *EhuxLAB* (n. l. = no loss).

	polysaccharide degradation				assimilation of hydrolysates		
	hydrolysis by α-, β-glucosidase[a]		loss of combined glucose (< 1 kDa)[b]		uptake[c]		support BBP[d]
	h^{-1}	nmol l^{-1} h^{-1}	nmol l^{-1}	nmol l^{-1} h^{-1}	h^{-1}	nmol l^{-1} h^{-1}	%
380 µatm CO_2							
day 0 - 2	0.005	37	4825	101	0.023	2.31	16
day 2 - 4	0.005	12	1787	37	0.027	1.00	6.3
day 4 - 7	0.003	2	n. l.	-	-	-	-
day 7-14	0.001	1	n. l.	-	-	-	-
750 µatm CO_2							
day 0 - 2	0.017	297	14072	293	0.034	10.0	68
day 2 - 4	0.021	69	1634	34	0.024	0.82	5.6
day 4 - 7	0.012	21	678	9	0.018	0.17	2.0
day 7-14	0.003	3	88	1	0.020	0.01	0.3

[a] A ratio α-glucose : β-glucose of 1 : 1 was assumed to calculate the hydrolysis of combined glucose by α- and β-glucosidase.

[b] The loss rate of combined glucose (nmol l^{-1} h^{-1}) was calculated from the loss as determined by chemical analysis (nmol l^{-1}) divided by hours of time interval.

[c] The uptake rate (nmol l^{-1} h^{-1}) represents the uptake of glucose derived from the degradation of combined glucose (<1 kDa).

[d] support BBP = glucose uptake (nmol C l^{-1} h^{-1}) / BBP x 100, i.e. the fraction of carbon derived from assimilated combined glucose in bacterial biomass

Table 3. Final concentration (nmol l^{-1}) and relative abundance (%) of neutral and acidic sugars in polysaccharides derived from monospecific *Emiliania huxleyi* cultures in *EhuxLAB* (OC = organic carbon, TOC = total organic carbon).

	380 µatm CO_2		**750 µatm CO_2**	
	nmol l^{-1}	%	nmol l^{-1}	%
glucose	**949**	**18**	**943**	**15**
galactose	1095	22	1088	16
arabinose	429	8	491	8
mannose+ xylose	1061	21	1668	25
fucose	318	6	352	5
rhamnose	397	8	594	9
Σ deoxy sugars	**715**	**14**	**946**	**16**
glucuronic acid	141	3	209	3
galacturonic acid	701	14	1083	17
Σ uronic acids	**842**	**17**	**1292**	**20**
OC in polysaccharides				
[µmol carbon l^{-1}]	**29.6**		**37.2**	
[% of TOC]	**4.9**		**5.2**	

FIGURE CAPTIONS

Figure 1. Map of the northern Bay of Biscay with stations sampled during the campaign in May 2007.

Figure 2. Microscopic view on transparent exopolymer particles (TEP) and on cells of *Emiliania huxleyi* stained with Alcian Blue.

Figure 3. Glucose uptake rate constants as a function of α-glucosidase and β-glucosidase activity in the Gulf of Biscay (α-glucosidase: $r^2 = 0.66$, $p = 0.027$, $n = 7$; β-glucosidase: $r^2 = 0.65$, $p = 0.002$, $n = 12$). Open symbols represent datapoints not included in the regression analysis (st.=station, s=surface, sub= subsurface depth of 40 m).

Figure 4. Bacterial biomass production (BBP) as a function of glucose uptake rate constants in the Gulf of Biscay ($r^2 = 0.63$, $p < 0.001$, $n = 16$). Regression includes all data from surface and 40 m depth of all stations.

Figure 5. *Emiliania huxleyi* cells collected at the surface of station 2 in the Gulf of Biscay (A) included in microaggregates (A) and (B) fecal pellets. Picture was taken by scatter electron microscopy.

Figure 6. Concentration of combined glucose and sum concentration of other combined neutral sugars (galactose, arabinose, mannose, xylose, fucose, rhamnose) at 380 and 750 µatm CO_2. Fitted curves show nonlinear regression with $A_t = A_0 e^{-kt}$, where A_t is the concentration of combined glucose, A_0 the initial combined glucose concentration, and k the decay rate

constant (380 µatm CO_2: $A_t = 7.3\ e^{-0.53t}$, $r^2 = 0.96$, $p = 0.004$, $n = 5$; 750 µatm CO_2: $A_t = 17.4\ e^{-0.76t}$, $r^2 = 0.99$, $p < 0.001$, $n = 5$).

Figure 7. Bacterial biomass production (BBP) and bacterial cell numbers at 380 and 750 µatm CO_2.

Figure 8. Rate constants of α- and β-glucosidase and rate constants of glucose uptake at 380 and 750 µatm CO_2.

Figure 9. Concentration of total organic carbon (TOC) at 380 and 750 µatm CO_2. Fitted curve shows nonlinear regression with $A_t = A_0\ e^{-kt}$ for the incubation at 380 µatm CO_2, where A_t is the concentration of TOC, A_0 the initial TOC concentration, and k the decay rate constant ($A_t = 1097\ e^{-0.06t}$, $r^2 = 0.96$, $p = 0.04$, $n = 5$). A significant regression for the incubation at 380 µatm CO_2 could not be determined.

Figure 10. Concentration of TEP at 380 and 750 µatm CO_2. Fitted curves show nonlinear regression with $A_t = A_0\ e^{-kt}$, where A_t is the concentration of TEP, A_0 the initial TEP concentration, and k the decay rate constant (380 µatm CO_2: $A_t = 55.7\ e^{-0.11t}$, $r^2 = 0.96$, $p = 0.003$, $n = 5$; 750 µatm CO_2: $A_t = 80.2\ e^{-0.11t}$, $r^2 = 0.92$, $p = 0.01$, $n = 5$).

Figure 11. Changes in POC as a function of TEP at 380 µatm CO_2 ($r^2 = 0.90$, $p = 0.01$, $n = 5$) and 750 µatm CO_2 ($r^2 = 0.76$, $p = 0.05$, $n = 5$). Regressions yielded no significant offsets.

Figure 12. Ratios of [deoxy sugars + uronic acids] : [glucose] at 380 and 750 µatm CO_2.

Figure 13. Concentration of glucosamine at 380 µatm CO_2 ($r^2 = 0.98$, $p = 0.004$, $n = 5$) and 750 µatm CO_2 ($r^2 = 0.92$, $p = 0.08$, $n = 5$).

FIGURES

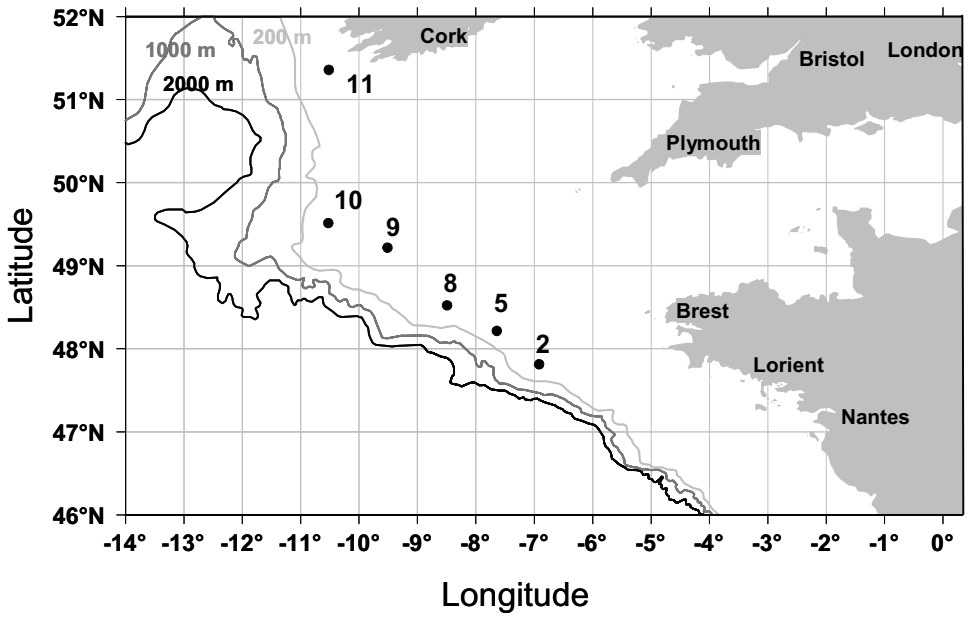

Figure 1

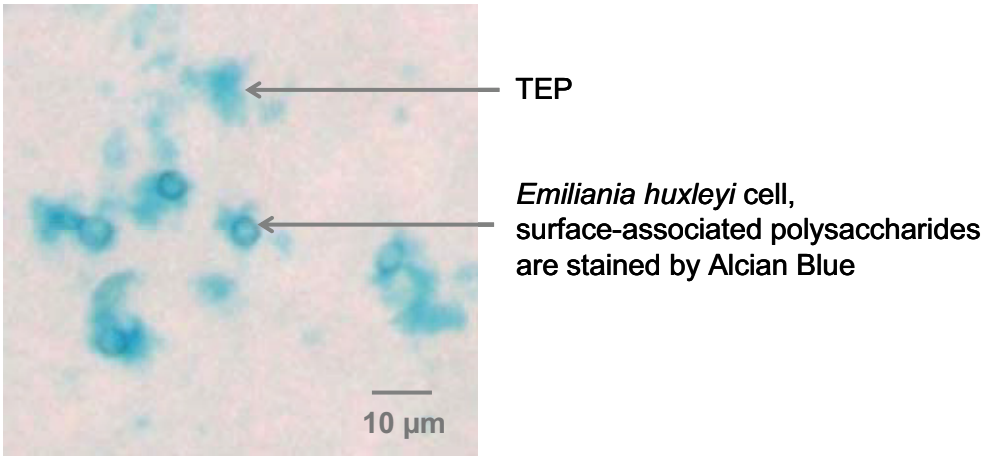
TEP
Emiliania huxleyi cell,
surface-associated polysaccharides
are stained by Alcian Blue
10 µm

Figure 2

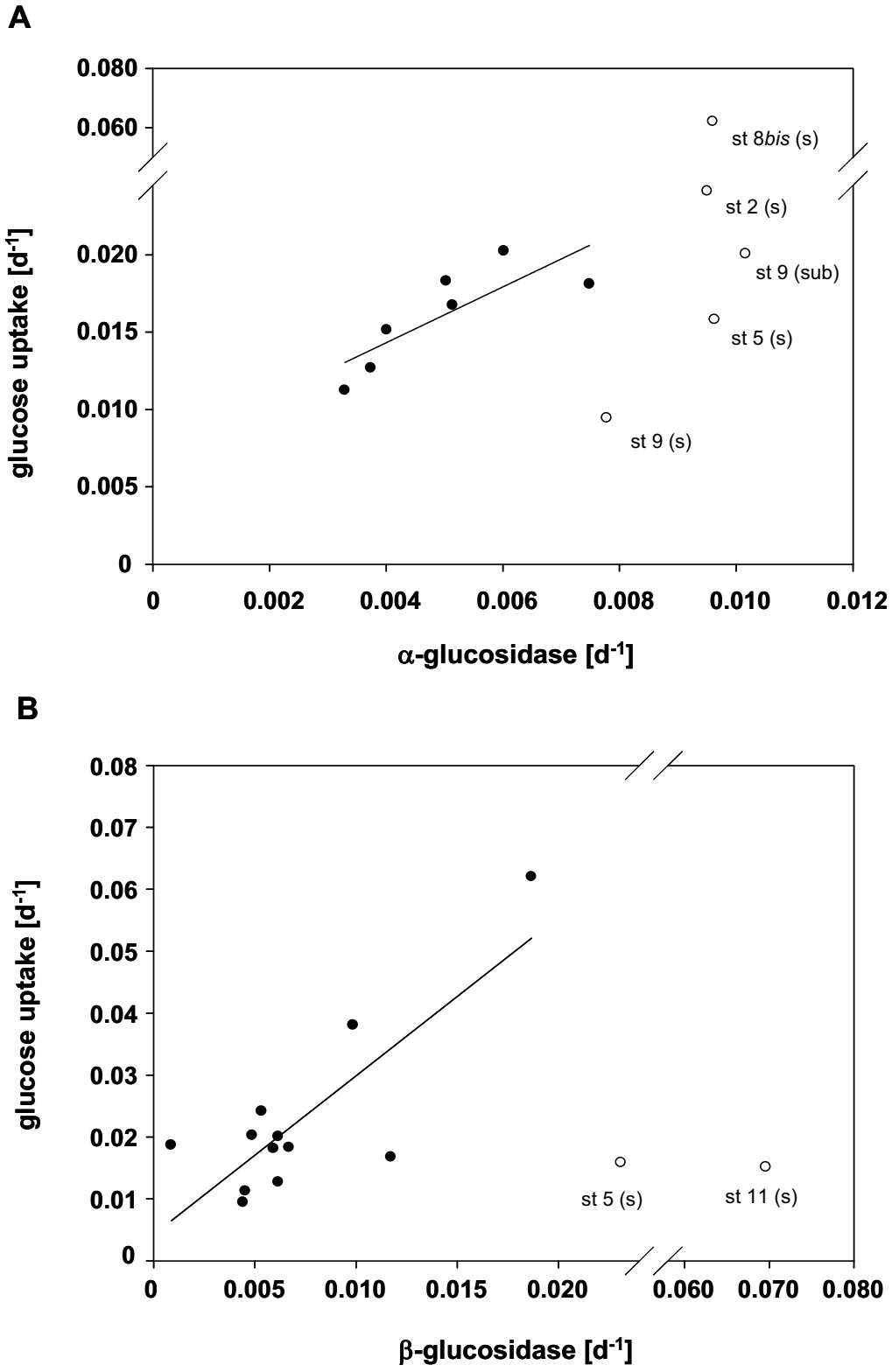
A
0.080
0.060
0.020
0.015
0.010
0.005
0
glucose uptake [d-1]
st 8bis (s)
st 2 (s)
st 9 (sub)
st 5 (s)
st 9 (s)
0
0.002
0.004
0.006
0.008
0.010
0.012
α-glucosidase [d-1]
B
0.08
0.07
0.06
0.05
0.04
0.03
0.02
0.01
0
glucose uptake [d-1]
st 5 (s)
st 11 (s)
0
0.005
0.010
0.015
0.020
0.060
0.070
0.080
β-glucosidase [d-1]

Figure 3

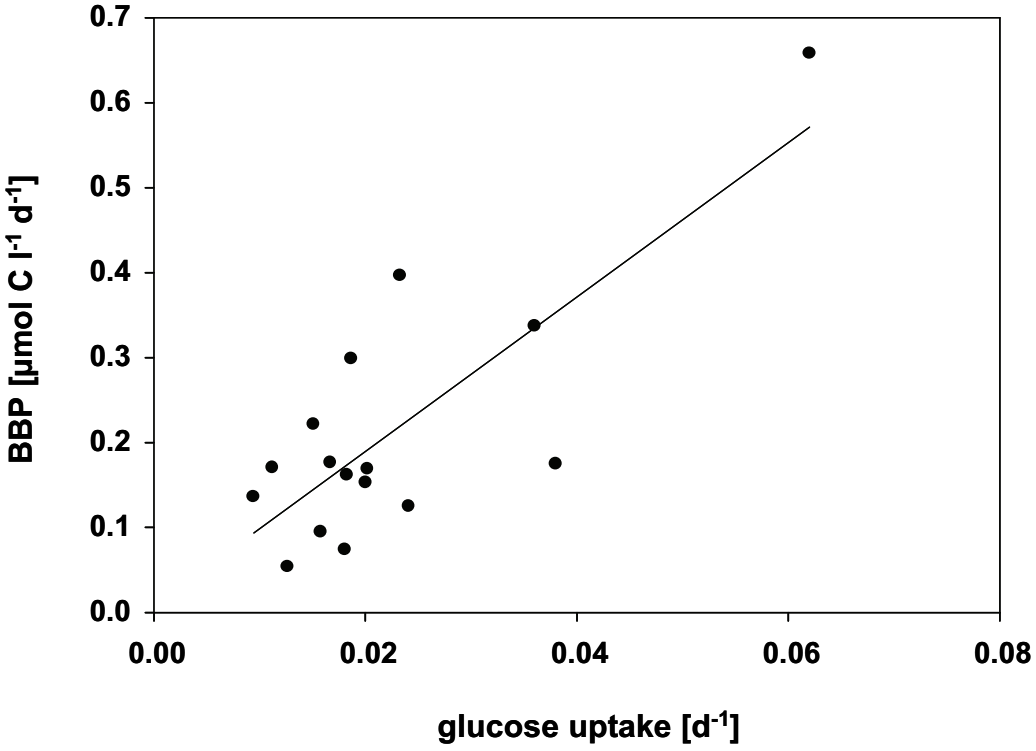
0.7
0.6
0.5
0.4
0.3
0.2
0.1
0.0
BBP [µmol C l-1 d-1]
0.00
0.02
0.04
0.06
0.08
glucose uptake [d-1]

Figure 4

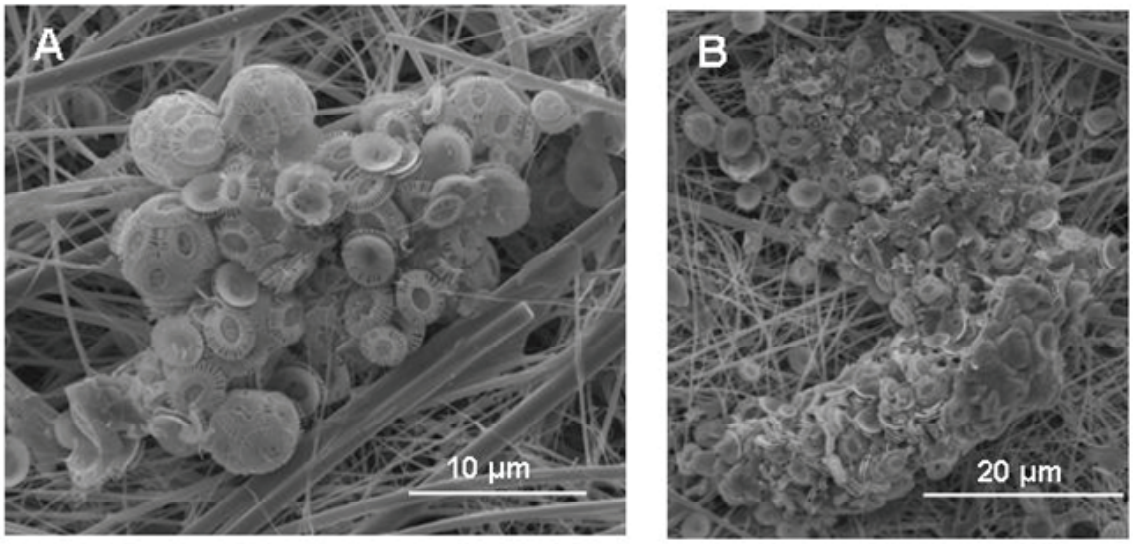

Figure 5

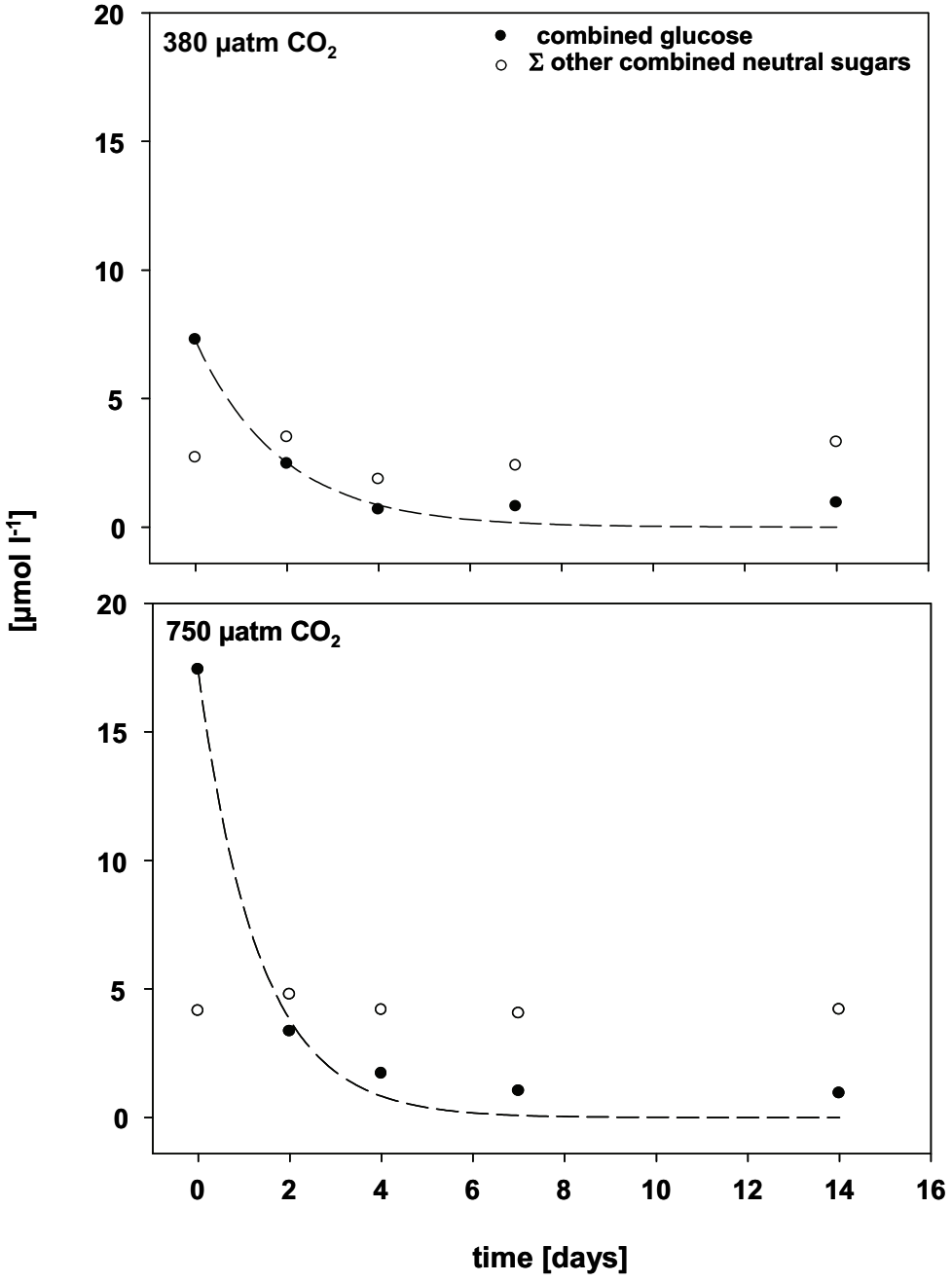
380 µatm CO_2
combined glucose
Σ other combined neutral sugars
750 µatm CO_2
[µmol l^{-1}]
time [days]
0
5
10
15
20
0
2
4
6
8
10
12
14
16

Figure 6

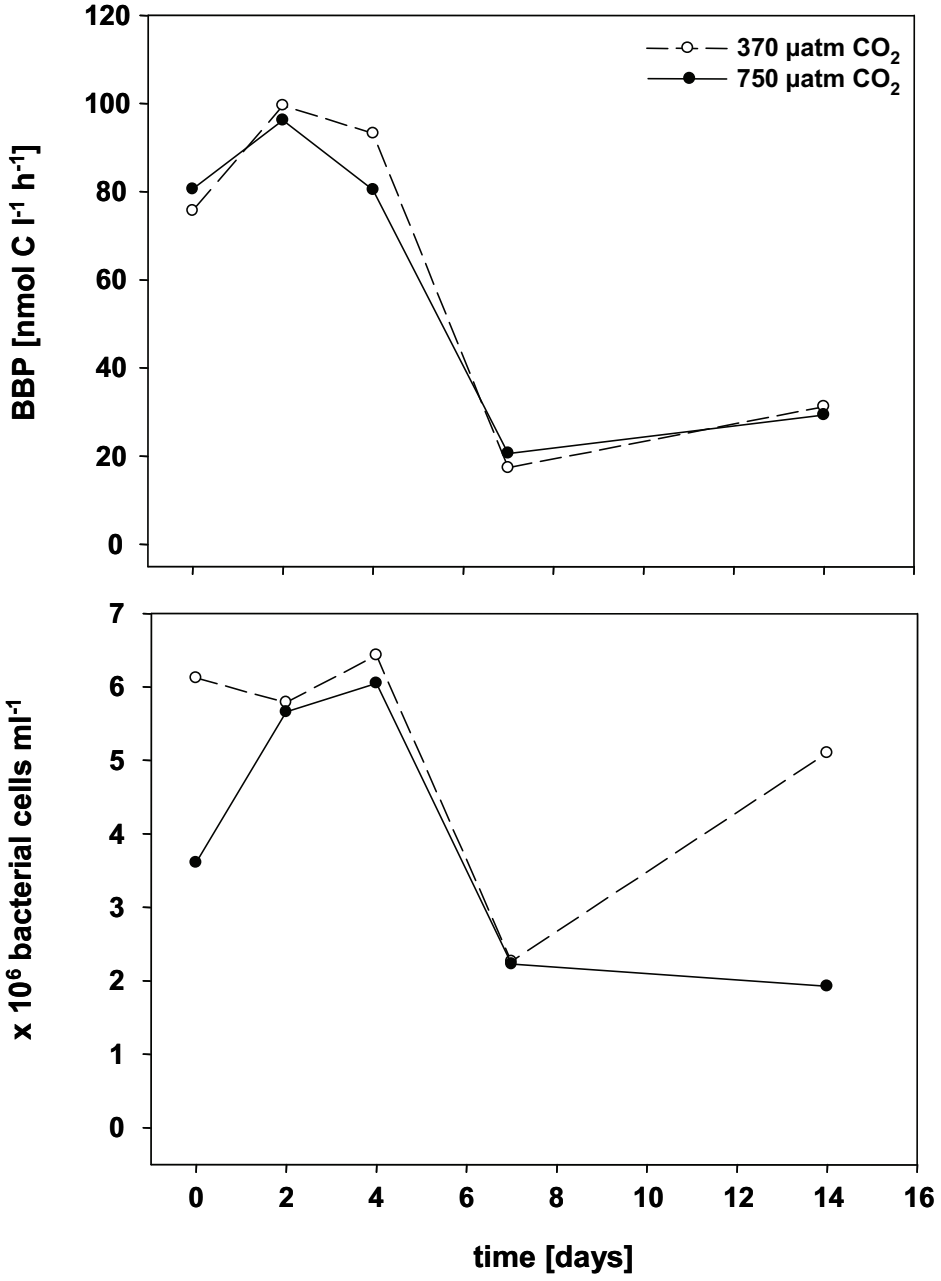
370 µatm CO2
750 µatm CO2
BBP [nmol C l-1 h-1]
x 10^6 bacterial cells ml-1
time [days]
0
20
40
60
80
100
120
0
1
2
3
4
5
6
7
0
2
4
6
8
10
12
14
16

Figure 7

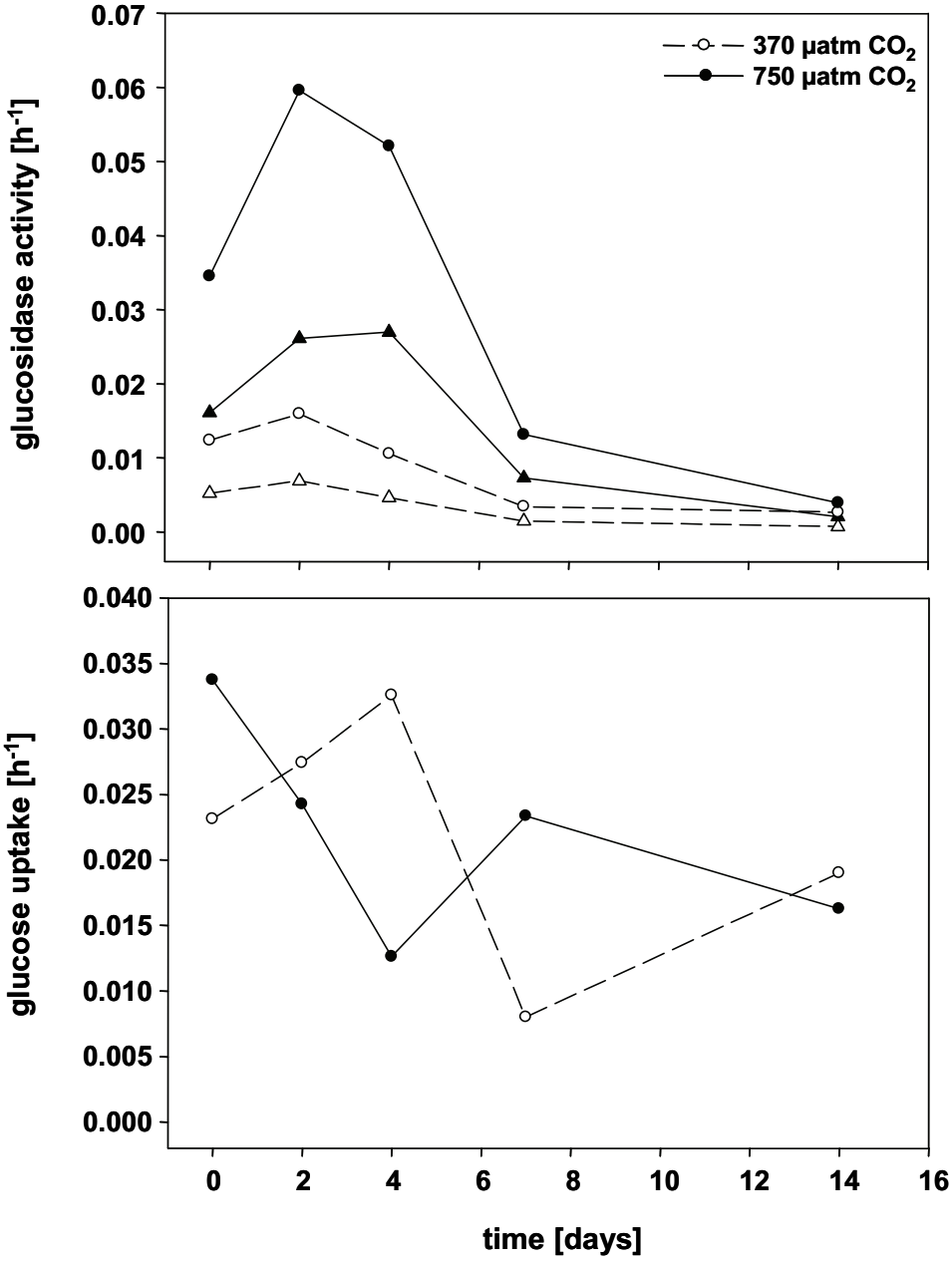
370 µatm CO2
750 µatm CO2
glucosidase activity [h-1]
0.07
0.06
0.05
0.04
0.03
0.02
0.01
0.00
glucose uptake [h-1]
0.040
0.035
0.030
0.025
0.020
0.015
0.010
0.005
0.000
0
2
4
6
8
10
12
14
16
time [days]

Figure 8

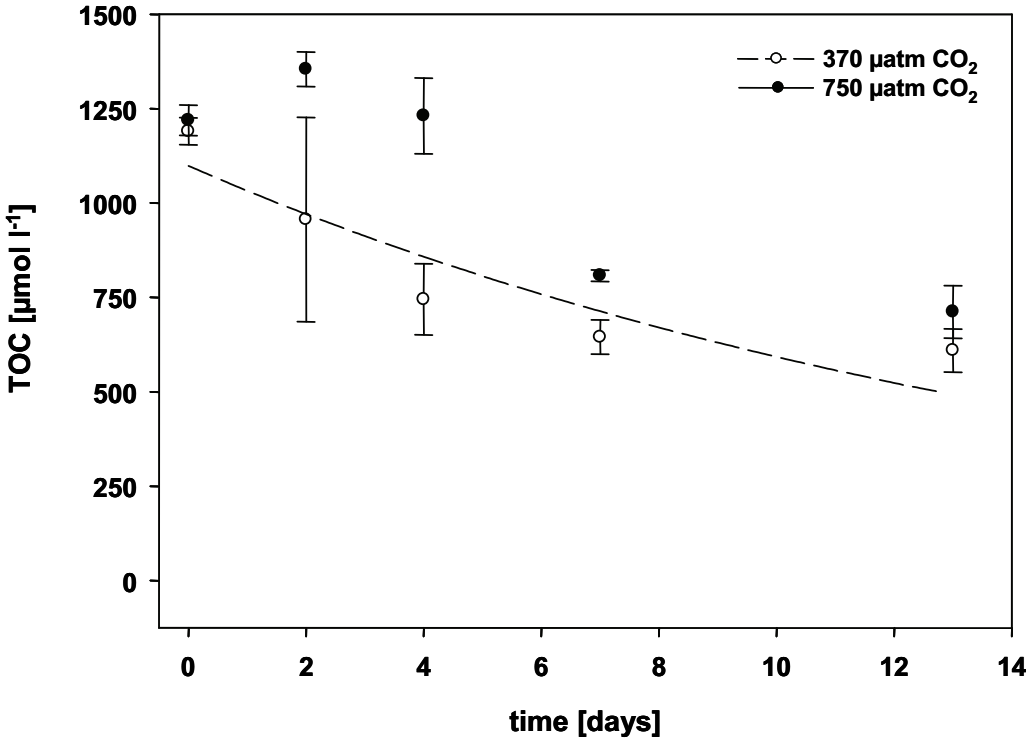
1500
1250
1000
750
500
250
0
TOC [µmol l-1]
0
2
4
6
8
10
12
14
time [days]
370 µatm CO2
750 µatm CO2

Figure 9

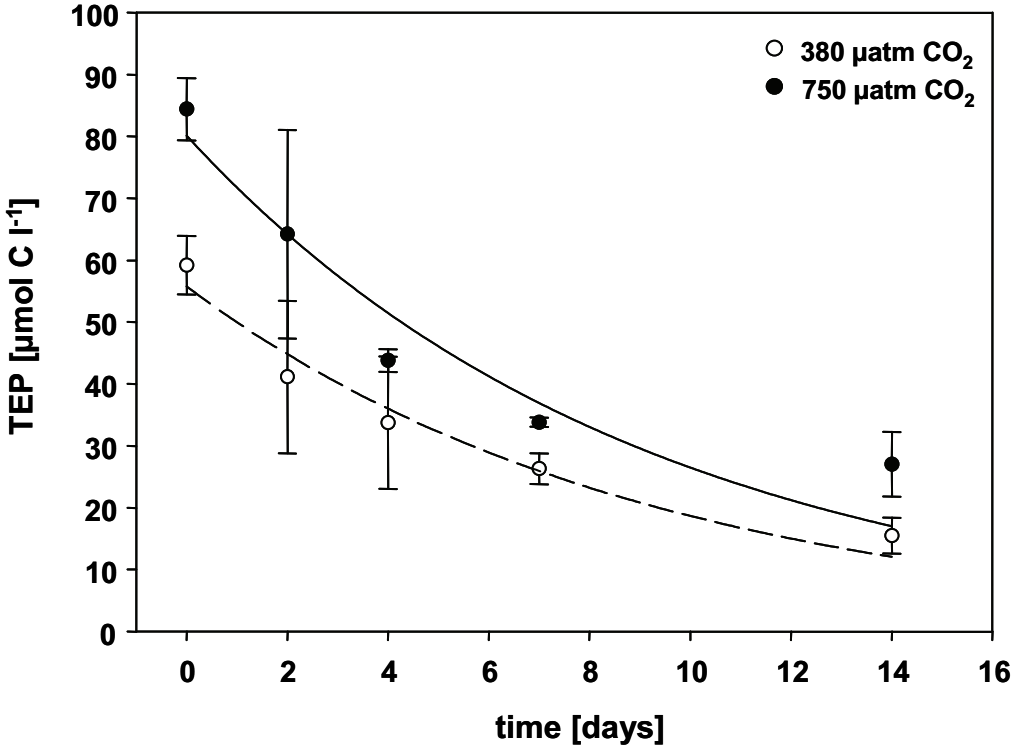
380 µatm CO2
750 µatm CO2
TEP [µmol C l-1]
time [days]
0
10
20
30
40
50
60
70
80
90
100
0
2
4
6
8
10
12
14
16

Figure 10

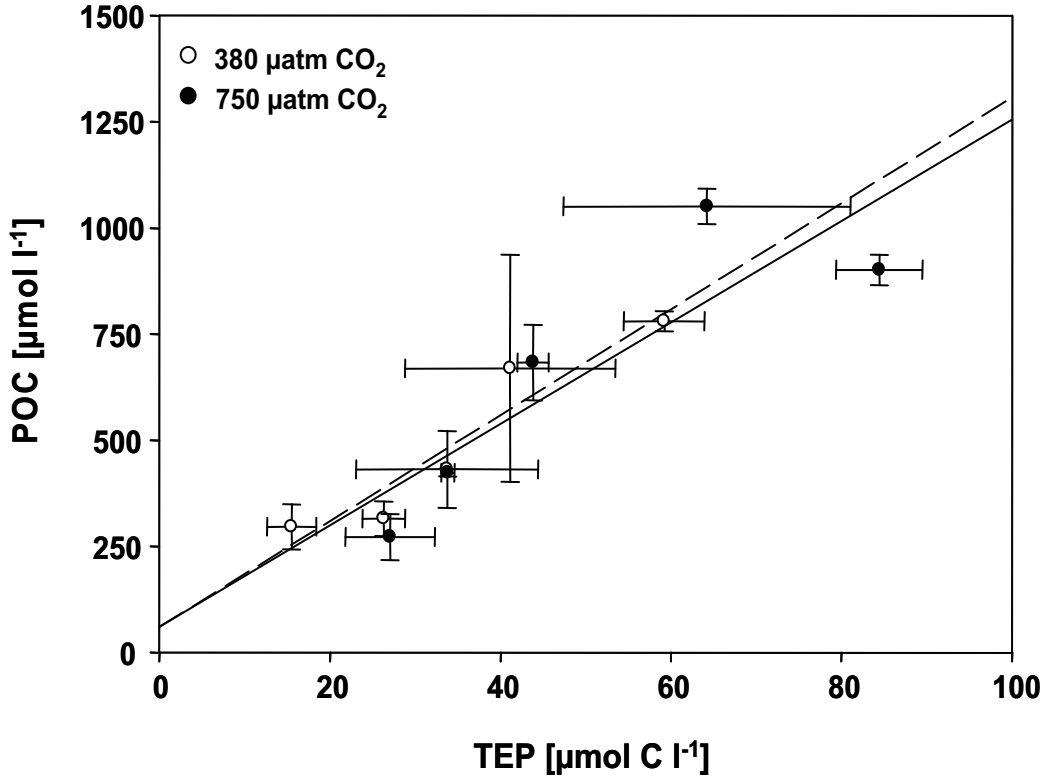
380 µatm CO2
750 µatm CO2
POC [µmol l-1]
TEP [µmol C l-1]
0
250
500
750
1000
1250
1500
0
20
40
60
80
100

Figure 11

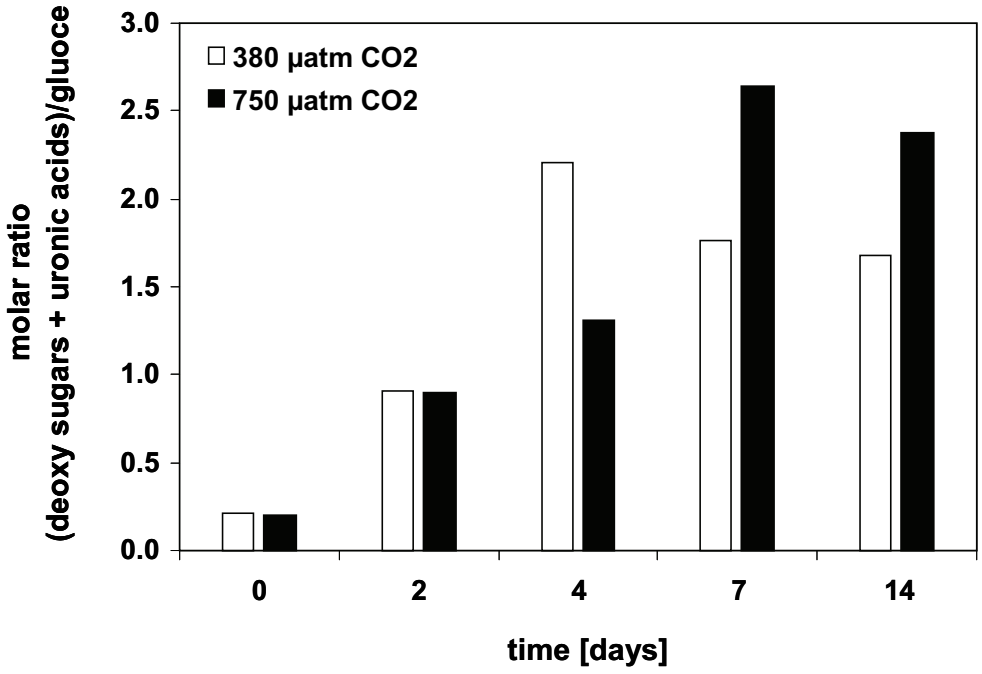
molar ratio
(deoxy sugars + uronic acids)/gluoce
3.0
2.5
2.0
1.5
1.0
0.5
0.0
380 µatm CO2
750 µatm CO2
0
2
4
7
14
time [days]

Figure 12

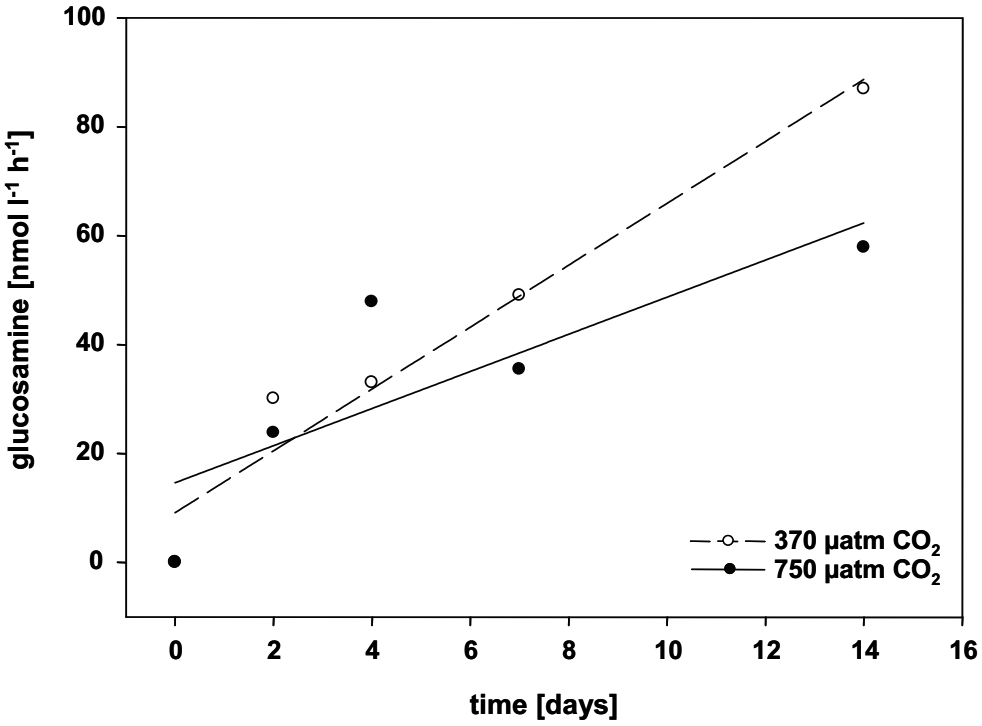
100
80
60
40
20
0
glucosamine [nmol l-1 h-1]
0
2
4
6
8
10
12
14
16
time [days]
370 µatm CO2
750 µatm CO2

Figure 13

Manuscript IV

Acidification increases microbial carbohydrate degradation in the ocean

Judith Piontek[1], Mirko Lunau[1], Nicole Händel[1], Corinna Borchard[1], Mascha Wurst[1] & Anja Engel[1]

Alfred Wegener Institute for Polar and Marine Research, Am Handelshafen 12, 27570 Bremerhaven, Germany

ABSTRACT: With the accumulation of anthropogenic carbon dioxide (CO_2), a proceeding decline in seawater pH has been induced that is referred to as ocean acidification. The ocean is one of the largest sinks for CO_2 on Earth in general and for anthropogenic emissions in particular. Thereby, the ocean's capacity for CO_2 storage is strongly affected by biological processes, whose feedback potential is difficult to evaluate. One dominant CO_2 source in the ocean is the bacterial degradation of organic matter and the subsequent respiration of organic molecules. Effects of decreasing ocean pH on marine bacteria and their degradation activity therefore provide a considerable climate feedback potential. This study reveals that the degradation of polysaccharides and particulate organic carbon (POC) by bacterial extracellular enzymes was significantly accelerated during experimental simulation of ocean acidification. Identified changes in the cycling of polysaccharides have a high potential to affect future carbon cycling and sequestration to the deep ocean. From a more general perspective, the identified responses of enzymes to decreasing pH have the potential to evoke effects of high complexity in the ocean, since this class of catalytic biomolecules drives innumerable metabolic pathways of the marine biota.

KEY WORDS: bacteria, polysaccharides, carbon pump, carbon cycle, CO_2, climate change

INTRODUCTION

Organic matter in the ocean is one of the largest dynamic carbon reservoirs on Earth that interacts with atmospheric CO_2 concentrations on time scales of 1,000 to 10,000 years (Hedges 1992). Biological consumption of CO_2 during photosynthesis and the related production of organic matter are counteracted by CO_2-regenerating processes with bacterial respiration being the predominant one (Rivkin & Legendre 2001). About 75-95% of organic matter produced by autotrophic organisms in the euphotic zone gets remineralized by heterotrophic bacteria within the upper water column (Martin et al. 1987, Boyd et al. 1999), the zone most strongly affected by ocean acidification (Raven et al. 2005). Potential effects of ocean acidification on the bacterial metabolism are therefore of utmost importance for the cycling of organic matter and the carbon balance in the ocean.

Phytoplankton cells and their debris are a main source of bioreactive organic matter in the ocean. Bacteria cluster around phytoplankton, colonizing particle surfaces and plumes of leaking solutes (Fig. 1). The bacterial degradation of organic matter is initiated by the activity of extracellular enzymes (Hoppe et al. 1988, Chróst 1991). Macromolecules are enzymatically hydrolyzed outside of bacterial cells into units of low molecular weight that are small enough to be transported across the cytoplasmic membrane (Hoppe et al. 1988, Chróst 1991). The pH is a crucial and omnipresent factor influencing enzymatic activity. Changing concentrations of hydrogen ions in the enzyme's environment alter the ionization state of amino acids, and thus affect the three-dimensional protein structure of the active site. Enzymatic reactions exhibit a specific narrow range of pH, where highest activity is apparent, but already small deviations from this pH optimum result in decreased reaction rates. In contrast to intracellular enzymes, acting in the cell's buffered cytoplasm, bacterial extracellular enzymes directly experience the pH of the outer environment. Equilibration of seawater with rising CO_2 in the atmosphere has already lowered the ocean

pH by 0.12 units compared to pre-industrial values, which in turn has increased the concentration of hydrogen ions by 30% (Houghton et al. 2001, Sabine et al. 2004, Raven et al. 2005). Today, it is not known how present and upcoming changes induced by ocean acidification will affect the bacterial turnover of organic matter.

MATERIAL AND METHODS

Experiments

In order to examine the effect of ocean acidification on the bacterial degradation of organic matter we conducted a series of four experiments, referred to as *Ehux_lab1*, *Ehux_lab2*, *Biscay_nat*, and *Biscay_ch* (Tab. 1). Particulate and dissolved organic matter derived from coccolithophore-dominated natural phytoplankton communities and from monospecific cultures of the bloom-forming coccolithophore *Emiliania huxleyi* was degraded by natural bacterioplankton communities in chemostat systems and in batch incubations. Degradation of organic carbon and activities of bacterial extracellular enzymes at the present-day pCO_2 level of 380 µatm were compared with treatments representing near-future (750 µatm pCO_2) conditions (Houghton et al. 2001, Raven et al. 2005).

Organic matter in *Ehux_lab1* was derived from a continuous culture of *Emiliania huxleyi* (strain PML B92/11). A 16/8 hours light/dark cycle and a photon flux density of 300 µmol photons m^{-2} s^{-1} were applied. The culture was grown for 12 days under nutrient-deplete conditions before the bacterial inoculum was added. In *Ehux_lab2*, a batch culture of *Emiliania huxleyi* (strain PML B92/11) was grown in sterile-filtered seawater enriched with 50 µM nitrate and 3 µM phosphate, applying a 16/8 hour light/dark cycle and a photon flux density of 200 µmol photons m^{-2} s^{-1}. Culture-derived organic matter was inoculated with a natural bacterial community collected at the North Sea after 27 days,

when decreasing growth rates of *Emiliania huxleyi* indicated exhaustion of inorganic nutrients. *Biscay_ch* and *Biscay_nat* were conducted with natural assemblages, including phyto- and bacterioplankton, collected at the Gulf of Biscay (North Atlantic) in June 2006 (47°05'34"N, 7°16'63"E) and May 2007 (47°07'83"N, 6°92'01"E), respectively. The phytoplankton communities at these sites were dominated by coccolithophores. The autotrophic production of organic matter under nutrient-deplete conditions and the co-occurring degradation by bacterioplankton were investigated by the use of a chemostat system in *Biscay_ch*. In *Biscay_nat*, the degradation of organic matter by the bacterioplankton community was conducted in bottle incubations.

The pH of seawater was modified either by aeration with defined CO_2-air-mixtures or by addition of dilute hydrochloric acid. Incubations were continuously aerated with CO_2-air-mixtures containing 380 µatm and 750 µatm CO_2 in *Ehux_lab1* and *Biscay_ch*. In *Ehux_lab2* and *Biscay_nat*, degradation of organic matter in incubations with unmodified pH, representing 'present day' conditions, was compared with incubations acidified with CO_2 gas and 0.1 M hydrochloric acid, respectively. The target pH equivalent to 750 µatm CO_2 was calculated from the unmodified pH and the initial total alkalinity by the use of the program CO_2sys (Lewis & Wallace 1998). Total alkalinity was determined by the Gran electrotitration method (Gran 1952). The pH was measured using a combined temperature- and pH-probe (WTW 340i).

Furthermore, effects of pH on purified enzymes were tested with α-glucosidase of *Bacillus staerothermophilus* (Sigma).

Analytical Methods

The analysis of total combined carbohydrates (TCCHO) was carried out by ion chromatography (HPAEC-PAD, Dionex) (Engel & Händel, submitted). Samples were

desalted by the use of dialysis membranes (1 kDa). Prior to analysis, dissolved and particulate carbohydrates were hydrolyzed with hydrochloric acid at a final concentration of 0.8 M for 20 hours at 100°C. Samples for particulate organic carbon (POC) were filtered onto precombusted glass fibre filters (GF/F, Whatman). Filters were acidified with 0.2 M hydrochloric acid to remove all particulate inorganic carbon. After drying, concentrations of POC were determined with an elemental analyzer (EuroEA, Euro Vector).

Activities of extracellular enzymes were determined by the use of fluorogenic substrate analogues (Hoppe 1983). The activities of α-glucosidase and β-glucosidase were estimated from the enzymatic hydrolysis of 4-methylumbelliferyl-α-glucopyranoside (MUF-α-gluco) and 4-methylumbelliferyl-β-glucopyranoside (MUF-β-gluco), respectively. Samples were incubated at *in-situ* temperature for 3 to 5 hours with fluorogenic substrates added to a final concentration of 1 µM in all experiments. The fluorescence emitted by 4-methylumbelliferone (MUF) molecules was detected at 355 nm excitation and 460 nm emission wavelength, using a plate reader (FLUOstar OPTIMA, BMG Labtech, and Fluoroskan Ascent, Thermo Labsystems) or a cuvette fluorometer (F-2000, Hitachi). Calibration was carried out with solutions of MUF. In order to consider the effect of pH on the fluorescence intensity of MUF, standard solutions were adjusted to pH 7.6, 7.8, 8.0, 8.2, and 8.3, buffered with 1% 3-(N-Morpholino)-propanesulfonic acid. The activities of α-glucosidase purified from *Bacillus staerothermophilus* (Sigma) was calculated from the turnover time of 50 µM MUF-α-gluco in 1 mM n-2-hydroxyethylpiperazone-n-2-ethanesulfonic acid adjusted to pH 7.55, 7.70, 7.90, and 8.10. Fluorescence was measured in time intervals of 5 minutes for 2 hours using a plate reader (FLUOstar OPTIMA, BMG Labtech).

Bacterial cell numbers were determined by flow cytometry (FACSCalibur, Beckton Dickinson) in *Ehux_lab1*, *Ehux_lab2*, and *Biscay_nat*. Nucleic acid was stained with SybrGreen I (Invitrogen). Bacterial abundances were estimated after visual inspection of the dot plot of SSC vs. FL1, and manual gating of the bacterial subpopulation. Yellow-green fluorescent latex beads (diameter 0.94 µm, Polyscience) were used to normalize the counted events to a reference volume. TruCount beads (Beckton Dickinson) were used for daily intercalibration and absolute volume calculation (Gasol & Del Giorgio 2000). Bacterial cells were counted by epifluorescence microscopy in *Biscay_ch*. For this purpose, samples were filtered onto black 0.2 µm polycarbonate filters and stained with 4',6-diamidino-2-phenylindole (DAPI) (Porter & Feig 1980). Bacterial abundances were calculated from cell counts of 10 randomly selected fields per filter that contained at least 100 cells each.

RESULTS

Our results demonstrate that acidification had a substantial effect on the bacterial degradation of polysaccharides and POC by extracellular enzymes. The loss of TCCHO, which contribute largely to the reactive organic carbon pool in the ocean (Pakulski & Benner 1994), was in average 21 ± 6% higher in incubations at 750 µatm CO2 than at 380 µatm CO_2. Also the loss of phytoplankton-derived POC at 750 µatm CO_2 was between 8 and 40% higher than in incubations at 380 µatm CO_2 (Fig. 2). The significantly higher loss of TCCHO (p=0.03, n=4) and of POC (p=0.05, n=3) was accompanied by higher glucosidase activity at lowered pH (p=0.03, n=6) (Fig. 2). The activity of glucosidases cleaves glycosidic linkages in polysaccharides (Barmann 1969, Béguin 1990). Relative to present-day pH, the hydrolytic activities of α- and β-glucosidase increased at predicted

future pH conditions by a factor of 1.5 to 11.3 and 2.7 to 5.6, respectively, depending on the increase in hydrogen ions. The observed increase in activity of extracellular glucosidases at decreasing pH is consistent with the pH characteristics of purified bacterial glucosidase. The activity of α-glucosidase isolated from *Bacillus stearothermophilus* increased by a factor of 15.5, when pH dropped from 8.10 to 7.55. Linear regression revealed that α- and β-glucosidase activity was directly related to the increase in hydrogen ions across all laboratory and field experiments (α-glucosidase: r^2=0.86, n=7, p<0.0001; β-glucosidase: r^2=0.88, n=4, p=0.0008) (Fig. 3).

DISCUSSION

The impact of ocean acidification on the cycling of organic carbon in polysaccharides mediated by increased activities of bacterial extracellular glucosidases has the potential to provide a positive feedback on the atmospheric CO_2 (Fig. 4). The accelerated bacterial degradation of polysaccharides included in sinking particles may affect the vertical export of organic carbon. In the ocean, the flux of sinking particles is strongly reduced by the activity of extracellular enzymes in the surface layer and in the mesopelagic zone (Smith et al. 1992). Based on our findings, it can be assumed that the amount of polysaccharide-derived carbon available for export in the future ocean will be curtailed due to increased extracellular glucosidase activity at lowered ocean pH. The export of organic carbon contained in particles sinking to the deeper ocean, referred to as biological carbon pump (Volk & Hoffert 1985), sustains a vertical gradient of dissolved inorganic carbon in the ocean that in turn drives the ocean's uptake of atmospheric CO_2. An enhanced degradation of polysaccharides in sinking particles potentially weakens the future biological carbon

pump, and thus the ocean's ability to absorb CO_2 from the atmosphere. The most significant effect of accelerated polysaccharide degradation at lowered ocean pH on the cycling of organic carbon must be expected during the decline of phytoplankton blooms, when increasing bacterial degradation activity coincides with high proportions of polysaccharides in POC (Handa et al. 1992, Lochte et al. 1993).

The degradation of organic matter by extracellular enzymes generates the supply of substrates for bacterial uptake and metabolism in the ocean (Chróst 1991). Increased glucosidase activity at lowered ocean pH will enhance the release of monomeric glucose from the hydrolysis of particulate and dissolved polysaccharides. Among the great diversity of organic carbon compounds in the ocean, free glucose monomers must be considered as key carbon source for bacteria (Rich et al. 1996). Concentrations of glucose monosaccharides in the ocean are usually below 100 nM (Rich et al. 1996, Skoog et al. 2002), but high glucose uptake rate constants reveal high fluxes and underscore the importance of glucose as a major carbon and energy source for the bacterial metabolism. An enhanced enzymatic hydrolysis of polysaccharides at lowered ocean pH will increase the fraction of glucose available for bacterial utilization. Up to 60% of glucose taken up by marine bacteria is respired to CO_2 (Rich et al. 1996). It can therefore be assumed that increased glucose availability at lowered pH will fuel the bacterial respiratory production of CO_2. The proportion of bacterial production supported by glucose largely depends on the availability of appropriate nitrogen compounds to meet stoichiometric requirements of bacterial growth (Rich et al. 1996, Skoog et al. 2002). To compensate an insufficient supply of organic nitrogen, marine bacteria may increase their share in dissolved inorganic nitrogen (DIN) consumption. In particular, increasing glucose availability was shown to increase the bacterial consumption of ammonium (Kirchman et al. 1990). Since bacteria compete for DIN with phytoplankton, an increased bacterial consumption of DIN can

change the partitioning of inorganic nutrients between the two groups for the disadvantage of autotrophic production (Kirchman et al. 1990, Kirchman 2000).

Changing activities of bacterial extracellular glucosidases at elevated CO_2 concentration represent a direct biochemical response to increased proton concentration. Further research, however, will have to elucidate potential secondary effects of acidification on organic matter degradation induced by changes in the community composition, and in the associated functional capabilities of marine bacterioplankton. Since enzymes mediate metabolic processes in all life forms, it can be assumed that effects of decreasing pH on enzymatic activities will impact a variety of biological processes in the future ocean, thus evoking consequences of unprecedented complexity. It has previously been shown that enzymes in muscle tissues of fish respond to ocean acidification (Michaelidis et al. 2007), same as enzymes involved in growth and carbon acquisition of phytoplankton species (Hansen et al. 2007). Here, extracellular enzymes of bacteria were identified as pH-sensitive keystone in the turnover of organic matter, playing a decisive role for marine biogeochemical cycles (Azam 1998, Azam & Malfatti 2007). In the face of rapidly changing marine ecosystems, a better understanding of acidification effects on the metabolism of marine organisms influencing biogeochemical cycles becomes a matter of urgency.

REFERENCES

AZAM F (1998) Microbial control of oceanic carbon flux: The plot thickens. Science 280:694-696

AZAM F, MALFATTI F (2007) Microbial structuring of marine ecosystems. Nature Reviews Microbiology 5:782-791

BARMANN TE (1969) Enzyme handbook, vol.2 (Springer Verlag, Berlin)

BÉGUIN P (1990) Molecular biology of cellulose degradation. Annu Rev Microbiol 44:219-248

BOYD PW, SHERRY ND, BERGES JA, BISHOP JKB, CALVERT SE, CHARETTE MA, GIOVANNONI SJ, GOLDBLATT R, HARRISON PJ, MORAN SB, ROY S, SOON M, STROM S (1999) Transformations of biogenic particulates from the pelagic to the deep ocean realm. Deep-Sea Res Part II 46:2761-2792

CHRÓST R (1991) Environmental control of the synthesis and activity of aquatic microbal ectoenzymes. In: Chróst R (ed) Microbial enzymes in aquatic environments. (Springer, Berlin)

GASOL JM, DEL GIORGIO PA (2000) Using flow cytometry for counting natural planktonic bacteria and understanding the structure of planktonic bacterial communities. Sci Mar 64:197-224

ENGEL A, HÄNDEL N (submitted) Simultaneous determination of the neutral-, amino-, and acidic sugar composition of polysaccharides in seawater using High Performance Anion Exchange Chromatography with Pulsed Amperometric Detection

GRAN G (1952) Determination of the equivalence point in potentiometric titrations of seawater with hydrochloric acid. Oceanol Acta 5:209–218

HANDA N, NAKATSUKA T, FUKUCHI M, HATTORI H, HOSHIAI T (1992) Vertical fluxes and ecological significance of organic materials during the phytoplankton bloom during austral summer in Breid Bay, Antarctica. Mar Biol 112:469-478

HANSEN PJ, LUNDHOLM N, ROST B (2007) Growth limitation in marine red-tide dinoflagellates: effects of pH versus inorganic carbon availability. Mar Ecol Prog Ser 334:63-71

HEDGES JI (1992) Global Biogeochemical cycles - progress and problems. Mar Chem 39:67-93

HOPPE HG (1983) Significance of Exoenzymatic Activities in the Ecology of Brackish Water - Measurements by Means of Methylumbelliferyl-Substrates. Mar Ecol Prog Ser 11:299-308

HOPPE HG, KIM SJ, GOCKE K (1988) Microbial decomposition in aquatic environments - combined process of extracellular enzyme-activity and substrate uptake Appl Environ Microbiol 54:784-790

HOUGHTON JT, DING Y, GRIGGS DJ, NOGUER M, VAN DER LINDEN PJ, DAI X, MASKELL K, JOHNSON CA (2001) Climate Change 2001: The Scientific Basis: Contribution of Working Group I to the Third Assessment Report of the Intergovernmental Panel of Climate Change, (Cambridge University Press)

KIRCHMAN DL (2000) Uptake and regeneration of inorganic nutrients by marine heterotrophic bacteria (Wiley, New York)

KIRCHMAN DL, KEIL RG, WHEELER PA (1990) Carbon limitation of ammonium uptake by heterotrophic bacteria in the sub-arctic pacific. Limnol and Oceanogr 35:1258-1266

LEWIS E, WALLACE DWR (1998) Program developed for CO_2 System Calculations. ORNL/CDIAC-105, Energy USDo)

LOCHTE K, DUCKLOW HW, FASHAM MJR, STIENEN C (1993) Plankton succession and carbon cycling at 47°N 20°W during the JGOFS North Atlantic bloom experiment. Deep-Sea Res Part II 40:91-114

MARTIN JH, KNAUER GA, KARL DM, BROENKOW WW (1987) VERTEX - Carbon cycling in the northeast pacific. Deep-Sea Res Part A 34:267-285

MICHAELIDIS B, SPRING A, PÖRTNER HO (2007) Effects of long-term acclimitation to environmental hypercapnia on extracellular acid-base status and metabolic capacity in Mediterranean fish Sparus aurata. Mar Biol 150:1417-1429

PAKULSKI JD, BENNER R (1994) Abundance and distribution of carbohydrates in the ocean. Limnol and Oceanogr 39:930-940

PARRY M, CANZIANI O, PALUTIKOF J, VAN DER LINDEN PJ, HANSON C (2007) Climate Change 2007: Impact, Adaption and Vulnerability: Contribution of Working Group II to the Fourth Assessment Report of the Intergovernmental Panel of Climate Change, (Cambridge University Press)

PORTER KG, FEIG YS (1980) The use of DAPI for identifying and counting aquatic microflora. Limnol and Oceanogr 25:943-948

RAVEN J, CALDEIRA K, ELDERFIELD H, HOEGH-GULDBERG O, LISS PS, RIEBESELL U, SHEPHERD J, TURLEY C, WATSON A (2005) Ocean acidification due to increasing atmospheric carbon dioxide. The Royal Society 12:68

RICH JH, DUCKLOW HW, KIRCHMAN DL (1996) Concentrations and uptake of neutral monosaccharides along 140 degrees W in the equatorial Pacific: Contribution of glucose to heterotrophic bacterial activity and the DOM flux. Limnol Oceanogr 41:595-604

RIVKIN RB, LEGENDRE L (2001) Biogenic carbon cycling in the upper ocean: Effects of microbial respiration. Science 291:2398-2400

SABINE CL, FEELY RA, GRUBER N, KEY RM, LEE K, BULLISTER JL, WANNINKHOF R, WONG CS, WALLACE DWR, TILBROOK B, MILLERO FJ, PENG TH, KOZYR A, ONO T, RIOS AF (2004) The oceanic sink for anthropogenic CO2. Science 305:367-371

SKOOG A, WHITEHEAD K, SPERLING F, JUNGE K (2002) Microbial glucose uptake and growth along a horizontal nutrient gradient in the North Pacific. Limnol Oceanogr 47:1676-1683

SMITH DC, SIMON M, ALLDREDGE AL, AZAM F (1992) Intense hydrolytic enzyme-activity on marine aggregates and implications for rapid particle dissolution. Nature 359:139-142

VOLK T, HOFFERT MI (1985) The Carbon Cycle and Atmospheric CO_2. Natural Variations Archean to Present (Am Geophys Union, Washington DC)

TABLES

Table 1. Setup of degradation experiments.

Bacterial cell numbers and particulate organic carbon (POC) concentrations given as mean values ± standard deviation (SD); * for *Biscay_nat* one field sample was subdivided into acidified and non-acidified replicates.

experiment	sample origin	incubation mode (period)	T [°C]	light regime	initial bacteria [x10^6 cells ml^{-1}]	initial POC [µM]	pCO_2 [µatm]	pH (replicates)
Ehux_lab1	culture of *Emiliania huxleyi* (PML B92/11)	batch (13 days)	15	permanent dark	4.9 ± 1.8	840 ± 86	380 750	7.9 (n=1) 7.7 (n=1)
Ehux_lab2	culture of *Emiliania huxleyi* (PML B92/11)	batch (30 days)	14	permanent dark	21.4 ± 5.3	522 ± 168	380 750	8.3 (n=2) 8.1 (n=2)
Biscay_ch	natural community (Gulf of Biscay, 2006)	chemostat (8 days)	16	light/dark 16/8 h, 200 µmol photons m^{-2} s^{-1}	6.2 ± 2.5	48 ± 12	380 750	7.9 (n=2) 7.6 (n=2)
Biscay_nat	natural community (Gulf of Biscay 2007)	batch (12 days)	10	permanent dark	0.08 *	14 *	380 750	8.2 (n=3) 7.9 (n=3)

FIGURE CAPTIONS

Figure 1

Marine bacteria clustered around cells of the coccolithophore *Emiliania huxleyi*.

Bacterial cells were stained with SybrGreen I, a cyanine dye that binds to double-stranded DNA, and emits green fluorescence. Chlorophyll in cells of *Emiliania huxleyi* fluoresces in red. The picture was taken by epifluorescence microscopy at 1000-fold magnification.

Figure 2

Microbial activity and degradation of organic carbon in marine systems at present-day and future pCO_2 conditions. Bacterial cell numbers, glucosidase activity, loss of total combined carbohydrates (TCCHO) and particulate organic carbon (POC) were determined in treatments of 380 µatm pCO_2 (open bars) and 750 µatm pCO_2 (solid bars), respectively. Organic matter was derived from monospecific cultures of *Emiliania huxleyi* in the experiments *Ehux_lab1* and *Ehux_lab2*. The experiment *Biscay_nat* was conducted with a natural plankton community sampled in the Bay of Biscay. Bacterial cell numbers and glucosidase activity are mean values over incubation time. Loss of TCCHO and POC was calculated by subtracting initial from final concentration (n.d.: no loss detectable). Error bars denote the standard deviation from replicate incubations in *Ehux_lab2* (n = 2) and *Biscay_nat* (n = 3). Standard deviation was not calculated for the loss of TCCHO in *Biscay_nat*, since replicate incubations were pooled for analysis. Significance between CO_2 treatments was assessed by means of *t*-tests (n.s.: not significant). Data of all experiments were summarized for statistical tests.

Figure 3

Changing activity of extracellular glucosidases in response to rising hydrogen ion concentrations. Changes in α- and ß-glucosidase activities (solid circles: marine α-glucosidase, triangles-down: purified α-glucosidase, open circles: β-glucosidase). The relative change in glucosidase activity (C_A) was calculated according to $C_A = (A_{fu}-A_{pr})/A_{pr}$, where A_{pr} is the enzymatic activity [nmol l^{-1} h^{-1}] at present-day pCO_2 conditions of 380 µatm, and A_{fu} the enzymatic activity [nmol l^{-1} h^{-1}] at the future pCO_2 levels of 750 µatm and 1400 µatm, respectively. The corresponding increase in hydrogen ion concentration (Δ hydrogen ions) [nmol l^{-1}] was calculated from the difference in pH between the CO_2 treatments. Dashed lines represent linear regressions (α-glucosidase: $r^2 = 0.86$, n = 7, $p < 0.0001$; β-glucosidase: $r^2 = 0.88$, n = 4, $p = 0.0008$).

Figure 4

Expected effects of ocean acidification on the degradation of organic carbon mediated by increasing glucosidase activity. Increased glucosidase activity (GA) at lowered ocean pH enhances the degradation of polysaccharides included in the pools of dissolved organic carbon (DOC) and particulate organic carbon (POC). As a consequence, the amount of POC available for export to the deeper ocean decreases. The increased availability of the hydrolytic product of polysaccharides, i.e. free glucose, for bacterial uptake supports bacterial respiration, resulting in higher CO_2 concentration in seawater and subsequently in the atmosphere.

FIGURES

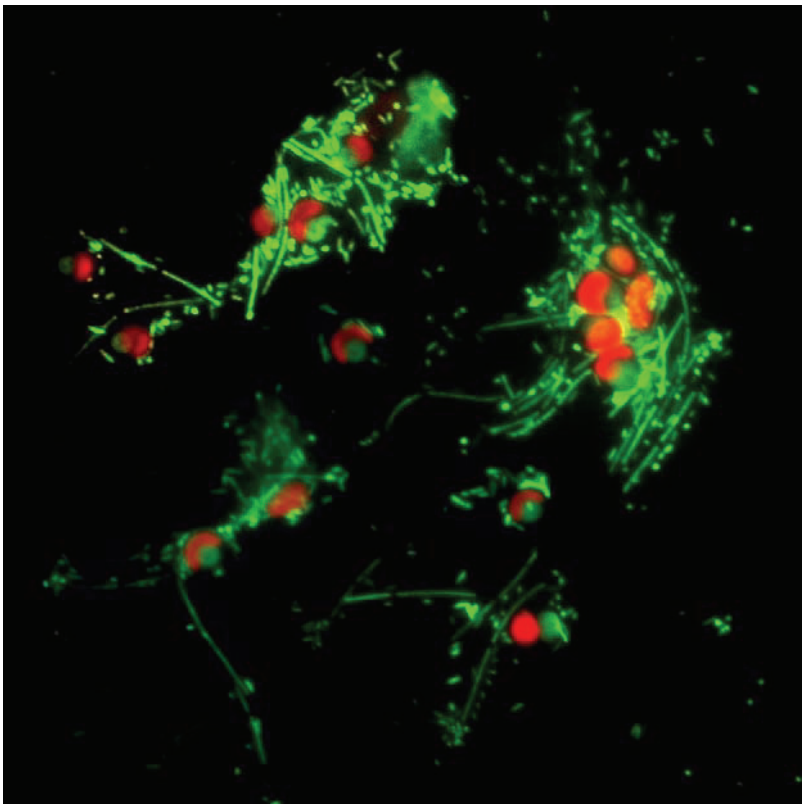

Figure 1

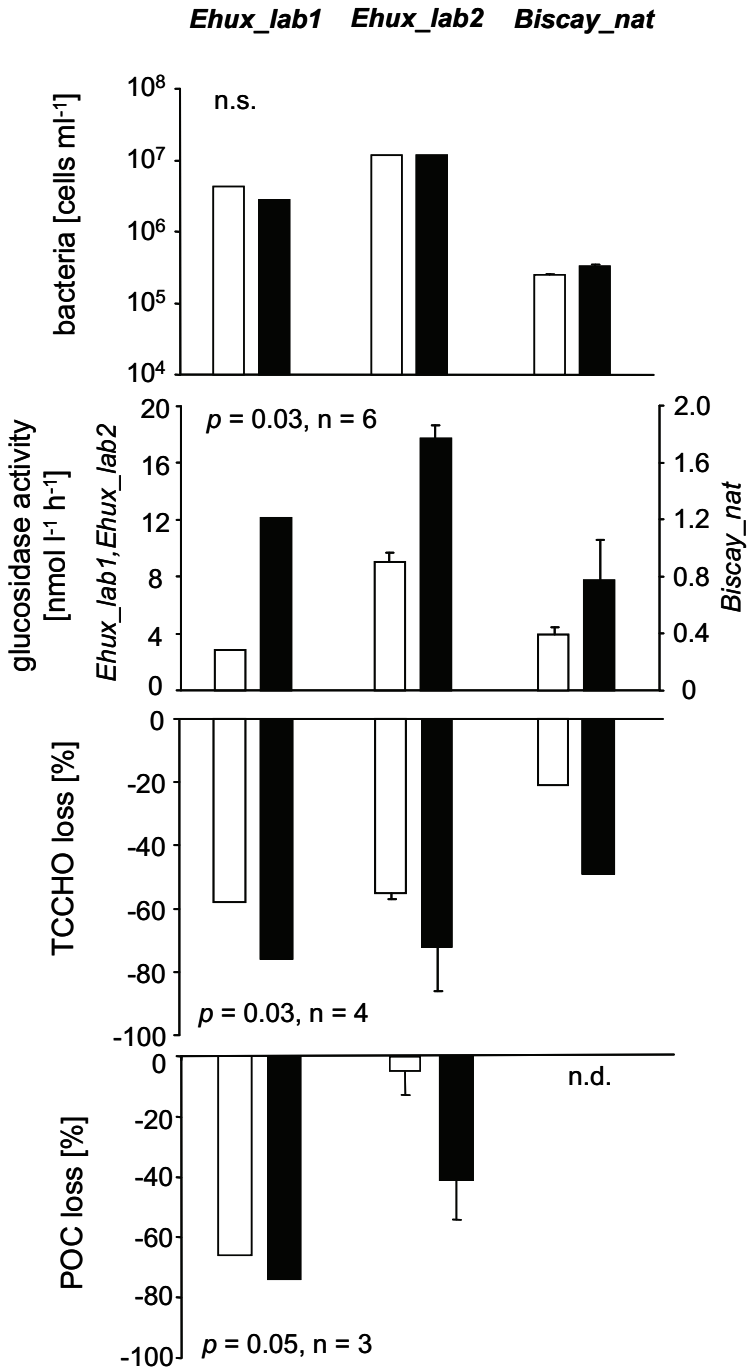
Ehux_lab1
Ehux_lab2
Biscay_nat
bacteria [cells ml-1]
n.s.
glucosidase activity [nmol l-1 h-1]
Ehux_lab1,Ehux_lab2
Biscay_nat
p = 0.03, n = 6
TCCHO loss [%]
p = 0.03, n = 4
POC loss [%]
n.d.
p = 0.05, n = 3

Figure 2

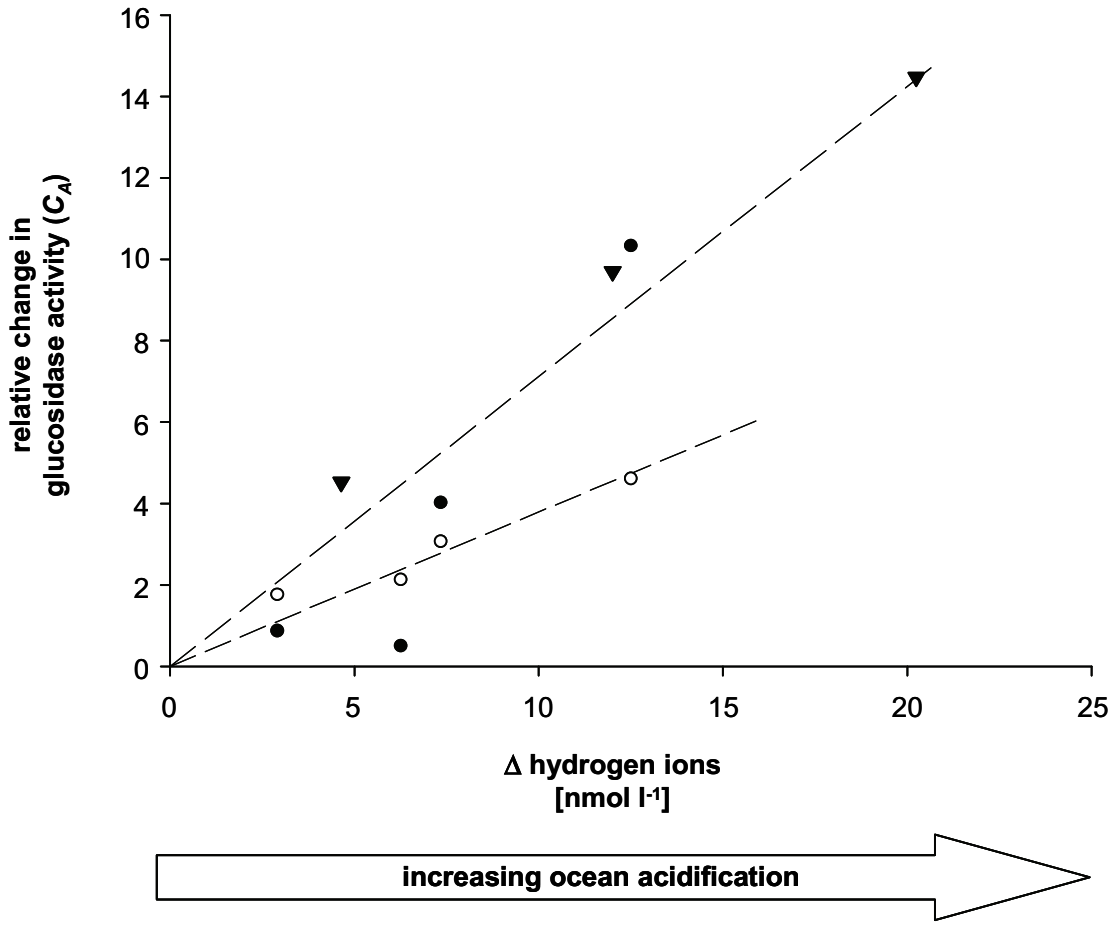
relative change in glucosidase activity (C_A)
16
14
12
10
8
6
4
2
0
0
5
10
15
20
25
Δ hydrogen ions
[nmol l-1]
increasing ocean acidification

Figure 3

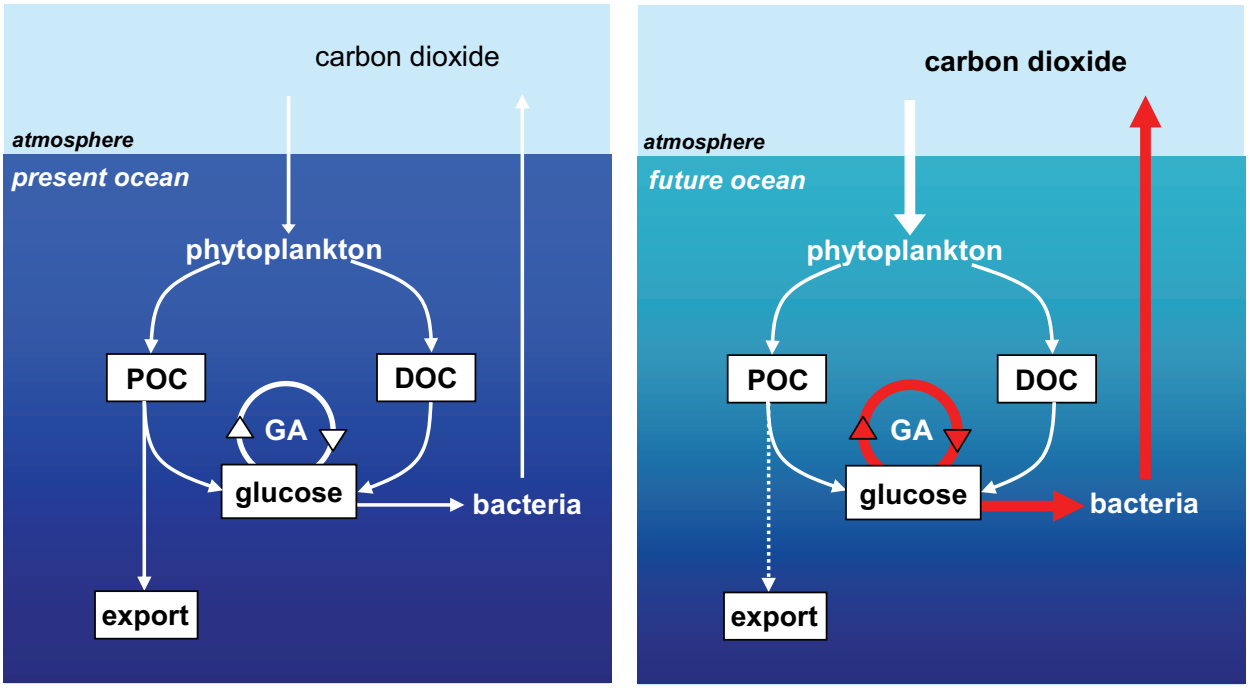
carbon dioxide
atmosphere
present ocean
phytoplankton
POC
DOC
GA
glucose
bacteria
export
carbon dioxide
atmosphere
future ocean
phytoplankton
POC
DOC
GA
glucose
bacteria
export

Figure 4

3. Conclusions

Manuscripts included in this thesis deal with effects of changing ocean temperature and partial pressure of carbon dioxide (pCO_2) on the bacterial degradation of organic matter. In this chapter, investigated effects are characterized, explaining how changes of temperature and pCO_2 affected bacterial degradation activity and how effects on heterotrophic bacterioplankton in turn influenced organic matter cycling. Implications of experimental results for organic matter fluxes in the future ocean are discussed in context of recent research on ocean warming and acidification. Furthermore, an outlook on future research perspectives as emerging from this thesis is given.

3.1 Bacterial degradation activity at rising ocean temperature and pCO_2

Effects of rising ocean temperature and pCO_2 on the degradation activity of natural bacterioplankton communities were investigated by encompassing manipulation experiments conducted by the use of mesocosms (manuscript I), chemostat systems (manuscripts III, IV), and batch incubations (manuscripts I, III, IV). Experimental temperature and pCO_2 manipulation simulated future impacts on marine ecosystems that will be induced by climate change. Bacterial activity was monitored in the context of complex interactions between autotrophic production and heterotrophic turnover of organic matter. Methods using fluorescent and radiolabelled substrate analogues were applied to estimate the bacterial hydrolytic activity (Hoppe 1983), substrate assimilation (Wright & Hobbie 1965, Azam & Hodson 1981, Rich et al. 1996), and biomass production (Fuhrman & Azam 1990, Ducklow & Carlson 1992). A newly developed method for carbohydrate analysis by ion chromatography (Engel & Händel, submitted) and well-established

methods for the analysis of bulk organic carbon concentrations (Qian & Mopper 1996) provided convenient tools to determine the loss of organic matter driven by heterotrophic bacterial activity.

Present studies revealed that changes in seawater temperature and pCO_2 simulating ocean warming and acidification affected the degradation of organic matter in marine pelagic ecosystems due to temperature and pH effects on bacterial extracellular enzymes. By synthesis and release of extracellular enzymes marine heterotrophic bacteria generate their substrate supply by the hydrolysis of organic macromolecules (Chróst 1991, Hoppe 1991, Hoppe et al. 1993). Experimental results showed that elevated temperature and lowered pH significantly increased the reaction velocity of extracellular hydrolases produced by natural bacterioplankton communities. The activity of polysaccharide- and protein-hydrolyzing enzymes associated with aggregates formed from a natural diatom assemblage increased in response to an increase of *in-situ* temperature by 6°C (manuscript I). Rates of polysaccharide-hydrolyzing extracellular enzymes produced by natural bacterioplankton communities of the North Sea and of the northern Bay of Biscay increased, when the *in-situ* pH was decreased by 0.2 and 0.3 units, respectively (manuscripts III, IV). Thus, experimental manipulation shifted ambient temperature and pH closer towards the specific optima of tested extracellular enzymes, suggesting that *in-situ* conditions of investigated marine ecosystems did not allow for maximum potential rates of these enzymatic reactions. This observation is in good accordance with previous studies that revealed temperature and pH as regulating factors of bacterial extracellular enzymes in marine environments, and determined optima for enzymatic reactions not corresponding to *in-situ* conditions (King 1986, Christian & Karl 1995, Arnosti et al. 1998). Present studies further suggest that future changes in ocean temperature and pH induced by climate change will be sufficient

to substantially alter the environmental control of bacterial extracellular enzymes in marine pelagic ecosystems, increasing rates of enzymatic polymer degradation.

The hydrolytic activity of extracellular enzymes represents the initial step in the bacterial turnover of organic matter (Chróst 1991, Hoppe 1991), and drives the loss of particulate organic matter (POM) in the ocean (Smith et al. 1992, Hoppe et al. 1993, Huston & Deming 2002). In the present studies, effects of elevated temperature and lowered pH on bacterial extracellular enzymes were strong enough to mediate significant impacts on pools and fluxes of organic carbon. Stimulating effects of lowered pH on bacterial extracellular glucosidases coincided with an increased loss of polysaccharides (manuscripts III, IV), which account for a major fraction of semilabile organic carbon in the ocean (Benner et al. 1992, Pakulski & Benner 1994, Hedges et al. 2001). Furthermore, increased rates of extracellular hydrolases at elevated temperature and lowered pH coincided with an enhanced loss of particulate organic carbon (POC) derived from diatom aggregates (manuscript I) and monospecific cultures of *Emiliania huxleyi* (manuscripts III, IV), respectively. Thus, direct effects of elevated temperature and lowered pH on bacterial extracellular enzymes increased degradation rates of both reactive organic carbon and bulk particulate carbon. Therefore, it can be assumed that ocean warming and acidification will evoke a significant acceleration of the bacterial carbon processing in marine pelagic ecosystems.

3.2 Contribution to current research on ocean warming and ocean acidification

The world's ocean is one of the largest dynamic carbon reservoirs on Earth (Hedges 1992), and provides an important sink for anthropogenic carbon dioxide (CO_2). The oceans have absorbed approximately half of the CO_2 produced by fossil fuel burning during the last 200

years (Sabine et al. 2004). Since the oceanic uptake of atmospheric CO_2 is strongly affected by biological processes, marine research currently undertakes strong efforts to explore the feedback potential provided by marine biota and biogeochemical cycles to climate change. Degradation and remineralization of organic carbon by heterotrophic bacteria co-determine the flux of atmospheric CO_2 to the ocean, but potential impacts of ocean warming and acidification on heterotrophic bacterioplankton are yet hardly considered. Manuscripts included in this thesis revealed that bacterial degradation activity in the ocean is likely to respond to environmental impacts of climate change, implying changes in the future marine carbon cycle.

Effects of rising temperature and pCO_2 enhancing the enzymatic hydrolysis of biogenic particles in the ocean can provide a positive feedback to the atmospheric level of pCO_2. The efficiency of particle hydrolysis by bacterial extracellular enzymes co-determines the partitioning of organic carbon between the particulate and dissolved pool, and is therefore an important factor influencing the sinking flux of carbon in the ocean (Smith et al. 1992, Hoppe et al. 1993). The downward export of carbon contained in biogenic particles, referred to as biological carbon pump, promotes the flux of CO_2 from the atmosphere to the ocean and plays a significant role in controlling the atmospheric level of pCO_2 (Volk & Hoffert 1985). In the modern ocean, the biological carbon pump transfers around 5 - 15 Gt carbon yr^{-1} to depth (Falkowski et al. 1998). A strengthening of the biological carbon pump reduced the atmospheric pCO_2 by approximately 30 µatm during the last glacial maximum (Sigman & Boyle 2000). An enhanced bacterial degradation of aggregated (manuscript I) and suspended (manuscripts III, IV) POC in response to ocean warming and acidification may decrease the magnitude of carbon export and weaken the biological carbon pump in the future ocean, mediating a biologically driven feedback to climate change.

Increased enzymatic degradation of polysaccharides at rising temperature and decreasing pH will potentially provide cascading effects on bacterial respiration, and increase the production of CO_2 in the future ocean. Carbohydrates contribute substantially to the bacterial carbon supply in the open ocean, with glucose representing the most important carbohydrate species (Rich et al. 1996, Skoog et al. 1999, Kirchman et al. 2001). Approximately 40 - 60% of consumed glucose fuels bacterial respiration, and thus the production of CO_2 (Rich et al. 1996). Increased activities of extracellular glucosidases in response to ocean warming and acidification will improve the supply of glucose to bacterioplankton (manuscripts I, III, IV), and potentially increase the bacterial production of respiratory CO_2, what in turn can reduce the net flux of atmospheric CO_2 to the ocean.

Autotrophic production and subsequent bacterial remineralization of organic carbon are key processes in the marine carbon cycle. In particular in the open ocean, a large fraction of organic carbon is produced and recycled during the growth and decline of phytoplankton blooms. Phytoplankton production of particulate and dissolved organic matter in the Bay of Biscay was shown to generate substrates for heterotrophic bacterioplankton (manuscripts II, III). Recently, it has been demonstrated that elevated seawater pCO_2 increases the autotrophic CO_2 consumption of a natural phytoplankton community, suggesting a negative feedback to rising atmospheric CO_2 (Riebesell et al. 2007, Arrigo 2007). The additional uptake of CO_2 was likely balanced by an increased production of phytoplankton exudates. The production of carbon-rich exopolymers represents a mechanism for cellular carbon overflow, and typically increases under nutrient-limited conditions during the decline of phytoplankton blooms (Wood & van Walen 1990, manuscript II). The abundance of transparent exopolymer particles (TEP) that

form from phytoplankton exudates was shown to be affected by changing seawater pCO_2 (Engel 2002, Engel et al. 2004). However, current research on effects of ocean warming and acidification on the activity of heterotrophic bacterioplankton suggests that organic matter derived from increased autotrophic carbon consumption in a high-CO_2 world will not escape bacterial remineralization. The lag time between maximum primary production and bacterial secondary production in the succession of a diatom bloom was shown to diminish at elevated seawater temperature. Hence, the peak of bacterial degradation activity will occur earlier during the course of phytoplankton blooms and potentially accelerate the remineralization of organic matter in response to ocean warming (Hoppe et al. 2008). Furthermore, the addition of labile organic carbon as produced by phytoplankton at elevated seawater pCO_2 to a carbon-limited microbial food web reduced phytoplankton biomass and the rate of organic carbon accumulation due to stimulated bacterial competition for inorganic nutrients (Thingstad et al. 2008). Present studies suggest that also higher rates of bacterial carbon turnover in response to ocean warming and acidification may counterbalance an increased autotrophic CO_2 consumption.

It is noteworthy that the feedback mechanisms identified by Riebesell et al. (2007) and by this thesis are supported by different chemical effects of rising ocean pCO_2 on enzymatic reactions. Effects of elevated seawater pCO_2 on the autotrophic fixation of inorganic carbon are attributed to an increased availability of aqueous CO_2, the preferred substrate of the primary carboxylating enzyme ribulose-1,5-bisphosphate carboxylase/oxygenase (RubisCO) (Raven 1990, Rost et al. 2003). In contrast, effects of elevated seawater pCO_2 on bacterial extracellular enzymes are mediated by lowered pH, i.e. by an increased concentration of protons in seawater, which affects the enzymatic protein structure

(manuscripts III, IV). Hence, enzymes sensitive to rising temperature and pCO_2 may become key drivers of a changing carbon cycle in the future ocean.

3.3 Future research perspectives

This thesis provides new information on the environmental control of bacterial organic matter degradation by ocean temperature and pCO_2, suggesting impacts of ocean warming and acidification on heterotrophic processes in the marine carbon cycle. It is therefore a matter of urgency to consider the response of heterotrophic bacterioplankton to ocean warming and acidification when assessing consequences of climate change for the future ocean. Several issues for future research arise from present findings.

Experimental results revealed that effects of ocean warming and acidification on extracellular enzymes of bacterioplankton communities will accelerate the initial step in bacterial carbon remineralization. Future research needs to test effects of projected changes in ocean temperature and pH on subsequent processes of bacterial organic matter turnover. In particular, effects on bacterial respiration and on the bacterial growth efficiency, i.e. on the partitioning of consumed organic carbon between bacterial biomass production and respiration would imply essential consequences for the microbial loop and the marine carbon cycle. Future research should also verify whether the use of molecular tools can improve the mechanistic understanding of physiological feedbacks of heterotrophic bacterial communities to changes in ocean temperature and pH.

Increased rates of extracellular hydrolases induced by elevated temperature and lowered pH in seawater accelerated the degradation of bulk organic carbon. Future research should examine impacts of increased bacterial degradation activity on the chemical composition of dissolved and particulate organic matter. Present studies revealed that the enzymatic

breakdown of polysaccharides was accelerated at elevated temperature and lowered pH. Further studies should investigate whether other components of organic matter like proteins, lipids, and organic phosphate compounds are also affected, and whether potential changes in the quantity of these compounds are sufficient to mediate effects on the elemental stoichiometry of marine organic matter.

Temperature and pH are only two factors controlling bacterial degradation activity in the ocean. Other factors like the availability and lability of organic substrates and the abundance of bacteriovores and bacteriophages also exert influence on the activity of bacterioplankton communities. In order to better assess consequences of ocean warming and acidification on the organic matter turnover in marine ecosystems, it will be important to investigate combined effects of temperature and pH and interactions of both individual parameters with other abiotic and biotic factors on heterotrophic bacterial activity in the ocean.

3.4 References

ARNOSTI C, JØRGENSEN BB, SAGEMANN J, THAMDRUP B (1998) Temperature dependence of microbial degradation of organic matter in marine sediments: polysaccharide hydrolysis, oxygen consumption, and sulfate reduction. Mar Ecol Prog Ser 165:59-70

ARRIGO K (2007) Marine manipulations. Nature 450:491-492

AZAM F, HODSON RE (1981) Multiphasic kinetics for D-glucose uptake by assemblages of natural marine bacteria. Mar Ecol Prog Ser 6: 213-222

BENNER R, PAKULSKI JD, MCCARTHY M, HEDGES JL, HATCHER PG (1992) Bulk chemical characterization of dissolved organic matter in the ocean. Science 255:1561-1564

CHRISTIAN JR, KARL DM (1995) Bacterial ectoenzymes in marine waters: activity ratios and temperature responses in three oceanographic provinces. Limnol Oceanogr 40:1042-1049

CHRÓST RJ (1991) Environmental control of the synthesis and activity of aquatic microbial ectoenzymes. In: Chróst RJ (ed) Microbial enzymes in aquatic environments (Springer Verlag, Heidelberg)

DUCKLOW HW, CARLSON CA (1992) Oceanic bacterial production. Adv Microb Ecol 12:113-181

ENGEL A (2002) Direct relationship between CO2 uptake and transparent exopolymer particles production in natural phytoplankton. J Plankt Res 24:49-53

ENGEL A, HÄNDEL N (submitted) Simultaneous determination of the neutral-, amino-, and acidic sugar composition of polysaccharides in seawater using High Performance Anion Exchange Chromatography with Pulsed Amperometric Detection

ENGEL A, DELILLE B, JACQUET S, RIEBESELL U, ROCHELLE-NEWALL E, TERBRUGGEN A, ZONDERVAN I (2004) Transparent exopolymer particles and dissolved organic carbon production by Emiliania huxleyi exposed to different CO2 concentrations: a mesocosm experiment. Aquat Microb Ecol 34:93-104

FALKOWSKI PG, BARBER RT, SMETACEK V (1998) Biogeochemical controls and feedbacks on ocean primary production. Science 281:200-206

FUHRMAN JA, AZAM F (1980) Bacterioplankton secondary production estimates for coastal waters of British Columbia, Antarctica, and California. Appl Environ Microbiol 39: 1085-1095

HEDGES JI (1992) Global Biogeochemical cycles - progress and problems. Mar Chem 39:67-93

HEDGES JI, BALDOCK JA, GELINAS Y, LEE C, PETERSON M, WAKEHAM SG (2001) Evidence for non-selective preservation of organic matter in sinking marine particles. Nature 409:801-804

HOPPE HG (1983) Significance of exoenzymatic activities in the ecology of brackish water: measurements by means of methylumbelliferyl-substrates. Mar Ecol Prog Ser 11:299-308

HOPPE HG (1991) Microbial extracellular enzyme activity: a new key parameter in aquatic ecology. In: Chróst RJ (ed) Microbial enzymes in aquatic environments (Springer Verlag, Heidelberg)

HOPPE HG, DUCKLOW H, KARRASCH B (1993) Evidence for dependence of bacterial growth on enzymatic hydrolysis of particulate organic matter in the mesopelagic ocean. Mar Ecol Prog Ser 93:277-283

HOPPE HG, BREITHAUPT P, WALTHER K, KOPPE R, BLECK S, SOMMER U, JÜRGENS K (2008) Climate warming during winter affects the coupling between phytoplankton and bacteria during the spring bloom: Results from a mesocosm study. Aquat Microb Ecol 51: 105-115

HUSTON AL, DEMING JW (2002) Relationship between microbial extracellular enzyme activity and suspended and sinking particulate organic matter: seasonal transformations in the North Water. Deep Sea Res II 49:5211-5225

KING GM (1986) Characterization of β-glucosidase activity in intertidal marine sediments. Appl Envrionm Microbiol 51(2):373-380

KIRCHMAN DL, MEON B, DUCKLOW HW, CARLSON CA, HANSELL DA, STEWARD GF (2001) Glucose fluxes and concentrations of dissolved combined neutral sugars (polysaccharides) in the Ross Sea and Polar Front Zone, Antarctica. Deep-Sea Res Part II 48:4179-4197

PAKULSKI JD, BENNER R (1994) Abundance and distribution of carbohydrates in the ocean. Limnol Oceanogr 39:930-940

QIAN J, MOPPER K (1996) Automated high-performance, high-temperature combustion total organic carbon analyser. Anal Chem 68:3090-3097

RAVEN JA (1990) Predictions of Mn and Fe use efficiencies of phototrophic growth as a function of light availability for growth. New Phytol 116:1-18

RICH JH, DUCKLOW HW, KIRCHMAN DL (1996) Concentrations and uptake of neutral monosaccharides along 140 degrees W in the equatorial Pacific: Contribution of glucose to heterotrophic bacterial activity and the DOM flux. Limnol Oceanogr 41:595-604

RIEBESELL U, SCHULZ KG, BELLERBY RGJ, BOTROS M, FRITSCHE P, MEYERHÖFER M, NEILL C, NONDAL G, OSCHLIES A, WOHLERS J, ZÖLLNER E (2007) Enhanced biological carbon consumption in a high CO2 ocean. Nature 450:545-549

ROST B, RIEBESELL U, BURKHARDT S, SÜLTEMEYER D (2003) Carbon acquisition of bloom-forming marine phytoplankton. Limnol Oceanogr 48:55-67

SABINE CL, FEELY RA, GRUBER N, KEY RM, LEE K, BULLISTER JL, WANNINKHOF R, WONG CS, WALLACE DWR, TILBROOK B, MILLERO FJ, PENG TH, KOZYR A, ONO T, RIOS AF (2004) The oceanic sink for anthropogenic CO2. Science 305:367-371

SIGMAN DM, BOYLE EA (2000) Glacial/Interglacial variations in atmospheric carbon dioxide. Nature 407:859-869

SKOOG A, BIDDANDA B, BENNER R (1999) Bacterial utilization of dissolved glucose in the upper water column of the Gulf of Mexico. Limnol Oceanogr 44, 1625-1633

SMITH DC, AZAM F (1992) A simple, economical method for measuring bacterial protein synthesis in seawater using ^{3}H-leucine. Mar Microb Food Webs 6:1007-114

SMITH DC, SIMON M, ALLDREDGE AL, AZAM F (1992) Intense hydrolytic enzyme-activity on marine aggregates and implications for rapid particle dissolution. Nature 359:139-142

THINGSTAD TF, BELLERBY RGJ, BRATBAK G, BØRSHEIM KY, EGGE JK, HELDAL M, LARSEN A, NEILL C, NEJSTGAARD J, NORLAND S, SANDAA R-A, SKJOLDAL EF, TANAKA T, THYRHAUG R, TÖPPER B (2008) Counterintuitive carbon-to-nutrient coupling in an Arctic pelagic ecosystem. Nature 455:387-390

VOLK T, HOFFERT MI (1985) The Carbon Cycle and Atmospheric CO_2. Natural Variations Archean to Present (Am Geophys Union, Washington DC)Wood MA, van Walen

LM (1990) Paradox lost? On the release of energy-rich compounds by phytoplankton. Mar Microb Food Webs 4:103–116

WRIGHT RJ, HOBBIE JE (1965) The uptake of organic solutes in lake water. Limnol Oceanogr 10:22-28

Acknowledgements – *Danksagung*

Anja Engel sei für ihr Vertrauen in meine Fähigkeiten, für viele Freiheiten und alle Unterstützung herzlich gedankt. Karin Lochte danke ich sehr für die spontane Bereitschaft meine zweite Gutachterin zu sein und für ihre terminliche Flexibilität. Mein Dank gebührt ebenfalls Kai Bischof, Christoph Völker, Lena und Aneta, die alle ohne zu zögern Mitglieder meines Prüfungsausschusses geworden sind.

Alle aktuellen und ehemaligen Mitglieder der HGF-Nachwuchsgruppe GloCar haben zum Gelingen dieser Arbeit beigetragen: Nicole, danke für das jederzeit angenehme und unkomplizierte Miteinander, deine Arbeit im Labor, deinen unermüdlichen Einsatz und dafür, dass wir nie die Nerven verloren haben - egal, ob in der überschäumenden Biskaya oder auf der Suche nach verschollenen Proben bei erfrischenden -20°C. Corinna, danke für deine große Unterstützung, meinen konstanten Koffein-Spiegel und dafür, dass du mich immer wieder motiviert und aufgemuntert hast. Mirko, Mascha und Markus sei sehr für Hilfe mit Rat und Tat gedankt.

Gerald und Sandra, eure Hilfsbereitschaft war grenzenlos, ihr hattet immer ein offenes Ohr für mich und durch euch habe ich mich im AWI-Kosmos nie verloren gefühlt. Tausend Dank, ihr Spitzenforscher!

Allen noch nicht genannten Mitgliedern des mittlerweile nicht mehr existierenden Kaffeekränzchens - Anja T., Ina, Gernot - sei für die sinnvollen und auch für die sinnlosen Diskussionen herzlich gedankt!

Danke an die vielen helfenden Hände - Christiane, Erika, Friedel, Julia, Petra und viele mehr. Jérôme, Caroline, Nicolas, Lei - thanks for your help on board of the *Belgica*!

Rita und Susanne - danke für eure Hilfe in längst vergessenen dunklen Zeiten und die daraus entstandene Freundschaft.

Ein großes Dankeschön an alle meine Bochumer - für die Unterstützung und die wissenschaftliche Ahnungslosigkeit.

Anlage zur Dissertation

Judith Piontek
Weißenburger Str. 13
27570 Bremerhaven

Bremerhaven, den 6. Januar 2009

Erklärung gem. §6(5) Nr. 1-3 PromO

Hiermit erkläre ich, dass ich

1. die Arbeit ohne unerlaubte fremde Hilfe angefertigt habe
2. keine anderen, als die von mir angegebenen Quellen und Hilfsmittel benutzt habe
3. die den benutzten Werken wörtlich oder inhaltlich entnommenen Stellen als solche kenntlich gemacht habe.

Ebenfalls erkläre ich hiermit, dass die drei von mir abgegebenen Exemplare der Arbeit identisch sind.

_____